Ann. Rev. Astron. Astrophys. 1983. 21: 271–342

ASYMPTOTIC GIANT BRANCH EVOLUTION AND BEYOND[1]

Icko Iben, Jr.

Departments of Astronomy and Physics, University of Illinois, Urbana, Illinois 61801

Alvio Renzini

Osservatorio Astronomico, Universita di Bologna, I-40100 Bologna, Italy

1. INTRODUCTION

In this review, attention is concentrated on progress in understanding the last stages of evolution of low- and intermediate-mass stars. We define low-mass stars to be those that develop an electron-degenerate helium core immediately following the main sequence phase; this places an upper limit of about 2–2.3 $M_\odot$ and a lower limit of about 0.8–1.0 $M_\odot$ on the initial main sequence mass of such stars, the precise limits being a function of initial composition. Intermediate-mass stars are those that ignite helium "non-degenerately," but develop an electron-degenerate carbon-oxygen (C-O) core following the exhaustion of helium at the center; this places an upper limit of about 8–9 $M_\odot$ on the initial mass of such stars, with the precise value again a function of composition. Low-mass stars also develop an electron-degenerate C-O core after the exhaustion of central helium; during their subsequent evolution they behave qualitatively like intermediate-mass stars in the same (nuclear) stage of evolution. This common phase we refer to as the asymptotic giant branch (AGB) phase of evolution (since, for low-mass stars, the evolutionary track in the H-R diagram approaches that of the first giant branch).

[1] Supported in part by National Science Foundation Grants (AST 78-20124 and AST 81-15325).

0066–4146/83/0915–0271$02.00

In Section 2 we concentrate on the thermal pulse phase of AGB evolution. In Section 3 we review estimates and implications of non-catastrophic mass loss (winds) and ejection (planetary nebulae) from AGB stars, and in Section 4 we present the concept of synthetic AGB evolution and use the algorithms that follow from this concept to review estimates of ages of stellar aggregates that contain AGB stars.

Evolution to the white dwarf state (for those stars that lose their hydrogen-rich envelopes before establishing a core of mass $\sim 1.4\ M_{\odot}$), as well as the nature of type I $\frac{1}{2}$ supernovae (for those that do not), are discussed in Section 5; and Sections 6 and 7 are devoted to comparisons with the observations, with particular emphasis on the predictions about surface abundances given by "canonical" stellar evolution versus abundances estimated from spectroscopic observations (e.g. CNO abundances in Cepheids and in AGB stars).

Throughout, it is assumed that the reader is familiar with general evolutionary concepts as described in earlier reviews in this series (99, 100) or elsewhere (e.g. 106, 187, 222), and emphasis is placed on developments over the past eight years.

2. THE EARLY AGB AND THE THERMALLY PULSING PHASE

A number of exciting features of AGB evolution have been revealed over the past decade. The first of these is that, in the helium-burning convective shell that develops during thermal pulses, neutron-rich isotopes are produced naturally, and, in sufficiently massive AGB model stars, they are produced in the solar-system *s*-process distribution. The second is that, during the first portion of the quiescent helium-burning phase that follows a pulse in model stars of sufficiently large mass in which core mass $M_{\rm H}$ exceeds $\sim 0.62 M_{\odot}$, the freshly produced neutron-rich isotopes and freshly produced carbon are "dredged up" into the convective envelope. Finally, some of the dredged-up ^{12}C may be converted into ^{13}C and ^{14}N at the base of the envelope during the interpulse phase in AGB stars of the largest initial mass. Surface mass loss via a wind during the AGB phase and/or via catastrophic ejection at the end of the AGB phase (ejection of a planetary nebula or explosion as a supernova of type I $\frac{1}{2}$) carries freshly processed matter into the interstellar medium. One of the most exciting aspects of these physical processes is the fact that they permit the calculation of theoretical carbon star distributions that can be compared with observable distributions, and, furthermore, they permit the calculation of the contribution of AGB stars to the galactic nucleosynthesis of ^{4}He, ^{12}C, ^{13}C, ^{14}N, ^{22}Ne, and neutron-rich isotopes.

Stellar model calculations of relevance include the following: (18, 84, 88, 89, 101–105, 112, 117, 118, 171, 208–210, 218, 223, 253, 266, 268, 271).

2.1 *The First and Second Dredge-Up and Attendant Changes in Surface Composition*

From the point of view of comparisons with the observations, the surface abundance changes that occur prior to the AGB phase are potentially of high significance. These changes are brought about when the base of the convective envelope extends inward to "dredge up" material that has experienced hydrogen burning during preceding phases. During the first dredge-up phase, which occurs in every star as it becomes a red giant for the first time (following the exhaustion of central hydrogen), the major results are the following: a doubling (roughly) of the surface ^{14}N abundance, a reduction in surface ^{12}C abundance by approximately 30%, the formation of a surface $^{12}C/^{13}C$ ratio of about 20–30, a reduction in surface Li and Be by several orders of magnitude, and practically no change at all in the surface abundance of ^{16}O. These changes are extensively reviewed elsewhere (e.g. 21, 99, 106).

The second dredge-up phase accompanies the formation of an electron-degenerate core, following the exhaustion of central helium. In the dredged-up material, which can be as high as 1.0 $M_\odot$ in the most massive intermediate-mass stars, hydrogen has been completely converted into helium, and both ^{12}C and ^{16}O have been converted almost completely into ^{14}N. Figure 1 [adapted from (20)] illustrates how the base of the convective envelope moves inward in mass through matter that is being pushed out from the helium-burning shell during this second dredge-up phase. It is the increase in opacity and drop in temperature in the expanding layers, coupled with an increase in the outward flux of energy produced by helium burning and the release of gravitational potential energy from the contracting core, that forces the local radiative gradient to increase above the adiabatic gradient in matter ever closer (in mass, not radius) to the helium-burning shell.

During the second dredge-up phase, temperatures in the rapidly contracting helium-exhausted core at first increase as a result of the release of gravitational potential energy, and then decrease as energy loss via neutrinos becomes important. The net result is a highly electron-degenerate core in which temperatures do not become high enough for carbon to burn until core mass approaches the Chandrasekhar mass.

For a given initial composition, the final mass M_H in the hydrogen-exhausted core at the end of the second dredge-up phase is a monotonically increasing function of initial stellar mass. This mass reaches a maximum of only slightly larger than 1.0 $M_\odot$ in the most massive stars that develop an

electron-degenerate core. The maximum initial mass M_i^{max} of a star that forms a degenerate core is $M_i^{max} \cong 8.95 + 69.4\Delta Z - 31.3\Delta Y$, where M_i is in solar units, and the minimum initial stellar mass for which the second dredge up occurs is $M_i^{min} \cong 4.59 + 82.5\Delta Z - 6.88\Delta Y$ (20). Here, Z and Y are, respectively, the abundances by mass of elements heavier than helium and of helium, and $\Delta Z = Z - 0.02$ and $\Delta Y = Y - 0.28$. Thus, only the most massive intermediate-mass stars experience a change in surface composition as they settle onto the AGB. This contrasts with the first dredge-up phase, when every star that becomes a giant experiences a change in surface composition after hydrogen exhaustion in the center.

It is worthwhile to give a simple example of the magnitude of surface composition changes that one might expect as a consequence of the first and second dredge-up episodes in a single star. Let us begin with an initial composition of CNO elements in the ratio $(C:N:O)_0 = 1/2:1/6:1$ so that, in units of the initial oxygen abundance, the sum of all CNO elements is 5/3. During the first dredge-up phase, the CNO abundances become $(C:N:O)_1 \cong 1/3:1/3:1$, very roughly independent of stellar mass. For

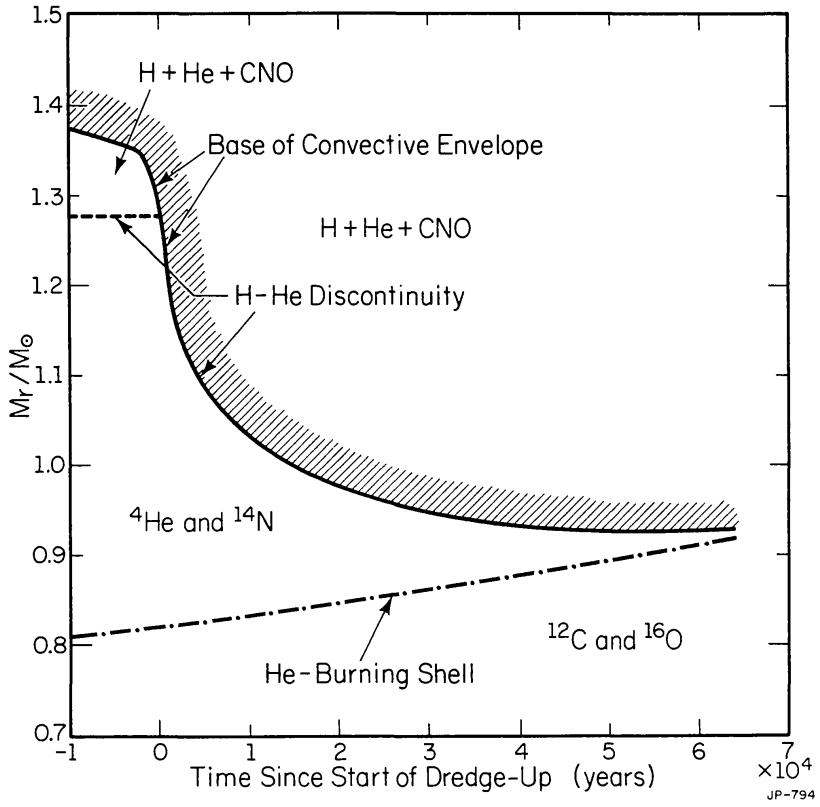

Figure 1 The variation with time of the location (in mass) of the base of the convective envelope and of the center of the helium-burning shell during the second dredge-up phase in a model of mass 5 $M_\odot$ and initial composition $(Y, Z) = (0.28, 0.001)$.

those stars of composition $Y = 0.28$, $Z = 0.02$, that experience the second dredge up, the mass in the hydrogen-exhausted core just before dredge up is $M'_H \cong 0.2954M_i - 0.50$, and the mass of this core at the completion of dredge up is $M_H \cong 0.0526M_i + 0.59$, where $4.59 < M_i < 8.95$ (20). If Y_1 and Y_2 are, respectively, the surface abundances of element Y before and after the second dredge up and Y_p is the abundance of element Y after processing through the H-burning shell, then $Y_2 = [Y_p(M'_H - M_H) + Y_1(M_i - M'_H)]/(M_i - M_H)$. When, for example, $M_i = M_i^{max} = 8.95$, it then follows that $Y_2 \cong 0.137\ Y_p + 0.863\ Y_1$. Since $(C:N:O)_p \cong 0:5/3:0$, the final surface abundances of the CNO elements become $(C:N:O)_2 \cong 0.29:0.52:0.86$ and nitrogen rivals oxygen in abundance.

2.2 *The Early-AGB Phase*

It is convenient to group AGB stars into two classes. Those which have not yet begun to thermally pulse we designate as early-AGB (E-AGB) stars, while those that are in the thermally pulsing phase we designate as TP-AGB stars. While in the E-AGB phase, the hydrogen-burning shell is extinct, and helium burning in a narrowing shell provides most of the energy reaching the stellar surface.

With an unimportant exception, L and T_e are monotonic functions of time during the E-AGB phase. As an example, for the composition $Z = 0.001$, $Y \sim 0.25$, the expression $\log L \cong 2.23 + 2.68 \log (M_i/2) + 10^{-7.08}(M_i/2)^{3.6}t$ represents (to within $\Delta \log L = \pm 0.1$) the time dependence of the luminosity as a function of initial mass, and the duration of the phase is roughly $t_{E\text{-}AGB} \cong 10^7$ yr $(2/M_i)^{3.64}$. In these expressions, M_i is to be set equal to 2 for all $M_i < 2$.

The relationship between T_e and L is too sensitive to mass and composition to permit the construction of a simple analytic approximation that is valid for all masses and compositions. It must further be emphasized that the relationships between T_e and L found in any model calculation for a given mass (cf. Figure 5) are at best acceptably reliable only with regard to the slope. The normalization is so sensitive to the choice of ℓ/H and to the details of the opacity (including molecular lines, etc.) that it requires an observational calibration.

The designation "asymptotic" in the acronym AGB comes from the fact that, for $M_i \gtrsim 1$, the T_e-L relationship for AGB stars of low mass is very close to (but slightly to the blue of) the T_e-L relationship for low-mass stars on the first giant branch. For more-massive stars, the term "asymptotic" has no morphological significance.

Toward the end of the E-AGB phase, hydrogen is reignited in a thin shell and the star begins to thermally pulse. The location in mass (M_H) of the

hydrogen-burning shell when thermal pulsing begins is a well-defined function of initial mass M_i. For intermediate-mass stars of Population I composition, this mass is given approximately by $M_H \simeq 0.59 + 0.0526\, M_i$. For low-mass stars, M_H is only slightly larger than the mass of the hydrogen-exhausted core at the onset of the helium flash, or, $M_H \sim 0.53$.

2.3 *General Characteristics of Thermal Pulses*

As in the case of the helium-core flash, the dominant energy source for a thermal pulse is the triple alpha reaction. However, since burning occurs in a region in which electrons are not degenerate [between the hydrogen-helium (XY) discontinuity and the electron-degenerate C-O core], the energy that is liberated goes directly into raising the local pressure and initiating an expansion. Once the expansion has progressed far enough, cooling sets in and helium burning begins to die down.

The expansion initiated by helium burning takes matter at and beyond the XY discontinuity out to such low temperatures and densities that hydrogen burning is effectively shut off. Ultimately, when the helium-burning luminosity L_{He} drops below the surface luminosity L, the matter that has been propelled outward falls back inward and heats until hydrogen is reignited. The helium-burning rate continues to drop and the hydrogen-burning rate continues to increase until a steady state is reached in which the hydrogen-burning luminosity L_H nearly equals L and $L_{He} \ll L_H$. Then ensues a long period during which quiescent hydrogen burning in a shell eats its way outward in mass until, after a critical mass ΔM_H has been processed, another thermal pulse is initiated.

The time dependence of L_{He}, L_H, and L are shown in Figure 2 for an intermediate-mass star shortly after it has begun thermally pulsing (102). In this particular case ($M_H \sim 0.96$, $M = 7$, and 7 prior pulses have occurred), the global characteristics (radius R, L, and T_e) are not affected very dramatically by a pulse. This is not true for very-low-mass stars, as is emphasized in Section 2.8. Note that the surface luminosity L plummets downward immediately following the rapid increase in L_{He}. After reaching a relative minimum, L increases for a short period before decreasing again at a more leisurely pace to an absolute (postflash) minimum. In the following, we refer to the initial decline and increase in L as a rapid dip and rise, respectively. The subsequent, more leisurely decline in surface luminosity to the absolute (postflash) minimum is called the extended postflash dip. During this extended dip, $L \simeq L_{He}$ and $L_H \simeq 0$.

Pulse amplitude grows with each succeeding pulse, rapidly for the first 5 or 10 pulses, then much more slowly for the next 5 or 10 pulses, until a "locally asymptotic" limit is approached (see 85). At this limit, L_{He}^{max} can reach from a few times 10^7 to almost 10^8 (see 18 and 113).

Toward the end of each interpulse phase, L reaches a limit L_{max} given by

$$L_{max} \cong 5.925 \times 10^4 (M_H - 0.495), \quad 1.$$

as first shown by Paczyński (167) and Uus (241). For low-mass stars, $L_H \sim L$ during the interpulse phase, but in intermediate-mass stars, the gravitational potential energy that is liberated as matter flows through the hydrogen-burning shell contributes appreciably to L (by an amount L_g) and, roughly (105, 120)

$$L_{max} = (L_H + L_g)_{max} \cong 6.34 \times 10^4 (M_H - 0.44)(M/7)^{0.19}. \quad 1.'$$

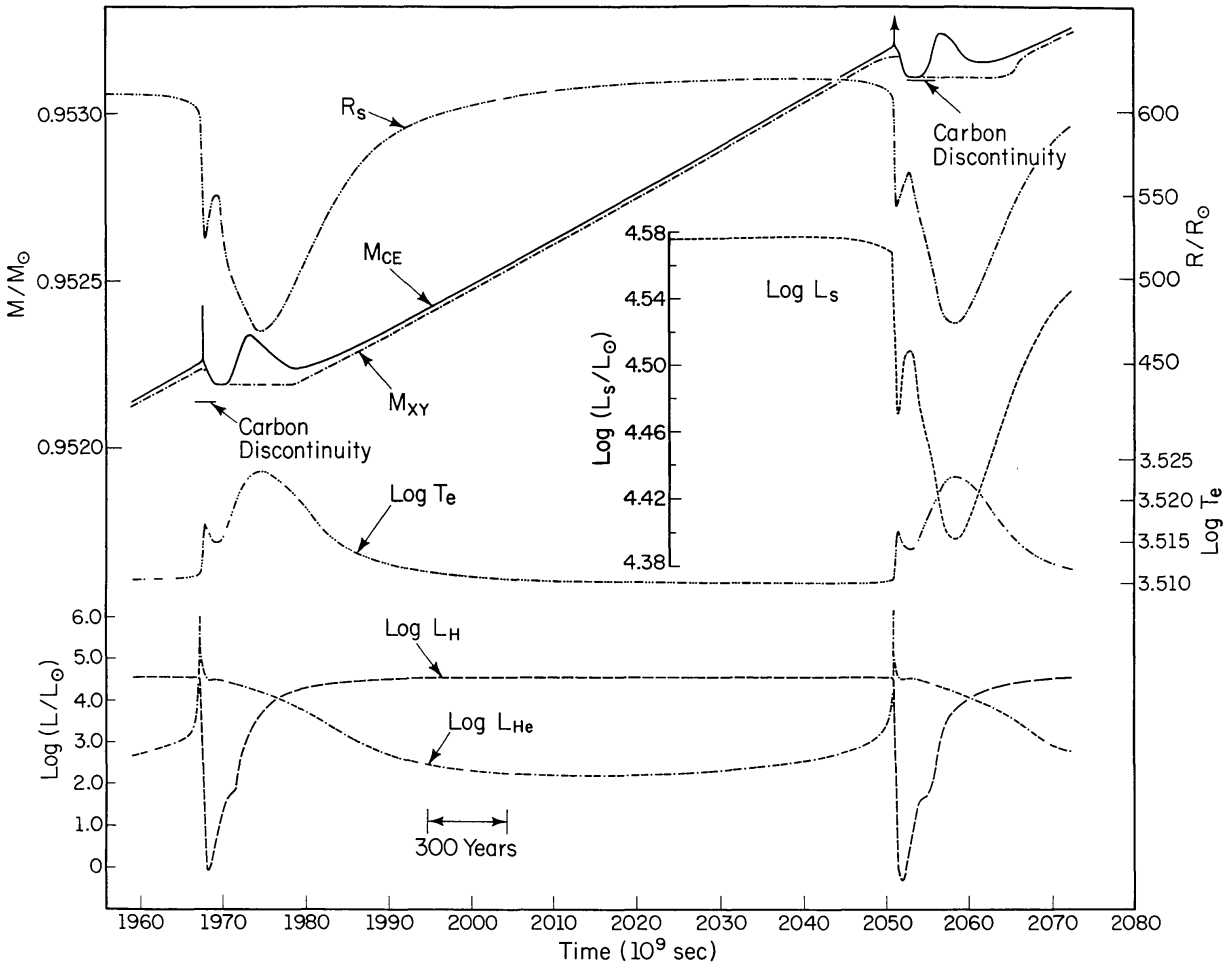

Figure 2 The variation with time of several internal and external characteristics in a model of mass $7M_\odot$ and initial composition $(Y, Z) = (0.28, 0.02)$ during and between its seventh and eighth thermal pulses as an AGB star. Here, L_H is the rate of energy production by hydrogen-burning reactions, L_{He} the rate of energy production by helium-burning reactions, L the surface luminosity, M_{XY} the location in mass of the hydrogen-helium discontinuity, M_{CE} the location in mass of the base of the convective envelope, R_s the radius of the star, and T_e the surface temperature of the star. Surface temperature is in degrees Kelvin and all other quantities are in solar units.

An approximation that fits results for low-mass stars somewhat better is (109)

$$L_{\max} \cong (5.925+0.415x)(M_{\rm H}-0.495+0.0505x)\ 10^4, \qquad 1.''$$

where $x = [(M-M_{\rm H})/6.04]^{1.83}$.

Yet another complication arises if, during the interpulse phase, temperatures at the base of the convective envelope are high enough for hydrogen-burning reactions to occur. Then, $L_{\max}$ at the end of the interpulse phase is even larger than the value given by (1.) or (1.′). Since temperatures at the base of the envelope are a function of ℓ/H, the luminosity-core mass relationship is also a function of ℓ/H. For example, when ℓ/H is increased from 0.7 (no envelope burning) to 1.0 (envelope burning), the quiescent luminosity of a 7-$M_\odot$ model with $M_{\rm H} \cong 0.96$ increases by about 15% (105).

The amount of time that elapses between pulses increases as the locally asymptotic limit is approached. This elapsed time $\Delta t_{\rm ip}$ initially obeys $\log \Delta t_{\rm ip}({\rm yr}) \cong 3.05-4.5\,(M_{\rm H}-1.0)$ (170) and grows until $\log \Delta t_{\rm ip}$ is larger than this by about 0.25 (21). During a pulse, the flux produced by helium burning becomes so large that a convective shell forms. At its maximum size this shell extends from the base of the burning region almost, but not quite, to the XY discontinuity. At limiting amplitude the maximum mass $\Delta M_{\rm CSH}$ of the shell is given approximately (105) by $\log \Delta M_{\rm CSH} \cong -1.835+1.73\ M_{\rm H} -2.67\ M_{\rm H}^2$. The maximum temperature $T_{\rm CSB}^{\max}$ at the base of the shell is another important characteristic that increases with each pulse. In low-mass AGB stars, $T_{\rm CSB}^{\max}$ grows typically from about 2×10^8 K to nearly 3×10^8 K. In intermediate-mass AGB stars, it grows even larger. Very approximately one has, in the locally asymptotic limit, $T_{\rm CSB}^{\max} \cong 2.9 \times 10^8$ K, for $M_{\rm H} \lesssim 0.9$, and $T_{\rm CSB}^{\max} \sim [3.1+2.85\,(M_{\rm H}-0.96)] \times 10^8$ K, for $M_{\rm H} \gtrsim 0.9$. Much work remains to be done to establish the exact relationship between $M_{\rm H}$ and $T_{\rm CSB}^{\max}$, and these expressions are only a rough summary of the results of many different authors for stars of many different total masses and compositions (see 18).

Still another important characteristic is the degree of overlap between successive convective shells. This overlap is illustrated in Figure 3 (104) for the same star described in Figure 2. The shaded regions indicate the presence of convection, and it is evident that the fraction of matter in the second shell that was once in the first shell is $r = 1-\Delta M_{\rm H}/\Delta M_{\rm CSH}$, where $\Delta M_{\rm H}$ is the amount of matter traversed by the hydrogen-burning shell during the interpulse phase. At limiting amplitude, $r \simeq 0.6$–$0.555(M_{\rm H}-0.6)$. For a given star, r decreases with each pulse until limiting amplitude is reached. For example, in a model of mass $M = 0.6$, r takes on values 0.85, 0.80, 0.75, 0.71, 0.67, and 0.65 as pulse number increases from 5 to 10 and $M_{\rm H}$ increases from 0.54 to 0.59 (113).

In concluding this section we comment on a paper by Prialnik et al. (182), which asserts that, as a consequence of diffusion, thermal pulses do not occur. The authors argue that diffusion spreads out composition profiles in both the hydrogen- and helium-burning shells in such a way that not only is the thermal instability damped out, but the two shells remain stationary in mass(!), with hydrogen flowing inward into the H-burning shell and helium flowing outward from this shell into the envelope.

This idea is certainly an interesting one, but the exploration of the idea is seriously flawed. First, effects of thermal, pressure, and gravitational diffusion are ignored, and only the effect of a concentration gradient is explored. This results in a maximal estimation of the rate of diffusion of any species. Second, the time scale for diffusion is stated to be comparable to time scales for changes in composition variables that are due to nuclear reactions. This can be shown to be false. For example, with the diffusion coefficient used by Prialnik et al., the time scale τ_d for diffusion out of the hydrogen-burning shell is very roughly $\tau_d \sim 2.2$

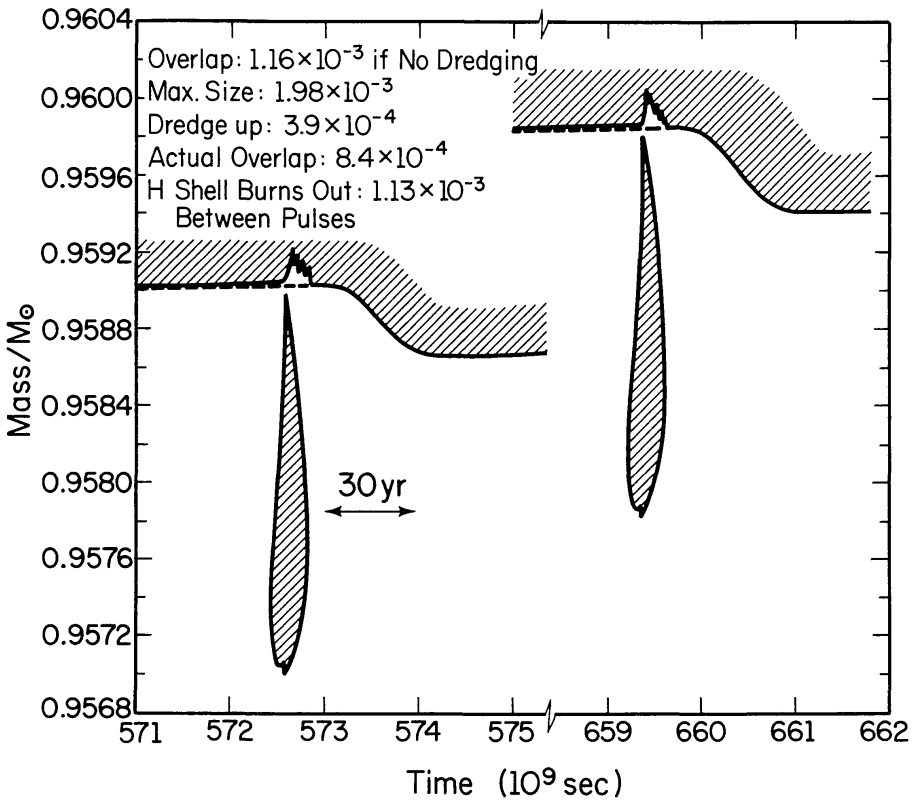

Figure 3 Convective regions during the fifteenth and sixteenth pulses in a model of mass $7M_\odot$ and initial composition $(Y, Z) = (0.28, 0.02)$. Shading indicates where convection occurs, and the dashed lines indicate the location of the hydrogen-helium interface before dredging up begins.

$\times 10^{20}(\delta M_H)^2 R^{-4}\rho^{-1}T_6^{-5/2}$ s, where δM_H is the thickness of the H-burning shell, R is the distance of the shell from the center in solar units, ρ is the mean shell density in g cm^{-3}, and T_6 is the mean temperature in the shell in units of 10^6 K. The time scale for changes in the hydrogen abundance can be measured by $\tau_X \equiv \delta M_H/\dot{M}_H$, where $\dot{M}_H$ is the rate at which the center of the hydrogen-burning shell moves outward in mass during the interpulse phase. Since approximately 6×10^{18} erg are released by the conversion of one gram of hydrogen into helium, it follows from (1.) that $\dot{M}_H \approx 6 \times 10^{-7}$ yr^{-1} $(M_H - 0.44)$ X_e^{-1}, where X_e is the abundance by mass of hydrogen at the surface. From Iben (105), $\delta M_H \cong 2.1 \times 10^{-7}$, 1.8×10^{-6}, and 1.05×10^{-5} for $M_H \sim 1.36$, 1.16, and 0.96, respectively, and, from Iben (113), $\delta M_H \sim 1.2 \times 10^{-4}$ for $M_H \sim 0.6$. Using the values of R, ρ, and T from the last two references to find τ_d, we find $\tau_X/\tau_d \sim 8.3 \times 10^{-3}$, 8.1×10^{-4}, 1.0×10^{-4}, and 7.8×10^{-3} for $M_H \simeq 1.36$, 1.26, 0.96, and 0.6, respectively. Thus, diffusion may definitely be neglected during the major hydrogen-burning phase.

How, then, does one interpret the Prialnik et al. results? They are possibly due to a simple arithmetic error. They are also possibly a consequence of choosing a time step that is comparable with τ_X, rather than at least ten times smaller, as in most previous work. Prialnik et al. are able to find solutions only because the composition changes due to nuclear reactions are calculated implicitly, a procedure that, for large time steps, can produce nonsense. Certainly, the random oscillations in structural quantities that Prialnik et al. find when diffusion is neglected (as well as when it is not) must be due either to the choice of time step, which forces the hydrogen shell to move through a substantial part of its thickness in each time step, or to some other source of numerical noise. They assert that these random oscillations are equivalent to the "minipulses" defined by Becker & Iben (20). This is not true, since minipulses are simply thermal pulses of low amplitude that precede the first "major" pulse, which is defined as the first pulse of sufficient amplitude to generate a convective shell in the helium-burning region. The time between minipulses does not vary randomly but increases uniformly with increasing pulse amplitude.

Finally, Prialnik et al. claim that the manner in which the surface luminosity changes after a pulse varies in an apparently uncontrolled way from one worker to the next, and that their "results, which seem to resolve the controversy, are due to the rigorous evolutionary calculations (without any artificial shifting) of the interflash period." In fact, (*a*) their calculations are more crude (huge time step) and introduce more error than does a shell-shifting technique, and (*b*) the variations from one careful worker to the next are due to different choices in model parameters (M_H, M, etc.); in particular, in *all* models the surface luminosity drops immediately after a pulse, and

whether or not there is a subsequent luminosity peak that exceeds the prepulse luminosity in magnitude depends on the stellar mass (cf. Figures 2 and 4).

2.4 *Synthesis of Major Isotopes During Thermal Pulses*

Since the dominant energy source for a thermal pulse is the triple alpha reaction, it is not surprising that the most abundant element produced in the helium-burning convective shell during a pulse is ^{12}C. The ^{16}O that follows from the reaction $^{12}C(\alpha,\gamma)^{16}O$ is produced at an abundance that is roughly an order of magnitude smaller than the final shell ^{12}C abundance. At limiting amplitude this latter abundance is about 0.2 to 0.3 by mass (e.g. 102, 105, 113). Where helium burning goes to completion, as in matter between the base of the region defined by the convective shell at its maximum extent and the edge of the helium-exhausted core, the final abundances by mass of ^{12}C and ^{16}O are roughly in the ratio 2 to 1, if one adopts the most current estimates (72) of the triple alpha and the $^{12}C(\alpha,\gamma)^{16}O$ reaction rates. However, only matter that at some time resides in the convective shell can make its way to the surface during pulse powerdown.

During the interpulse phase, almost all of the envelope ^{12}C and ^{16}O that enters the hydrogen-burning shell is converted into ^{14}N. As a pulse progresses, the convective shell engulfs the region containing fresh ^{14}N and subsequently, within the convective shell, ^{14}N is converted into ^{22}Ne via the reactions $^{14}N(\alpha,\gamma)^{18}F\,(\beta^{+}\nu)^{18}O(\alpha,\gamma)^{22}Ne$.

Whether or not further nucleosynthesis occurs in the convective shell depends, among other things, on the maximum temperatures reached there and on the duration of the pulse. As already discussed, maximum shell temperatures depend on both $M_{\rm H}$ and on the number of pulses that have occurred prior to the pulse under consideration. Since very-low-mass stars may experience only a few pulses before exhausting their hydrogen, the asymptotic limit in such stars may well not be reached. If it is reached, however, in stars with $M_{\rm H} \cong (0.6\text{–}0.9)$, roughly one percent of the ^{22}Ne in the convective shell experiences the reaction $^{22}Ne(\alpha,n)^{25}Mg$ (18, 113). At the temperatures achieved in the convective shells for stars with core mass larger than $M_{\rm H} \simeq 1$, more than one third of the ^{22}Ne initially in the shell is converted into ^{25}Mg and neutrons, the extent of the conversion increasing with increasing $M_{\rm H}$ (103, 234).

2.5 *The Synthesis of s-Process and Other Neutron-Rich Isotopes*

Our understanding of how *s*-process isotopes are made in the solar-system distribution has evolved over several decades. In the early work of Cameron

(39) and Burbidge et al. (36), the *s*-process isotopes are defined as those produced by neutron capture in an environment of sufficiently low neutron flux that, in most cases, any beta-unstable isotope that is formed will beta decay more rapidly than it can capture a neutron. Cameron (39, 40) identifies two key reactions as primary neutron sources: $^{13}C(\alpha, n)^{16}O$ and $^{22}Ne(\alpha, n)^{25}Mg$. In the following we sometimes refer to these reactions simply as the ^{13}C source and the ^{22}Ne source, respectively. Clayton et al. (45) show that, in order to achieve a solar-system distribution of *s*-process isotopes, it is necessary for different fractions of the matter containing these isotopes to have been exposed to different integrated neutron fluxes, and they find that an exponential distribution of exposures provides a good fit.

Identification of an explicit stellar site for *s*-process nucleosynthesis begins with the thermal pulse calculations of Weigert (253) and Schwarzschild & Härm (223). The Schwarzschild & Härm calculations suggest that, in some stars at least, the helium-burning convective shell might extend outward far enough to ingest proton-rich material, with the reactions $^{12}C(p, \gamma)^{13}N(e^+\nu)^{13}C(\alpha, n)^{16}O$ then providing a source of neutrons. Both calculations demonstrate that successive convective shells partially overlap one another in the mass coordinate. Ulrich (239) shows that this overlap property leads quite naturally to an exponential distribution of exposures, provided a source of neutrons exists that produces roughly the same number of neutrons in each pulse: if r is the fractional overlap of the Nth and the $(N-1)$th convective shells at their maximum extent, then $r^N = \exp(N \log r)$ gives the fraction of matter in the Nth shell that has experienced N neutron exposures, $r^{N-1} = \exp[(N-1) \log r]$ is the fraction of matter that has experienced $N-1$ exposures, and so on. Ulrich goes on to show that, for beta-stable isotopes, $n_{i-1}\sigma_{i-1}/n_i\sigma_i = 1 + \Lambda/\sigma_i$, where isotope i is the neutron-capture progeny of isotope $i-1$, the n's are number densities, and the σ's are neutron capture cross sections at the relevant energies (30 keV). Further, Λ is a universal parameter that is a function of r and of the neutron flux per pulse and that must take on a value in the neighborhood of 4–5 mb if a solar-system distribution is to be achieved.

Subsequently, it has been shown that contact between the helium-burning convective shell and the hydrogen-rich region of the star is inhibited in stars by an entropy barrier (104) and that, in stars for which M_H exceeds about 0.95, the ^{22}Ne source provides a potent flux of neutrons (101, 102, 104, 105). It has been shown further that the light-element neutron-capture progeny of ^{22}Ne and ^{25}Mg filter out most of the neutrons produced and that, to a first approximation, when a substantial fraction of ^{22}Ne is

burned, the universal characteristic Λ is essentially the average (number-weighted) cross section σ_1 for neutron capture on ^{25}Mg and its neutron-capture progeny (103, 234). In the same approximation, the average number of neutrons captured by ^{56}Fe and its neutron-rich progeny is simply the ratio of the average cross section σ_s for neutron capture on ^{56}Fe and its progeny to σ_1. These simple results are primarily a consequence of the fact that the number of neutrons released is identical to the number of fresh light-element filters. By good fortune, average cross sections are such that $\Lambda \cong \sigma_1 \cong (4\text{–}6)$ mb, which is precisely what is required to produce *s*-process isotopes in the solar-system distribution. Similarly, the number of neutrons per ^{56}Fe seed is $\sigma_s/\sigma_1 \sim 3\text{–}5$.

Many details remain to be worked out, but it seems clear that, if real intermediate-mass stars can achieve C-O core masses in excess of 0.9–1.0, they will then produce large quantities of *s*-process isotopes in the solar-system distribution. An example of current activity in the subject is provided by the work of Despain (63), Cosner et al. (52), and Ward (249). Despain shows that, for large (>0.95) core masses, the average neutron flux achieved in the helium-burning convective shells exceeds by several orders of magnitude those values traditionally thought to be an upper limit for the classical *s*-process; he concludes that intermediate-mass stars produce *s*-process distributions that are far from solar and also produce several isotopes that have traditionally been associated exclusively with the *r*-process (neutron capture more rapid than beta decay). However, Cosner et al. show that the time dependence of the neutron flux (decaying exponentially with time) plays a crucial role in determining final abundances and that the net result is still a solar-system-like *s*-process distribution. Most of the glaring departures from the solar-system distribution can be understood if, as suggested by Ward (249), isomeric levels of several relevant nuclei do not thermalize on a time scale short compared with the duration of a pulse. Nevertheless, several isotopes are made that have been traditionally assumed to be produced only in an *r*-process environment. In one sense this is encouraging, since it is really too much to expect that nature would supply only those neutron-capture environments that produce isotopes in two distributions that happen to be convenient for the terrestrial mathematician to reproduce!

In another development, critical neutron-capture cross sections continue to be measured (e.g. 23), and the classical nucleosynthesist's approach is followed whereby the *s*-process distribution is assumed as given and the necessary properties of the environment that produces this distribution are deduced (6, 128). A particularly important demonstration is that, even though the neutron-capture cross section for ^{22}Ne has been found to be an

order of magnitude larger than used in most earlier work, the character of the neutron-capture distribution produced in intermediate-mass stars with $M_H \gtrsim 1\ M_\odot$ is still dominated by captures on ^{25}Mg (6).

The characteristics of neutron-rich isotope distributions formed in the convective shells of AGB stars of small core mass (say, $M_H < 0.8$) will be considerably different from those produced in stars of large core mass. One reason for this is that only a percent or so of the ^{22}Ne formed in the helium-burning convective shell during any given pulse is burned to ^{25}Mg plus a neutron, so that, during any given pulse, the number of neutrons (from this source) captured by ^{56}Fe and its progeny (many of which have been produced during previous pulses) is much less than one. Thus, during early pulses, only the lightest isotopes beyond ^{56}Fe would be formed if ^{22}Ne were the only neutron source.

The primary distinguishing characteristic of neutron-capture nucleosynthesis when M_H is small is that the ^{13}C source may assume major importance (e.g. 214). The fact that, in model AGB stars with large M_H, *s*-process isotopes are produced in the solar-system distribution by the ^{22}Ne source suggests that the ^{13}C source is not important in such stars. However, since the ^{22}Ne source is so weak in model stars with small M_H, and since the observations show that AGB stars of small M_H produce neutron-rich isotopes (see Section 7), it is reasonable to suppose that some mechanism exists for activating the ^{13}C source in these stars.

Ulrich (239) and Scalo & Ulrich (217) have suggested a form of "plume" mixing that may cause small amounts of hydrogen to be mixed into the helium-burning convective shell during a pulse. Sackman et al. (211) have proposed much more extensive injections of hydrogen into the helium-burning region, but the net result is the same: ^{13}C is formed and acts as a source of neutrons. Unfortunately, the extent of the envisioned mixings cannot be determined from first principles, and we can therefore say no more about them.

A potentially more promising way of activating the ^{13}C source is by diffusive mixing during the interpulse phase. We have shown that diffusion is too slow to affect the hydrogen profile during the long quiescent hydrogen-burning phase. However, during the extended post-flash dip, when hydrogen burning is extinct, the diffusion time at the XY "discontinuity" may be comparable to the duration of the dip. Hence, hydrogen may diffuse inward and ^{12}C diffuse outward, transforming the XY discontinuity into a more complex profile, with a trace of hydrogen being present at the base of the profile where there is a very large abundance of ^{12}C. When hydrogen reignites, the hydrogen over the inner portions of the profile will be captured by ^{12}C to form ^{13}C (predominantly). The ^{13}C-enriched region will shortly be left behind as hydrogen burning progresses

outward. Finally, when the next thermal pulse occurs and convection engulfs the enriched region, the ^{13}C source will be activated. How large this effect will be has yet to be determined (but see 113 for preliminary estimates).

A still more promising sequence of events that may bring a large amount of ^{13}C into the helium-burning convective shell during pulse peak is initiated by semiconvective mixing occurring during the third dredge-up phase (see Section 2.6) following the peak of the preceding pulse (117, 118). This mixing carries hydrogen downward into the ^{12}C-rich region that has been produced during pulse peak. At the end of the mixing episode, there exists a fairly extensive region over which the number abundance of ^{1}H is comparable to or less than the number abundance of ^{12}C. When this region heats up enough to reignite hydrogen burning, the principal product is ^{13}C at an abundance greater than the abundance of ^{14}N. When the next pulse occurs, the ^{13}C-rich, ^{14}N-poor region is swept into the helium-burning convective shell and neutrons are produced copiously [in the example studied in (118), 26 neutrons are produced for every ^{56}Fe seed nucleus], and ^{14}N cannot prevent significant neutron capture by heavy-element seeds.

The precise amount of ^{13}C formed in this way that ultimately acts as a neutron source in any given pulse is expected to be a strong function of M_H and of the number of pulses that has preceded the given pulse. Since the sky abounds with low-mass AGB stars with different M_H and M, each of which has experienced a different number of pulses, one must expect a very wide variety of neutron-rich isotopic distributions to be formed in the convective shells of these stars during pulses. Furthermore, the neutron densities N_n that are formed are much larger than is compatible with the production of a neutron-rich isotopic distribution that resembles the solar-system *s*-process distribution (118), and the variability of N_n with pulse number and M_H will add still further to the diversity of created distributions.

2.6 *The Third Dredge Up*

From the standpoint of an external observer, the formation of carbon and of neutron-rich isotopes in the helium-burning region of AGB stars is interesting only if the nucleosynthetic products are somehow mixed to the surface of the star and/or in some fashion expelled into the interstellar medium.

One of the most straightforward ways of mixing to the surface follows naturally from solutions of the standard equations for quasi-static evolution. Near the peak of every thermal pulse, the nuclear energy that has been and is being converted locally into thermal energy is partially used up in expanding matter outward against gravity; matter at the hydrogen-helium interface and beyond is propelled outward to lower densities, and

temperatures and hydrogen burning is temporarily extinguished. Part of the stored energy also diffuses outward; the consequent increase in the local energy flux, coupled with the dropping temperature, causes the radiative gradient to exceed the adiabatic gradient at positions successively closer in mass fraction to the helium-burning region. Matter successively closer in mass to the region that has experienced extensive processing via helium burning and neutron capture is mixed outward toward the surface. The closest approach of the base of the mixing region to the region of highly processed matter is a function of pulse amplitude and is therefore also a function of both M_H and M.

For stars of sufficiently large core mass ($M_H \gtrsim 0.7$) and sufficiently large total mass ($M > 2$), it has been established for some time that, as pulse amplitude approaches limiting strength, the base of the convective envelope extends into the region containing highly processed material (18, 85, 101, 102, 104, 171, 209, 210, 229, 266, 268, 271). The resulting mixing of freshly synthesized ^{12}C and neutron-rich isotopes to the surface is called the "third dredge-up" process. The occurrence of this dredge-up process and the fact that its importance grows with pulse number are illustrated by Figures 2 and 3. If one defines ΔM_{dredge} as the mass of freshly processed matter that is mixed throughout the envelope, then the ratio $\lambda = \Delta M_{dredge}/\Delta M_H$ parameterizes the extent of dredge up. For core masses in excess of 0.96 $M_\odot$, λ is on the order of 1/3 (85, 104).

The situation with regard to stars of small total mass and small core mass is just now becoming clarified. No studies find dredge up for core masses as small as $M_H = 0.6$ (88, 89, 113, 208, 209, 218, 223, 266, 268). Wood (266, 268) shows that whether or not dredge up occurs depends not only on core mass M_H, but also on the total mass M, the metallicity Z, and the treatment of envelope convection (more precisely, on ℓ/H in the crude but standard treatment of convection). In particular, the minimum mass for dredge up decreases with (*a*) increasing ℓ/H, (*b*) increasing M, and (*c*) decreasing Z. Wood finds that, even for the lowest values of Z studied ($Z \gtrsim 0.001$), dredge up does not occur for core masses smaller than $M_H \sim 0.67$, a value too large to be consistent with the observed properties of carbon stars in the Magellanic Clouds (see Section 7). Another study (113) finds that, for $M \sim 0.7$, dredge up does not occur until M_H is considerably larger than 0.6; however, for matter in carbon-rich regions, this study makes use of opacity formulae that are valid only for temperatures in excess of 10^7 K, whereas, once M_H reaches about 0.6, matter at the outer edge of the carbon-rich zone formed during pulse peak is propelled out to low enough temperatures ($< 3 \times 10^6$ K) that carbon begins to recombine. The attendant increase in opacity might be expected to accelerate the expansion and cooling that promotes the inward motion of envelope convection (194) and/or to lead to

convective motions that carry carbon closer (in mass) to the surface, where it may more easily be dredged up (113).

In fact, when appropriate opacities are used, both of these effects occur (117, 118). Once the temperature at the outer edge of the carbon-rich zone drops below about 5×10^6 K, semiconvective mixing carries carbon outward in mass (117) and the degree of expansion and cooling is increased to such an extent that dredge up occurs for much smaller values of M_H and M than would otherwise be the case (118). For example, for $Z = 0.001$, $\ell/H = 1.5$, and $M = 0.7$, it is found that dredge up occurs when $M_H \cong 0.61$ (compared with the value $M_H \cong 0.7$ when incorrect carbon opacities are used). That Wood (266, 268) does not obtain similar results, despite the use of presumably correct opacities, may be due to the use of insufficiently small time steps during thermal pulses, leading to too small peak helium-burning luminosities [L_{He} typically smaller by an order of magnitude than found by (113)] and consequently to a less dramatic expansion and cooling phase following pulse peak.

2.7 *Nucleosynthesis in the Envelope Between Pulses*

What happens to ^{12}C once it is brought to the surface? In the first paper describing the third dredge-up process in detail (102), it is shown that, for $M = 7$, $M_H = 0.96$, $Z = 0.02$, and $\ell/ = 1.0$, ^{12}C is rapidly converted at the base of the convective envelope during the interpulse phase, first into ^{13}C and then into ^{14}N in such a way that the final surface ratio of $^{12}C/^{13}C$ approaches its equilibrium value (~ 3.5). On decreasing ℓ/H to 0.7, the temperature at the base of the envelope drops sufficiently that the destruction of ^{12}C effectively ceases. Thus, whether or not an intermediate-mass AGB model star becomes a carbon star ("C" star, C > O) depends critically on the treatment of envelope convection, as well as on the efficiency of the third dredge-up process. We henceforth refer to nuclear processing at the base of the convective envelope as the envelope-burning (EB) process.

Renzini & Voli (197) have shown that the efficiency of the EB process depends very strongly on the total mass of the star. In particular, they have shown that, for every choice of composition and ℓ/H, there is a minimum stellar mass M_{EB} below which the conversion of ^{12}C to ^{14}N does not occur at all. For masses in the range M_{EB} and $M_{EB} + \Delta M_{EB} \sim 1.25\ M_{EB}$, the conversion proceeds at a rate that increases very steeply with M, and for M larger than this, conversion occurs at a steady rate. For $Z = 0.02$, M_{EB} decreases from 6.8 $M_\odot$ to 4.0 $M_\odot$ as ℓ/H is increased from 1.0 to 1.5. At this point, it is important to emphasize that the normalization of the convective flux may be different from one study to the next. For example, Renzini & Voli (197) find significant envelope burning in a 7-$M_\odot$ model only for

"ℓ/H" $\gtrsim 1.2$, whereas Iben (102) finds it for "ℓ/H" $= 1.0$. This means simply that the normalization factor in Renzini & Voli is different from that in the Iben program.

Renzini & Voli have also shown how for $M_i > M_{EB}$, the EB process delays the time at which the star first becomes a C star. In the most massive AGB stars the EB process can of course even prevent the formation of C star characteristics. Moreover, those stars with $M_i > M_{EB}$ that succeed in becoming C stars (in spite of the EB process) are greatly enriched in ^{13}C and are expected to exhibit spectra with strong ^{13}C isotopic features. Obviously, all those stars that become C stars will have to pass through an S star phase (C $\simeq$ O). Finally, those stars with $M_i > M_{EB}$ that fail to become C stars, but that instead develop high surface N abundances, should show strong ^{12}CN and/or ^{13}CN features.

All in all, when both the third dredge up and the EB processes are simultaneously active, enormous variations in the surface abundances are generated in the course of the AGB evolution of a given stellar model, with extremely different abundance patterns being successively shown by models of different initial mass. To give an idea of the ranges, the ratios C/O and N/O can vary by factors of ~ 60, and the product $^{13}C \times N$ can vary by a factor of ~ 500.

2.8 *Variation of Global Characteristics*

In order to make meaningful comparisons with the observations, as is attempted in Section 7, it is important to be aware of the time dependence of the luminosity. Luminosity varies on four major time scales: one associated with dynamical oscillations of the envelope (as in Mira variables); one associated with the instability that initiates thermal pulses; a thermal relaxation time scale characterizing the return to a quiescent phase following a thermal pulse; and a final time scale associated with the build up of conditions that lead to a helium-burning runaway. The first time scale is measured by the time required for a sound wave to traverse the envelope (hundreds of days to a few years). The second time scale is measured roughly by the time required for nuclear energy to double the thermal energy content in the helium-burning region (a few years or less). The third and fourth time scales are comparable and vary pronouncedly with core mass (from a few times 10^5 yr when $M \cong 0.6$ to less than 30 yr when $M \cong 1.4$).

We do not discuss here dynamical pulsations (see, for example, 70, 267) but instead concentrate on those variations in surface luminosity that are found in the quasi-static approximation (dynamical pulsations suppressed). The qualitative features of the L and T_e variations shown in Figure 2 are characteristic of all AGB models with a large envelope mass. In particular, changes in surface characteristics are modest ($\Delta \log L \sim 0.2$) and are

confined to about twenty percent of the interpulse period. During the rest of the interpulse period, L grows according to Equation 1′.

In contrast, an AGB star with small envelope mass experiences much more dramatic surface changes, and Equation 1.′ is an inapplicable and misleading estimate of surface luminosity. Figure 4 describes a model characterized by $M = 0.6$, $M_H \cong 0.53$–0.60, $Z = 0.001$, and $Y = 0.25$ (113) and exhibits features already present in the work of other authors. In particular, the extremely rapid drop in luminosity that terminates the interpulse phase has been found by all authors, and the sharp rise in luminosity that immediately follows the initial dip has been found by all authors who have studied pulses with $M_e = (M - M_H) \gtrsim M_H$. The sharp

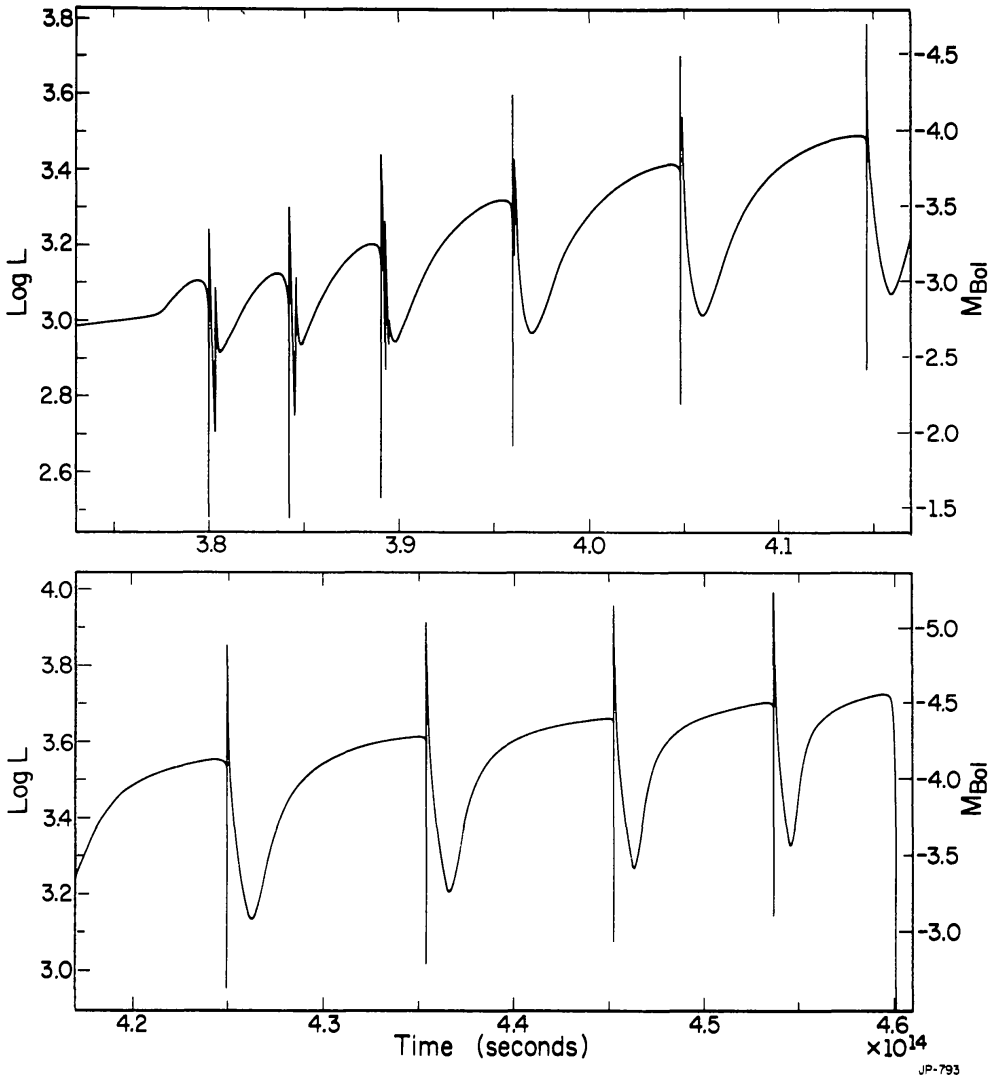

Figure 4 Surface luminosity (in solar units) as a function of time in a model of mass 0.6 $M_\odot$, and initial composition $(Y, Z) = (0.25, 0.001)$.

dip in luminosity is related to the extinction of hydrogen burning and to a dramatic decline in L_{He} brought about by the expansion and cooling engendered by the rapid injection of a large quantity of nuclear energy during pulse peak; the sharp rise is due to the emergence of energy from the helium-burning region and to the increase in L_{He}, which occurs as the lower portion of the helium-burning layer recontracts and reheats. It is during the sharp rise that convection extends inwards toward the highly processed region. For the earliest pulses, the light curve exhibits further rapid changes following the first dip and first rise.

The sharp dips and rises present in the light curves of low-mass models are much less pronounced in models of large mass, simply because a large envelope tends to damp out changes initiated in the burning regions. In particular, in models of large envelope mass ($M_e > 2$, say) the surface luminosity during the first (and only) rapid postflash rise does not reach as high a value as the luminosity prior to the initiation of the pulse.

Wood & Zarro (271) point out that the rates of change in (dynamical) pulsational period that are appropriate to the phase during and immediately following the first sharp rise are consistent with the rates at which periods of several Miras (R Hya, R Aql, and W Dra) are actually observed to change. This consistency might be interpreted as direct observational evidence for the occurrence of thermal pulses in low-mass stars.

Of course, the probability of finding a low-mass AGB star in a phase of rapid change ($\Delta t_{rapid} \sim$ few $\times$ 100 yr vs. $\Delta t_{ip} \sim$ few $\times 10^5$ yr) is very small and, for most purposes, more relevant characteristics of the light curve are the magnitude and duration of the extended postflash dip (defined in Section 2.3). During the first part of this dip, $L \sim L_{He}$; when L reaches a minimum, $L_{He} \sim L_H$ and $L \sim L_{He} + L_H$; as L climbs back to the next prepulse maximum, $L \sim L_H$. We repeat that, for stars with large envelope mass, the magnitude of the dip is about $\Delta \log L \sim 0.2$ and its duration is about $\Delta t_{dip} \sim 0.2\ \Delta t_{ip}$. In stars with low envelope mass, $\Delta \log L \sim 0.4$ and $\Delta t_{dip} \sim 0.4\ \Delta t_{ip}$. For a star of large envelope mass, the surface luminosity during eighty percent of the interpulse phase (after recovery from the dip) is given by Equation 1′. For a star of small envelope mass, it is only toward the very end of an interpulse phase that the luminosity approaches the value given by Equation 1.

In Figure 5 we show the evolution in the H-R diagram of the 0.6-$M_\odot$ model whose light curve is given in Figure 4. The locus of zero-age horizontal branch models (119) and the blue edge for pulsation in the fundamental mode for $M = 0.6$ (238) are shown, as well as rough evolutionary tracks for intermediate-mass stars during the core hydrogen- and helium-burning phases (22). The figure caption provides a detailed description.

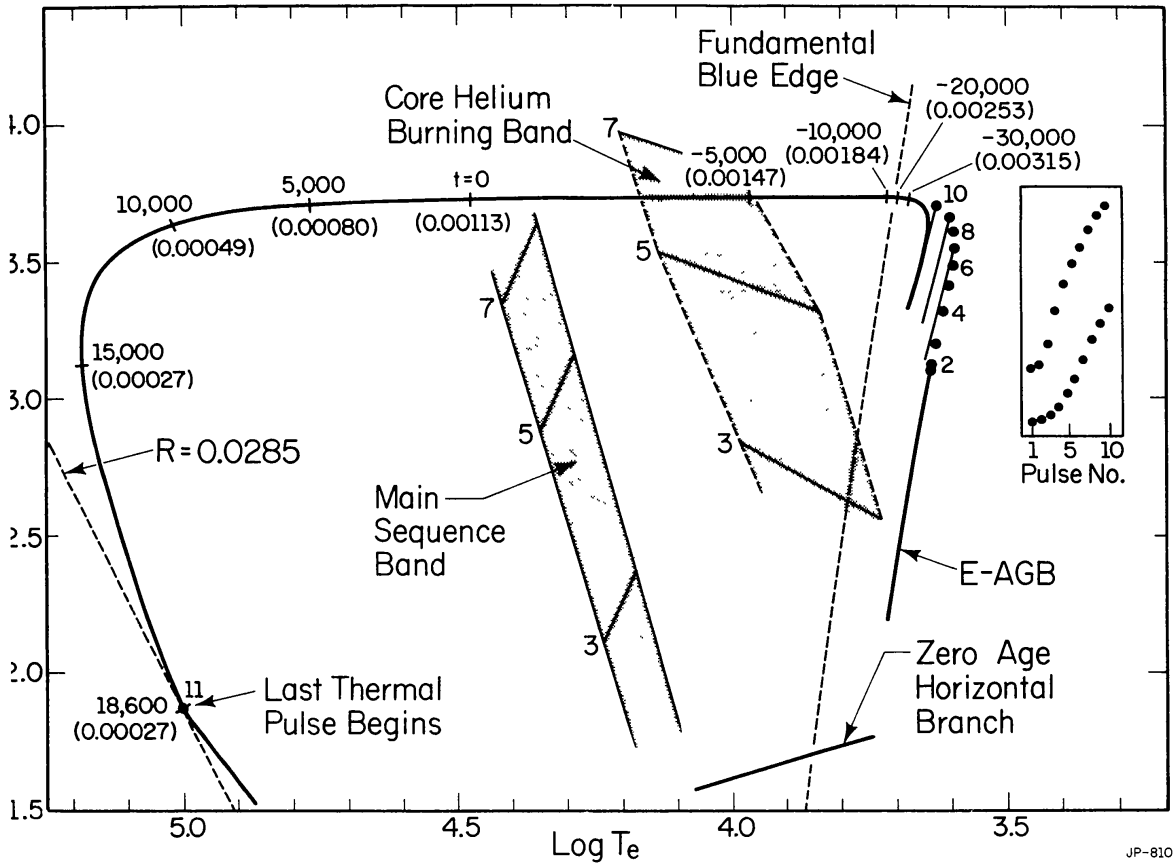

Figure 5 Evolutionary track in the H-R diagram of an AGB model of mass $0.6M_{\odot}$, initial composition $(Y, Z) = (0.25, 0.001)$. After burning helium in its core on the horizontal branch, the model arrives on the E-AGB to burn helium in a shell; the hydrogen-burning shell is extinguished. The E-AGB phase is terminated when hydrogen reignites and thermal pulsing begins. The location of the model at the start of each pulse is indicated by heavy dots. Excursions in the H-R diagram during the extended postflash dip and recovery period are shown for pulses 7, 9, and 10. Dots in the panel in the extreme right-hand portion of the diagram describe the excursion in luminosity during extended dips for all pulses that occur on the AGB. Evolution time ($t = 0$ when $T_e = 30{,}000$ K) and mass in the hydrogen-rich envelope (in parentheses) are shown at various points along the track leaving the AGB after the tenth pulse. Time is in yr, and M_e and R are in solar units. A line of constant radius passes through the location of the beginning of the eleventh pulse when the model has become a hot white dwarf. The dashed line is a blue edge for pulsation in the fundamental mode for a model of mass $0.6M_{\odot}$ and $(Y, Z) = (0.25, 0.001)$. Shown for orientation purposes are rough evolutionary tracks during core hydrogen- and core helium-burning phases for $(Y, Z) = (0.28, 0.001)$ and masses 3, 5, and $7M_{\odot}$.

3. MASS LOSS AND ENVELOPE EJECTION IN AGB STARS

AGB stars lose mass through stellar winds, many undergo radial pulsations, and some may eventually eject most of their residual H-rich

envelope through a quite fast mass loss process thought to be responsible for the formation of planetary nebulae (= PNe, singular = PN). These processes cannot at present be calculated from first principles, and their magnitudes can be ascertained only by analysis of observational features. They are, however, of unquestionable importance for the evolution of AGB stars.

3.1 *Stellar Winds*

Several observational lines of evidence indicate that red giants and supergiants support stellar winds with mass loss rates (MLRs) ranging from a detectability lower limit of $\sim 10^{-8}\, M_\odot\ \mathrm{yr}^{-1}$ to some $10^{-5}\, M_\odot\ \mathrm{yr}^{-1}$ [for a recent review, see (186)]. The physical nature of the mechanism(s) driving the winds remains substantially obscure (cf. 41, 43), in spite of the variety of theoretical models thus far proposed.

Reliable MLR determinations are restricted to a few stars, mainly wide binaries where the red-giant circumstellar envelope produces typical absorption features in the spectrum of a warmer companion (cf. 186). Reimers (184, 185) has proposed an empirical expression relating the MLR to basic stellar parameters:

$$\dot{M} = -4 \times 10^{-13}\, \eta L/gR, \qquad 2.$$

where $\dot{M}$ is in units of $M_\odot\ \mathrm{yr}^{-1}$, and luminosity L, surface gravity g, and radius R are in solar units. The parameter η is of the order of unity and is uncertain by perhaps a factor of 3; thus, $1/3 \lesssim \eta \lesssim 3$. The Reimers parameterization of the MLR has been widely used in conjunction with evolutionary calculations (e.g. 21, 86, 109, 111, 120, 155, 187, 188, 191, 192, 197, 213, 218). Very sharp limits on the value of η in Population II red giants are set by the distributions in the H-R diagram formed by stars in galactic globular clusters ($\eta \simeq 0.40 \pm 0.04$), while for intermediate-mass stars it is not easy to set equally stringent limits (187, 192). We emphasize that (2.) has been derived from a sample of stars that does not include very-metal-poor stars, large-amplitude red variables (Miras), or carbon stars. Thus, the Z-dependence of the MLR remains empirically indeterminate, although for galactic globular cluster stars the Z-dependence of the MLR must be rather mild, otherwise the correlation between horizontal branch morphology and Z would be exactly opposite to that observed in the clusters (192).

The MLR for an individual AGB star, if given by (2.), increases with time, reaching a maximum at the end of the star's AGB phase. This maximum MLR is shown in Figure 6 as a function of M_i for two values of η and for both "Case A" and "Case B" (see Section 3.2 for the definition of these two cases). The stellar model ingredients necessary for the construction of Figure 6 are described in Section 4. Note that there is an absolute maximum

to the MLR, which occurs for an initial mass $M_i = M_w$. For $M_i < M_w$, the wind "evaporates" the hydrogen-rich envelope before the mass of the C-O core reaches the Chandrasekhar limit; for $M_i > M_w$, the C-O core reaches the Chandrasekhar limit and the star explodes, thus terminating the AGB phase.

Many AGB stars become carbon stars, and the surface abundance of carbon not locked up in CO (hereinafter called "excess" carbon) may reach quite high values. The structure of both the atmosphere and the circumstellar envelope are probably greatly affected by the appearance of excess carbon (through molecular blanketing and formation of carbonaceous grains), and it is not yet clear what effect these variations will have on the MLR. Until accurate MLR determinations for normal carbon stars

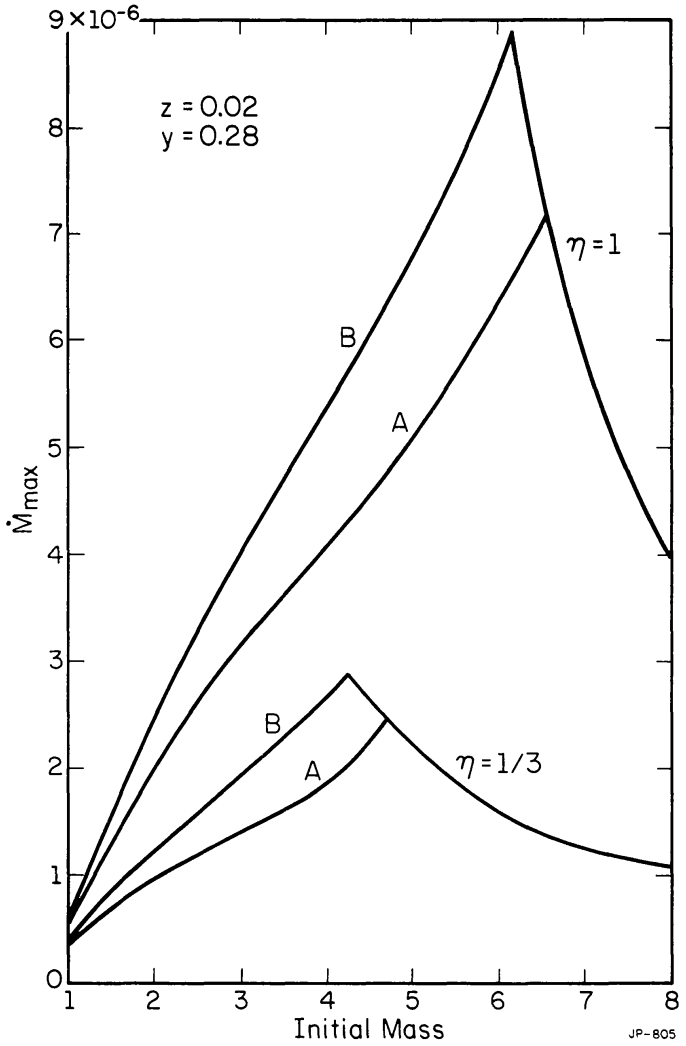

Figure 6 The maximum wind MLRs, when $L = L_{max}$, are shown as a function of the initial mass M_i for two values of η and for $b = 1$ "Case A" and $b = 1/2$ "Case B."

become available, there is no guarantee that (2.) can be correctly applied to both oxygen-rich stars and C stars.

Moreover, most AGB stars pass through a phase of large-amplitude radial pulsation, and the interaction of envelope pulsation with the wind may significantly enhance the MLR, as suggested by recent theoretical models (262, 265). The large MLRs determined for some type II OH/IR Miras also seem to support this possibiliiy (cf. 14, 15, 62, 67, 122, 254).

3.2 *Envelope Ejection From AGB Stars and the Termination of the AGB Phase*

The idea that planetary nebulae are ejected from red-giant stars was first suggested by Shklovski (225). Before stellar winds were recognized as important, attempts at identifying the physical mechanism responsible for envelope ejection focused on large-scale envelope instabilities, which operate on a dynamical time scale (e.g. 149, 172). Subsequent hydrodynamical studies refined and developed these early suggestions, but they did not achieve full quantitative reliability, the main uncertainties coming from (*a*) the adopted relationship between T_e, L, M, and composition, (*b*) the treatment of superadiabatic, time-dependent convection, and (*c*) atmospheric (molecular) opacities.

Since there is now overwhelming evidence that most red giants are losing mass through a relatively quiet wind, one can legitimately raise the question as to whether a more violent envelope ejection is actually required. In fact, evolutionary calculations show that, once their envelope mass drops below a critical value ($\ll \Delta M_H$; cf. 168), AGB stars will transform into condensed objects characterized by the high effective temperatures typical of PN nuclei, irrespective of the particular process responsible for the envelope reduction. One might therefore conjecture that planetary nebulae represent normal red giant wind material, excited by the hot post-AGB remnant (137–140).

However, there is an indirect argument suggesting that, although PNe may indeed be produced by a continuous wind, the strength of this wind must be considerably larger than is given by (2.). From estimates of the mass, radius, and expansion velocity of a PN, one may derive a lower limit for the MLR during PN formation (192, 193, 197). This lower limit is typically of the order of several $10^{-5}\ M_\odot\ \mathrm{yr}^{-1}$, thus exceeding by at least a factor of 10 the MLR predicted by (2.) for stars approaching the end of the AGB phase (cf. Figure 6). In the well-studied case of the PN K648 in the globular cluster M15, the MLR of the process that produced the nebula had to exceed by about 300 times the highest possible MLR of the normal wind in Population II AGB stars.

Since its physical nature is controversial, it has been suggested (192, 193)

that this very efficient mass loss process be provisionally called a *superwind*, to distinguish it clearly from the *normal* wind, which is described by (2.) and which dominates during most of the AGB phase. In this picture, low- and intermediate-mass stars ascend the AGB losing mass according to (2.), and, when a critical luminosity $L = L_{PN}$ (function of mass and composition) is reached, most of the residual H-rich envelope is ejected on a time scale very short compared with the previous AGB lifetime.

Hydrodynamical models of AGB stellar envelopes suggest that the superwind is triggered by the modal switch from overtone to fundamental pulsation, and that it consists of a series of discrete ejections repeating every few tens of pulsation periods (237, 264). At this rate, complete envelope removal should occur in about 1000 years, with average MLRs ranging from $\sim 10^{-5}\ M_\odot\ \mathrm{yr}^{-1}$ up to $\sim 10^{-3}\ M_\odot\ \mathrm{yr}^{-1}$, depending on the initial stellar mass. An AGB star undergoing such a process should be imbedded in a dusty and optically thick circumstellar envelope (optical depth in the visual up to about 100) and appear as a powerful IR source, with luminosity in the range from a few to 50,000, temperature as low as 100–150 K, and a typical linear dimension of $\sim 10^{16}$ cm (192). IR sources (50, 51, 61, 161, 183, 246) that are without any optical counterpart are the most obvious candidates for this type of object. Similarly, OH/IR sources without optical counterparts are also equally good candidates (14, 15, 62, 68), and the recent discovery in these objects of (nearly) periodic IR variations (68) strengthens such an interpretation. The common occurrence of very long periods of up to 4–5 yr (see also 93), may indicate that the imbedded stars are pulsating in the fundamental mode (cf. 166). Moreover, the expansion velocities of these CS envelopes, as judged from the separation of the 1612-MHz OH maser peaks, often approach or exceed 20 km s^{-1}, the typical expansion velocity of PNe.

Since model fundamental pulsators do not reach a limit cycle (see 68, and references therein), the modal-switch argument suggests that Mira variables are overtone pulsators. However, the pulsational mode of Miras has not yet been unambiguously identified. For example, Hill & Willson (94) and Willson (260) argue that Miras pulsate in the fundamental, and they offer another interpretation of the superwind as being due to atmospheric shocks produced by the pulsation itself (261, 262). Most Miras seem to have MLRs around $10^{-6}\ M_\odot\ \mathrm{yr}^{-1}$ (274, 275), a value consistent with the normal wind described by (2.), but some type II OH/IR Miras apparently support much stronger winds (see Section 3.1 and 254) and the transition to the superwind regime may have already occurred in such objects.

It follows that the identification of the pulsational mode of Miras bears directly on our understanding of the physical nature of the superwind, and further investigations are most welcome. More extensive grids of pulsating

model red-giant envelopes are required (see 73 for the latest developments), while crucial observations that may help in deciding the issue are needed of Miras with known distances, particularly those in the Magellanic Clouds (cf. 71, 269).

Another complication arises if an AGB star is also a carbon star in which the carbon excess is continuously increasing. It could be that the increase in excess carbon will cause an increase in the stellar radius, in turn triggering an early switch to the superwind regime; or, carbon-rich grains could suddenly condense near the photosphere, causing a catastrophic increase in the MLR due to radiation pressure (65). That excess carbon contributes to the development of a superwind seems clearly established by the observations of Knapp et al. (132).

The IR source IRC + 10216, optically known as the carbon star CW Leo, has received much attention in recent years. The very high MLR of $\sim 10^{-4}$ $M_\odot$ yr^{-1} reported for this object (Knapp 1979, referred to in 275, 132; see also 203, 248) indicates that CW Leo is in a superwind regime. Moreover, the detailed light curve of this star is highly reminiscent of the light curve of model fundamental pulsators, even to the extent that the amplitudes of both light curves increase at almost exactly the same rate (compare Figure 4 in 263 with Figure 27 in 264 or with Figure 12 in 237). If this interpretation is correct, CW Leo should experience a major mass ejection in just a few pulsation periods from now, that is, within 10 years or so!

Further extensive IR and microwave observations of AFCL and OH sources should eventually clarify the physical nature of the superwind and establish for which critical combination of the basic stellar parameters (L, R, M, and surface composition) the transition to the superwind regime actually takes place. Analysis of a selection of galactic stars that exhibit high mass loss rates and for which distances may be estimated (e.g. from the samples of 15, 132) may provide a good beginning (see 62). In the meantime, evolutionary model calculations for AGB stars have used semiempirical determinations of $L_{\rm PN}(M)$ (21, 109, 120, 180, 197, 270), but the adopted function $L_{\rm PN}(M)$ must still be regarded as very tentative.

Thanks to the luminosity-core-mass relation for AGB stars, the function $L_{\rm PN}(M)$ translates into a functional relationship between the envelope mass at ejection and the core mass, $M_{\rm PN}(M_{\rm H})$. During AGB evolution, $M_{\rm H}$ increases and the envelope mass $M_{\rm e}$ decreases. Once $M_{\rm e}$ falls below $M_{\rm PN}$, the envelope is assumed to be instantaneously ejected. The expression $M_{\rm PN}(M_{\rm H}) = b(1.69 - 8.09M_{\rm H} + 11.69M_{\rm H}^2 - 4.34M_{\rm H}^3)$ (197) nearly coincides with the functions used by others (120, 270) for $M_{\rm H} \geqq 0.8$ and $b = 1$; for $M_{\rm H} = 0.5$, it gives $M_{\rm PN} = 0.02$, thus fitting the case of PN K648 in M15, whose mass is particularly well determined (176). The parameter b is used to investigate the sensitivity of the results to the adopted value of $M_{\rm PN}$. Renzini

& Voli (197) have used two values of b (1 and 1/2), respectively called "Case A" and "Case B."

4. SYNTHETIC AGB EVOLUTIONARY MODELS AND THEIR USE

In order to compare the consequences of theoretical AGB evolution with the observations, it is necessary to have some first-order idea of the entire AGB evolutionary history of stars as a function of M_i. The number of thermal pulses that an AGB star experiences ranges from a few dozen for $M_i \sim 1$, up to about 9000 for a star whose core mass reaches the Chandrasekhar limit ($M_i \gtrsim 4$–5). Since the calculation of one thermal pulse and the following interpulse phase requires about 2000 models, it would be tremendously time consuming to follow the entire evolution by brute force. In practice, brute force is used only for those low-mass stars that experience only a modest number of pulses (e.g. 87, 113, 218, 223). On the other hand, most relevant stellar characteristics during the pulse portion of the AGB phase depend primarily on just the core mass M_H in a fashion that can be approximated by analytic formulae; the effects of mass loss processes occurring during the AGB phase can also be parameterized. Using these algorithms, the gross characteristics of the AGB evolution of a star of specified initial mass and composition can be rapidly computed for any choice of the mass loss parameters (η and M_{PN}) and of the mixing–length parameter ℓ/H controlling the efficiency of the EB process (120). However, the treatment of this process cannot be conveniently parameterized, and envelope integrations are required (197). We call the results of such calculations "synthetic" AGB evolution. They provide, among other things, the mean time dependence of several observable quantities, including L, T_e, $\dot{M}$, and the surface abundances of elements such as ^{4}He, ^{12}C, ^{13}C, ^{14}N, ^{16}O, and s-process isotopes.

4.1 *The Final Mass and the Maximum Initial Mass for White Dwarf Progenitors*

As an AGB model evolves, the mass M_e of the envelope above the hydrogen-burning shell decreases both as a consequence of hydrogen burning at the base and of mass loss at the outer edge of the envelope. When M_e drops below M_{PN}, the envelope is ejected, marking the termination of the AGB phase, and the remnant evolves toward its final white dwarf (WD) configuration. If, before this happens, M_H reaches a value of about 1.4, carbon is ignited in the degenerate C-O core and a supernova event follows (see Section 5). We define M_w as the maximum initial mass for which the final product of evolution is a C-O WD. For $M_i < M_w$, the mass of the WD

remnant M_f (equal to M_H at final envelope ejection) depends primarily on M_i and η, while the dependence on M_{PN} is rather slight. A quite accurate fit to the numerical results is $M_f \cong 0.53\ \eta^{-0.082} + 0.15\ \eta^{-0.35}\ (M_i - 1)$. Although this equation has been derived from models with $(Y, Z) = (0.28, 0.02)$, it is quite adequate for other compositions as well; for lower values of Z, M_f increases by only a few percent. Setting $M_f = 1.4$, we find $M_w \cong 1.0 + 9.33\,\eta^{0.35} - 3.53\,\eta^{0.27} + 0.8\,(b - 1.0)$, where the dependence on b (for $b \gtrsim 1$) has also been included. For $(\eta, b) = (1/3, 1)$, one has $M_w = 4.7$, while for $(\eta, b) = (1/3, 1/2)$, $M_w = 4.3$. For $(\eta, b) \cong (2, 1)$ one has $M_w = \sim 8$, which means that, for $\eta \gtrsim 2$, essentially all intermediate-mass stars produce WD remnants, and carbon is never ignited in them. However, if $\eta \gtrsim 0.6$, Population II red-giant stars would lose their envelopes before igniting helium in the core, and a horizontal branch would not exist (193). Similarly, for $\eta = 2$ and solar composition, the "clump giant" phase is absent for $M_i \gtrsim 1.15$. Therefore, the mere existence of horizontal branches and clump giants argues against such a high value of η.

4.2 *Maximum Luminosities and Ages of AGB Stars*

By inserting $M_H = M_f$ and $M = M_f + M_{PN}(M_f)$ (the actual mass at the onset of the superwind) in (1′.) one obtains, for $M_i < M_w$, an estimate of the maximum luminosity reached along the AGB: $L_{max} \cong 4.38 \times 10^4\ (M_f - 0.44)\,[M_f + M_{PN}(M_f)]^{0.19}$. In Figure 7, L_{max} is plotted vs. M_i (upper scale) for various values of η. The time required to evolve from the zero age main sequence to the AGB is reported in the lower scale of this figure as Age [estimated from Becker (16) and Rood (206) for $Y = 0.28$, $Z = 0.02$]. Since the AGB lifetime is much, much smaller than the main sequence lifetime, it is clear that, in a stellar system with a well-populated AGB, the determination of L_{max} (from the brightest AGB stars) can be used to estimate the initial mass of stars now on the AGB, and, therefore, the age of the system (or of its youngest stars).

The line marked "L_F" in Figure 7 represents the luminosity at the first thermal pulse; therefore, the TP-AGB phase of evolution is bounded by L_F and L_{max}. Also shown are the maximum stellar luminosity reached during the core helium-burning phase by intermediate-mass stars (18, 20) and the luminosity at helium ignition in the core for low-mass stars (231). Low-mass models spend most of their helium-burning lifetime at much lower luminosities ($\log L \sim 1.7$).

Quite a few stars can actually lie between the location of core helium-burning models and line L_F. These are stars in the E-AGB phase. Because of the much lower luminosities during the E-AGB phase than during the TP-AGB phase, mass loss along the E-AGB phase may be neglected in most cases, especially when the lifetime during the E-AGB phase is shorter than

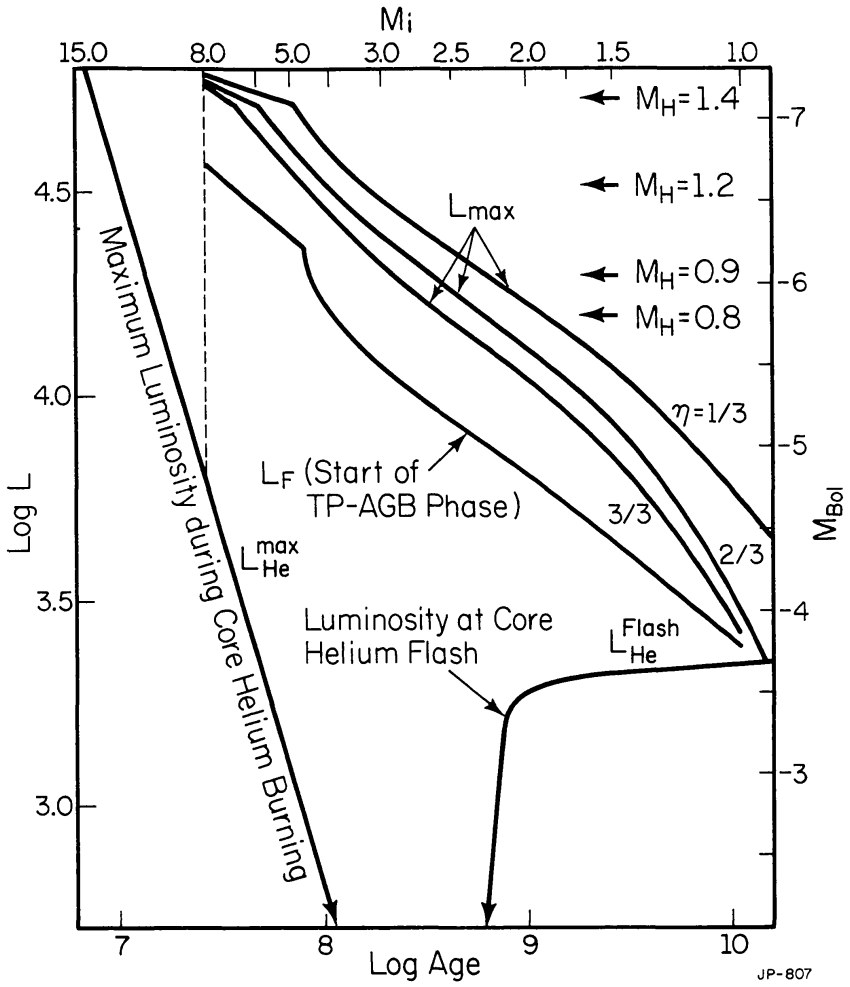

Figure 7 A number of relevant luminosities are shown vs. initial mass M_i (upper scale) and age (lower scale). We define age as the total nuclear-burning lifetime (from the beginning of the main sequence phase to stellar death). The luminosity L_{He}^{max} is the maximum luminosity reached during the core helium-burning stage for stars with $M_i \gtrsim 2.3$ (which ignite helium in a nondegenerate core). Stars with $M_i \gtrsim 8$ ignite carbon in a core where electrons are nondegenerate (at $L \simeq L_{max}$), and will finally produce type II SN events, with a pre-SN luminosity still very close to L_{He}^{max}. Stars with $M_i \lesssim 2.3$ ignite helium in an electron-degenerate core when $L = L_{He}^{flash}$, and then spend much of their helium-burning phase at lower luminosities ($\log L \sim 1.7$). All stars with $M_i \lesssim 8$, after helium exhaustion in the core, will evolve vertically in this diagram, through their E-AGB phase, until they experience a first thermal pulse when $L = L_F$ (start of the TP-AGB phase). Subsequent TP-AGB evolution comes to an end when $L = L_{max}$, where either the residual envelope is ejected (if $M_H < 1.4$) or carbon is ignited inside the electron-degenerate core (when $M_H \simeq 1.4$) and a supernova of type I $\frac{1}{2}$ is produced. The luminosity L_{max} depends on the mass loss parameters (η, b, and M_{PN}), and three different cases are exhibited for $b = 1$. Approximate values of M_H at the corresponding luminosities are also shown. The composition is $(Y, Z) = (0.28, 0.02)$.

during the TP-AGB phase. However, for stars of initial mass as low as those found in galactic globular clusters, the E-AGB phase lasts considerably longer than the TP-AGB phase and, for stars of sufficiently small M_i, mass loss during the E-AGB phase can actually evaporate the hydrogen-rich envelope before thermal pulses can begin (187). For simplicity, and because we are primarily interested in addressing the distribution of TP-AGB stars in the Magellanic Clouds, we have neglected here mass loss during the E-AGB phase.

For $8 \lesssim \log t \lesssim 10$, the relation between age and maximum AGB luminosity shown in Figure 7 can be approximated by $\log t = 14.46 + 0.93\, M_{\rm bol}^{\rm min} - 0.75\,(\eta - 1/3)$. (Note that $M_{\rm bol}^{\rm min}$ corresponds to $L_{\rm max}$.) This relationship has been obtained using the "Case A" criterion for PN ejection. Variations by a factor of 2 in the coefficient b do not produce significant changes in the derived ages. Although the t-$M_{\rm bol}^{\rm min}$ relationship has been obtained for $(Y, Z) = (0.28, 0.02)$, thanks to various compensating effects it also remains reasonably accurate for quite different metal abundances. We note that a change in η by a factor of 3 produces a factor of 3 change in the derived age.

4.3 *Age Estimates Using AGB Stars*

Absolute bolometric magnitudes of AGB stars in quite a few stellar systems are now available, and age estimates for these systems can therefore be attempted using the relationship between age and AGB luminosity just discussed. These estimates must be regarded as upper limits, particularly for those systems having a sparsely populated AGB (109). Moreover, derived ages depend on the parameter η and assume negligible circumstellar absorption.

4.3.1 GLOBULAR CLUSTERS IN THE MAGELLANIC CLOUDS Until recently, the term "globular cluster" has been restricted to the oldest (metal poor) clusters in the Galaxy that contain no single stars of initial mass larger than about 0.8 $M_\odot$. Now, however, it is commonly applied also to relatively young spheroidal aggregates in the Magellanic Clouds, some of which contain Cepheids! Several investigators (3, 78, 80, 157–159) have estimated $M_{\rm bol}$ values for a few AGB stars in several SMC and LMC globular clusters (GCs). Mould & Aaronson and Aaronson & Mould have also estimated cluster ages following the principles discussed in Section 4.2. These estimates, which range from 1 Gyr (1 Gyr = 10^9 yr) to $\gtrsim 10$ Gyr, are quite uncertain for a few clusters because of the very small number of AGB stars with measured $M_{\rm bol}$ (see also 98). From Hodge (96, 97), one knows that even younger GCs (10^7–10^8 yr) are present.

It is probably too early to speculate about the rate of GC formation in the

Clouds, but it is clear that, for $\eta \gg 1/3$, one would derive an exceptionally large rate of GC formation during the last billion years. Aaronson & Mould note that the LMC appears comparatively richer than the SMC in clusters younger than ~ 5 Gyr, although this effect could be due to the smaller number of clusters sampled in the SMC. The conclusion is that, for some reason, the Clouds have so far retained the ability to generate GCs, occasionally as massive as a typical galactic GC ($\sim 10^5\ M_\odot$; cf. 74), while our own Galaxy lost this ability very soon after its formation. This different behavior could be ascribed to the larger differential rotation of the galactic disk, which could prevent massive clouds from collapsing to the small volume typical of a GC.

When the main sequence turnoff is reached (probably with the Space Telescope), cluster ages obtained using the more traditional method based on turnoff luminosity will allow an independent calibration of the mass loss parameters. Moreover, age and metallicity determinations coupled with integrated spectrophotometry will provide a unique tool for the calibration of models of evolutionary population synthesis (cf. 47, 194, 224).

4.3.2. DWARF SPHEROIDAL GALAXIES The origin of dwarf spheroidal galaxies (DSGs) remains mysterious, but the observation of AGB stars may provide a clue to their past history. Their peculiar horizontal branch morphology and the average period of their RR Lyrae stars suggest that at least some component of DSGs may be younger than galactic GCs by several Gyr (e.g. 42, 190). Moreover, DSGs contain "anomalous" Cepheids, whose mass is $\sim 1.4\ M_\odot$ (273). These variables could be stars several Gyr younger than the bulk population in the parent system, or accreted secondaries in binaries (198). They might even be former binaries that have merged into single stars (190), as indicated by theoretical studies of close binaries (250). Deciding whether or not they are single from birth is obviously crucial for determining their age. If anomalous Cepheids are single stars (either from birth or as a consequence of merging), they will later evolve to the AGB, reaching higher luminosities (by ~ 1–2 mag; see Figure 7) than the stars of the bulk population. Whereas, if they are still binaries, Roche lobe overflow may prevent them from reaching the upper AGB. The possibility that a trace population of bright AGB stars in old stellar systems is the progeny of merged binaries should be kept in mind.

Absolute bolometric magnitudes of AGB stars are now available for Sculptor (77, 79) and Fornax (2, 77, 79). Sculptor does not contain AGB stars significantly brighter than the brightest AGB stars in galactic GCs, and therefore may not contain stars younger than ~ 10 Gyr. On the other hand, three anomalous Cepheids have been found in this system (242), and more could still be unrecognized. Arguing on the basis of relative lifetimes,

and assuming that these Cepheids are (now) single stars, one would expect to see one TP-AGB descendant for every 10–20 anomalous Cepheids (192).

Contrary to Sculptor, Fornax has a well-developed bright AGB reaching to at least $M_{bol} \cong -5.0$, and one star (DK46) is as bright as $M_{bol} \cong -5.6$. Correspondingly, Fornax should contain stars as young as ~ 5 Gyr, or even ~ 2 Gyr, if DK46 is included. Richer & Westerlund (202) estimate a total of 64 AGB stars in Fornax. (They are mostly carbon stars.) Could they all be the progeny of anomalous Cepheids? Fornax is ~ 100 times more massive than Draco (97), and, if its population is similar, it should contain ~ 500 anomalous Cepheids and some 10^4 RR Lyrae stars. We conclude that, within the uncertainties, the AGB stars in Fornax could be the progeny of anomalous Cepheids, and a search of such variables in this system should test this hypothesis. On the other hand, if anomalous Cepheids are merged binaries, the youngest AGB stars in Fornax could be considerably older than we have estimated. The brightest AGB stars in Carina (160) and in Draco (1) are, respectively, similar to those in Fornax and Sculptor.

The possible existence in Fornax of stars with ages covering a quite extended range (from more than ~ 10 Gyr to a few Gyr) has been interpreted as evidence of multiple stellar generations within this system (2, 81), and the presence of anomalous Cepheids may indicate the same for other DSGs. However, it is not clear how stars could have formed in such gas-free, low-density aggregates. Van den Bergh (243) argues that DSGs cannot have formed independently of the Milky Way and the Clouds, and we find rather more attractive the idea that DSGs were stripped from the Clouds by tidal interactions with the Milky Way (136, 150). Since gas would not have been retained by those fragments that managed to remain marginally bound, they should contain only stars with ages ranging from ~ 10 Gyr down to the age of the last stars formed before the stripping. In other words, multiple stellar generations would have occurred while these systems were still part of the Clouds. The close similarity of the DSG stellar populations with the old and/or intermediate populations of the Clouds (77, 79, 190) is a point in favor of this interpretation. Many-body simulations (87) support this picture.

4.3.3 THE GALACTIC BULGE The bulge population of spiral galaxies is generally thought to consist exclusively of old stars that have formed during an early galactic collapse phase. However, surprisingly enough, Frogel & Whitford (82) have discovered that there are red giants in the galactic nuclear bulge as bright as $M_{bol} \cong -5.5$, some 2 mag brighter than in galactic GCs. An immediate temptation is to take this result as evidence of current (less than several Gyr ago) star formation in the bulge. However, Whitford & Rich (2, 59) have found that the metallicity in several of these

bright giants may be considerably larger than in the Sun, and Frogel & Whitford have used this information (in conjunction with theoretical age estimates as a function of Z) to suggest that the temptation should be resisted. We agree with their conclusion (no age spread), but think it may follow for another reason. From Figure 7 it is apparent that an initial mass of at least 1.5 $M_\odot$ is required to reach $M_{\rm Bol} \sim -5.5$, even for stars with twice the solar metallicity. The corresponding age for a single star ($\sim$ Gyr) is much smaller than the age of the oldest star in the Galaxy ($\sim$15 Gyr). We can offer two possible interpretations of the presence in the galactic bulge of stars with $M_{\rm i} \cong 1.5$. (*a*) They could be merged binaries: after all, as suggested by the profusion of novae found in the bulge of M31 (207), the bulges of spirals are probably quite rich in binaries. (*b*) Alternatively, a galactic bulge may grow by incorporating stars from the innermost parts of disk density waves, as suggested by recent hydrodynamical simulations of disk galaxies (272). These calculations show that the amplitude of the inner part of a density wave can grow so large that a stellar velocity dispersion comparable to that of the bulge is reached. In any case, stars in the bulge are highly relevant for the problem of population synthesis in elliptical galaxies (75).

4.4 *AGB Luminosity Functions*

One straightforward application of synthetic AGB evolutionary models consists of the generation of theoretical luminosity functions (LFs) of assemblies of AGB stars produced by a given initial mass spectrum. Comparison of theoretical LFs with LFs observed in various stellar aggregates will then provide a crucial test for the theory (see Section 7.3).

The time spent during the TP-AGB phase is roughly proportional to $\Delta\log L = \log L_{\rm max} - \log L_{\rm F}$. This follows from (1.), using the fact that 6×10^{18} erg are liberated for every gram of hydrogen that is consumed. When the third dredge up is taken into account, one has (197) $t_{\rm TP\text{-}AGB} \cong 4.5 \times 10^6\ \Delta\log L$. In practice, the duration of the TP-AGB phase is typically $1\text{–}2 \times 10^6$ yr, depending on the chosen MLR and on $M_{\rm i}$ (120, 197).

Thanks to the third dredge-up process, TP-AGB stars can become C stars, and it is worth constructing separate LFs for C stars and for oxygen stars. Note that we prefer using the term oxygen stars (rather than M-type), as there is no guarantee that O-rich AGB stars are all M-type.

In the course of constructing AGB synthetic evolutionary histories, one obtains, for each value of the initial mass $M_{{\rm i}_j}$ (note that i is not a running index), the time Δt_{jk} spent in each of a number of predetermined luminosity intervals $\Delta L_k = L_k - L_{k-1}$. One needs also to assume some concrete mass function for the progenitors of AGB stars in the stellar system one is trying to theoretically reproduce. That is, one must guess the appropriate weights

$\psi(M_{ij})$ such that the number of stars in each magnitude interval is

$$N_k \propto \sum_j (M_{i_{j+1}} - M_{i_j}) \psi(M_{i_j}) \Delta t_{jk}.$$

The weighting function $\psi(M_{i_j})$, which we shall call the AGB mass function, is proportional to $\phi[T - t(M_i)] \times \mathrm{IMF}$ for $M_i > M_i(T)$, and $\psi = 0$ for $M_i < M_i(T)$. Here T is the age of the stellar system, $t(M_i)$ and the inverse function $M_i(t)$ follow from Figure 7, $\phi(t)$ is the overall rate of star formation at time t, and IMF is the initial mass function (e.g. using the Salpeter mass function, $\mathrm{IMF} \propto M_i^{-2.35}$). Since theoretical AGB LFs require two sets of information—the results of AGB model calculations and a guessed history of star formation—a failure in reproducing an observed LF can a priori be attributed to either of the two sets.

A realistic LF requires two additional refinements. Equation 1′ refers to the quiescent luminosity between two pulses, and one must take into account the effect of the extended postflash luminosity dip discussed in Section 2. A second effect that must be considered is stellar dynamical pulsation (Mira-like). We have assumed that all TP-AGB stars are variable, with an amplitude of 0.7 mag (bolometric). Both of these effects can easily be taken into account in the construction of the final LF (see 109 for numerical details). Of special interest is the LF of C stars, since observational LFs for oxygen stars are incomplete (cf. Section 7.2).

4.5 *AGB Stars, Nucleosynthesis, and Population Synthesis*

Matter lost by AGB stars (through both the wind and the superwind) is enriched by various nuclear-burning products, and therefore AGB stars can play an important role in galactic nucleosynthesis. More specifically, the envelope composition of AGB stars has been influenced by up to three dredge up processes and by the EB process. Further, CN-cycled materials could have been brought to the surface by additional slow mixing processes operating on the main sequence.

Iben & Truran (120) compute the amount and relative composition of *s*-process isotopes provided by AGB stars via the ^{22}Ne source plus third dredge up. They also estimate the contribution of AGB stars to the galactic enrichment of ^{3}He, ^{4}He, ^{12}C, ^{13}C, and ^{14}N when the EB process is neglected.

The amount of fresh ^{4}He, ^{12}C, ^{13}C, and ^{14}N ejected by intermediate-mass stars when the EB process is included is given in tabular form by Renzini & Voli (197). Particularly relevant is the possibility of producing substantial amounts of primary ^{13}C and ^{14}N, thanks to the combined effect of the third dredge up and the EB processes. The amount of ^{16}O produced (or consumed) by AGB stars is predicted to be negligible. The amounts of ejected ^{4}He, ^{12}C, ^{13}C, and ^{14}N depend primarily on the adopted third

dredge up law, on the mass loss parameters (η, M_{PN}), and on the mixing-length parameter (ℓ/H). The latter parameter controls the relative amount of ^{12}C and primary ^{13}C and ^{14}N produced by intermediate-mass stars. The production of *s*-process elements is primarily controlled by η and M_{PN} and, since the same parameters also determine the critical initial mass above which carbon is ignited, they also control the amount of iron-peak elements intermediate-mass stars may produce (cf. 111). Including the yields of the various elements produced by AGB stars in models of the chemical evolution of the Galaxy permits further astrophysical constraints to be imposed on the choice of η, M_{PN}, and ℓ/H.

A final consideration concerns interstellar grains. The circumstellar envelope of an AGB star is an obvious site for the formation of interstellar grains. Clearly, oxygen stars are candidates for the production of O-rich grains (e.g. silicates), while C stars should produce C-rich grains (e.g. graphite, soot, or carbyne). In this picture, the relative amount of O-rich and C-rich grains should ultimately depend on the familiar AGB parameters η, M_{PN} and ℓ/H, and the $^{12}C/^{13}C$ ratio in C-rich grains should exhibit enormous grain-to-grain variations (189). Moreover, several isotopic anomalies in primitive meteorites appear reminiscent of isotopic patterns induced by the ^{22}Ne neutron source (cf. 12, 66, 143, 226), while others could be ascribed to the EB process (165). Clearly, a great deal of valuable information should come from cooperative interactions among researchers studying AGB stars and those working on isotopic anomalies in presolar materials.

The contribution of stars in a given post-main-sequence stage to the integrated bolometric luminosity of a stellar system of coeval stars is directly proportional to the amount of fuel burned during that stage (194, 232). Preliminary calculations (194) show that AGB stars contribute roughly 50% of the integrated luminosity of a system $\sim 2 \times 10^8$ yr old, with only a mild dependence on η. The AGB contribution declines with age, reaching $\sim 10\%$ in a system as old as a galactic globular cluster. Correspondingly, the integrated light (particularly in the IR) of intermediate-age rich clusters can be dominated by AGB stars. Once again, more astrophysical constraints on η can be derived from population synthesis studies, notably for intermediate-age globular clusters in the Magellanic Clouds.

5. ESCHATOLOGY

This section focuses on the final chapters in the life of low- and intermediate-mass stars, discussing first those stars that become white dwarfs and then those that become supernovae.

5.1 *Formation of Planetary Nebulae and Evolution to the White Dwarf State*

The onset of the superwind regime, which perhaps temporarily hides the star from optical telescopes, marks the beginning of a dramatically rapid decrease in the envelope mass M_e of an AGB star. As M_e decreases, the star departs from the giant branch at a rate that increases with decreasing M_e (see Figure 5). In turn, the movement of the star to higher effective temperatures (smaller radii, but nearly constant luminosity) surely affects the superwind process, which must eventually cease when M_e falls below a critical "remnant" value M_{eR}. After the superwind has ceased, the ejected matter (whose composition is that of the envelope at the onset of the superwind) keeps expanding, while the remnant star continues its evolution toward higher temperatures. When T_e reaches sufficiently high values ($\sim$30,000 K), the ejected matter becomes ionized by the photons from the remnant and assumes the characteristics of a PN. Subsequent evolution brings the remnant star, which we now call a PN nucleus, closer and closer to the appropriate white dwarf cooling sequence, and the PN disperses.

This qualitative picture for post-AGB evolution is generally accepted, but the quantitative behavior of the various observables can be extremely sensitive to various stellar parameters (particularly M_i), and several details, which might at first sight appear to be inconsequential, can actually play a major role.

5.1.1 THE TRANSITION FROM THE AGB TO THE PN PHASE A first difficulty in understanding post-AGB evolution is that M_{eR} is essentially unknown from first principles. A zeroth-order guess for M_{eR} is the envelope mass for models that begin to depart from the giant branch (M_{eD}). This happens for $M_e = M_{eD} \cong (\sim 0.2\ \Delta M_H)$, moderately depending on the core mass of the remnant and on the input physics used to construct the envelope (cf. 88, 113, 168, 218). Thus, one can guess $M_{eR} \lesssim M_{eD}$, but this estimate may be uncertain by perhaps a factor of ten. The only attempt at deriving M_{eR} that is based on both evolutionary and hydrodynamical considerations is that of Härm & Schwarzschild (92). Although their numerical experiment is of great philosophical interest, the quantitative results are quite uncertain. If $M_{eR} > M_{eD}$, the star will remain close to the AGB until shell burning and surface mass loss reduces the envelope mass below M_{eD}. Then, as in the case when $M_{eR} < M_{eD}$, the star moves faster and faster toward higher effective temperatures, while the luminosity remains nearly constant and quite close to that given by the core-mass-luminosity relation (1′.). After having reached a maximum around $\log T_e \cong 4.0$, the evolutionary rate ($d \log T_e / d \log t$) starts decreasing (113, 168, 218).

The precise value of M_{eR} also directly controls the possibility of producing an observable PN (92, 191, 192). If mass loss following the end of the superwind can be neglected, the time t_{tr} required by the star to evolve from the end of the superwind phase to $T_e \cong 30{,}000$ K depends linearly on the quantity $\Delta M_e = M_{eR} - M_{eN}$ as $t_{tr} \cong X_e \Delta M_e E_H / L \cong 1.6 \times 10^6$ yr $\times \Delta M_e/(M_H - 0.44)$, where X_e is the envelope hydrogen abundance, $E_H = 6 \times 10^{18}$ erg, and M_{eN} is the envelope mass when the models reach $T_e = 30{,}000$ K. If mass loss actually dominates the envelope reduction, then $t_{tr} \cong -M_{eR}/\dot{M}$. If t_{tr} is too long (M_{eR} too large), the ejected envelope disperses before the remnant star becomes hot enough to excite the ejected matter, and no PN is produced. The mere fact that PNe do indeed exist shows that "quite often" M_{eR} is small enough for the formation of a PN. Nevertheless, the proportion of "lazy" post-AGB remnants, for which t_{tr} is too long, remains unknown.

Since the youngest PNe have an age of ~ 2000 yr, insisting that $t_{tr} \lesssim 2000$ yr and solving for M_{eR}, one obtains $\Delta M_e \lesssim 1.25 \times 10^{-3} \times (M_H - 0.44)$. For $M_H = 0.6$, one has $M_{eN} \cong 1.13 \times 10^{-3}$ (see Figure 5) and this implies that $\Delta M_e \lesssim 2 \times 10^{-4}$, which is about one order of magnitude less than the corresponding value of $M_{eD} - M_{eN}$. We conclude that either $M_{eR} < M_{eD}$ (and the transition occurs on a thermal time scale), or the normal wind may play a dominant role in further reducing M_e after the cessation of the superwind phase. A delicate interplay between wind and superwind appears to be critical if a PN is to be produced.

The value of M_{eR} is likely to depend somewhat on M_i, thus producing a dependence of the initial nebular radius ($= vt_{tr}$, v being the superwind velocity) on M_i. Moreover, because of the hydrodynamical nature of the superwind, M_{eR} could also exhibit erratic fluctuations even for stars with identical initial mass, and the precise pulse-cycle phase at the onset and termination of the superwind is also likely to generate sizable differences in M_{eR} in stars with virtually identical mass. Correspondingly, we can legitimately speculate that initially almost-identical stars can actually behave in extremely different ways during the post-AGB phase (e.g. generating or not generating an observable PN).

Only a few thousand years separate the superwind phase from the beginning of the PN phase. During this short time, the appearance of the evolving object (central star plus expanding circumstellar envelope) must change dramatically. Theoretical investigations on this "protoplanetary" phase are still in an exploratory stage and, since the evolution of the nebular properties is primarily driven by the evolution of the central star (through the rapid variation of the UV flux, the MLR, and the velocity of the stellar wind), it appears crucial to study the object as a whole. That is, a coupling of

the stellar with the nebular evolution is essential. The interaction of the fast wind ($v > 1000$ km s^{-1}) with materials ejected during the AGB phase has been the subject of several investigations (137–140, 152, 193).

Finally, we note that the superwind mass around the central star (i.e. M_{PN}), as well as the superwind composition and dust content, are all expected to be extremely sensitive to the initial mass M_i (cf. 189, 197). Extensive grids of models are therefore required.

5.1.2 THE EVOLUTION OF PN NUCLEI The qualitative features of the evolution of PN nuclei (= PNNi; singular = PNN) were first elucidated by Paczyński (168). An important property of the models is the "fading time" t_f that is required for the luminosity to fall by a factor of 10 after the stellar surface becomes hot enough to emit ionizing photons ($\sim$30,000 K). Paczyński's models give $t_f \cong 45$, 2000, and 33,500 yr, respectively, for $M_H = 1.2$, 0.8, and 0.6. This very strong dependence of t_f on core mass is easily understood. When models reach $T_e \lesssim 30{,}000$ K, their residual hydrogen-rich envelope has a mass M_{eN} ranging from $\sim 10^{-3}$ for $M_H = 0.6$, down to $\sim 4 \times 10^{-6}$ for $M_H = 1.2$; i.e. $M_{eN} \propto M_H^{-7.3}$! The envelope mass represents most of the available nuclear fuel that the star is consuming. Correspondingly, t_f is given by an expression similar to that reported in Section 5.1.1 for t_{tr}, with M_{eN} replacing ΔM_e. Thus, $t_f \sim M_H^{-9.6}$(!).

The 0.6-$M_\odot$ model computed by Schönberner (218, 219) fades in only 1/3 of the time required by the corresponding Paczyński model ($t_f \sim 10{,}000$ yr, rather than $\sim$30,000 yr); the Gingold 0.6-$M_\odot$ model fades in somewhat less than 36,000 yr, but the precise value cannot be derived from the data given in his paper. These differences can be qualitatively understood. Paczyński's starting models are the result of artificial AGB evolution in which thermal pulses have been suppressed, whereas Schönberner faithfully follows these pulses. A Paczyński model initially experiences a weak thermal pulse that is an attempt by the model to adjust the intershell chemical and thermal structure (which have been improperly chosen for the initial model) to that of a real post-AGB configuration. In a more realistic calculation, only a fraction of the carefully computed post-AGB models is actually expected to suffer a final flash (which, in any case, will be a large-amplitude flash!). The effect of the low-amplitude pulse on the Paczyński 0.6-$M_\odot$ model is to suppress hydrogen burning for $\sim$8000 yr, during which time helium burning is the dominant energy source. Even when hydrogen is reignited, the rate of helium burning decreases only gradually, and the star takes longer to consume its hydrogen-rich envelope. Without this artificial flash, t_f would have been much closer to the value found by Schönberner. Further, Schönberner's models are somewhat brighter than those of Paczyński, thus consuming their residual hydrogen more rapidly.

The large difference between t_f given by the Gingold and Schönberner models of the same mass can be traced in large part to the fact that Gingold's model departs from the AGB with a much larger M_{eD} ($\cong 0.005$) than in Schönberner's case ($\cong 0.0012$). This difference in M_{eD} may be due to differences in envelope opacities and ℓ/H. The value of $t_f = 15{,}000$ yr given by the 0.6-$M_\odot$ model described in Figure 5 is just 50% larger than that given by the Schönberner 0.6-$M_\odot$ model; this difference is due almost entirely to the difference in the calculated value of M_{eN} ($= 1.13 \times 10^{-3}$ in Figure 5, but only $\cong 6 \times 10^{-4}$ at the corresponding point along the Schönberner track).

Another theoretical consideration should be explored carefully by the construction of additional models. We have emphasized in Section 2.8 that, in stars with small M_H, the rate of consuming hydrogen changes considerably but only very gradually over the course of the interpulse phase. We may reasonably expect the mean luminosity of a PN nucleus (at $T_e > 30{,}000$ K) to be quite similar to the luminosity of the AGB progenitor of the PN, and that, correspondingly, both t_{tr} and t_f are quite sensitive to the time elapsed, or, equivalently, to the fraction of the critical mass ΔM_H through which the hydrogen-burning shell has advanced following the last thermal pulse.

We also note that mass loss by a stellar wind could accelerate the evolution of PN nuclei, reducing the amount of available fuel. However, the few MLRs so far determined for PNNi seem too small to have any significant evolutionary effect (193).

For the moment, in spite of the insufficient number of available theoretical evolutionary sequences, the following picture is emerging (188, 192). The production of an observable PN is primarily controlled by the transition time t_{tr}, which in turn depends on a delicate interplay between wind, superwind, and thermal pulses at the tip of the AGB. Some post-AGB stars produce PNe, others may not. The fading time t_f plays a crucial role in determining the properties of PNe and their central stars. It is a very strong function of the mass of the post-AGB remnant and, quite possibly, of the precise phase in the thermal pulse cycle at which the envelope is ejected. More-massive post-AGB stars ($M \simeq M_H > \sim 0.7$) have a very short fading time ($t_f < \sim$few 10^3 yr) and should generate PNe with very hot and bolometrically faint (log $L \lesssim 2.0$) nuclei, which are quite underrepresented in existing catalogs. Low-mass PN nuclei ($M \simeq M_H < \sim 0.57$) have a very long fading time ($t_f > \sim 30{,}000$ yr), and when they become dimmer than log $L \simeq 3.0$ the associated PN has already dispersed. These low-mass post-AGB stars should generate most of the bright PNNi (log $L \gtrsim 3.0$). Post-AGB stars of intermediate mass ($0.6 \lesssim M \lesssim 0.7$) also have intermediate fading times ($\sim$ few $10^3 \lesssim t_f \lesssim 30{,}000$ yr) and should exhibit a significant luminosity evolution during the nebular lifetime (219, 220). The anticorre-

lation between nebular radius and (visual) brightness found by Schönberner & Weidemann (220) could be produced by such stars, but their claim that all PNNi have virtually identical masses ($M \sim 0.58 \pm 0.02$) may apply, as they admit, just to the sample they have scrutinized. To settle this point, observational studies should concentrate on hot and faint ($M_v \gtrsim 6$) PNNi. Also, a dependence of t_{tr} and M_{PN} on M_i (which is very likely to exist) will produce a dependence of the initial PN radius and PN lifetime on M_i, and this point is subject to observational test (see also 196, 221).

At this stage the reader should have an appreciation of the unusual complexity of the problems involved in post-AGB evolution. A theory of post-AGB stars, with particular reference to PNNi, has not yet been worked out in detail, and the increasing flow of pertinent data (particularly in the UV) has not yet been matched by a parallel theoretical effort. However, in our opinion, this is one of the most interesting and rewarding topics in stellar (and nebular!) astrophysics.

5.1.3 THE COMPOSITION OF PLANETARY NEBULAE The idea that PNe owe their composition to the cumulative effects of the various mixings of nuclearly processed materials during the whole previous stellar history is obviously very old. However, the first attempt at using evolutionary models to predict PN composition is very recent (127). This attempt does not take into account the effect of the third dredge up, which has been included in subsequent investigations (21, 180, 197). In the latter paper, detailed nebular abundances are given for a variety of initial masses, and for various values of the parameters η, M_{PN}, and ℓ/H. These models do not include the possible influence of extramixing. Moreover, the uncertainty in the dredge-up law $\lambda(M_H)$ for small values of M_H makes rather uncertain the theoretical abundances of the nebulae produced by the less-massive stars (which, unfortunately, are also the most common). However, irrespective of the uncertainty in λ, a tight correlation is predicted between C and He enrichments (e.g. 21).

Theoretical nebular abundances are very sensitive to M_i, with He/H and C/O (or N/O, if the EB process is active) rapidly increasing with M_i. Since the mass of post-AGB models is also a function of M_i (at this stage $M \simeq M_H = M_f$), current AGB theory predicts a correlation between the nebular composition and the mass of the central star. Nebulae with high He/H and C/O should have more massive central stars, and since model PN nuclei of different mass have very different fading times, a correlation is expected between the nebular composition and the location of the central star in the H-R diagram (118, 192). Analyzing different samples of PNe, Renzini (192) and Schönberner & Weidemann (220) reach opposite conclusions about the existence of this correlation. Once again, the observations of PNe with very faint nuclei should provide a decisive test.

Peimbert (177, 178) has compared the Renzini & Voli (197) models with observed nebular abundances, finding reasonable agreement for He and C, and concluding that N is underproduced by the models. This may suggest that either in some stars the amount of CN cycling is larger than in the standard first dredge up (rotationally induced mixing required?), or that the efficiency of the EB process has been underestimated (overshooting at the lower boundary of the convective envelope?). On the other hand, Kaler (126) argues that the abundance of N predicted by the Renzini & Voli models exceeds observed values and that the milder burning suggested by Becker & Iben (21) is closer to the truth. All in all, theoretical nebular abundances of He encompass the observed range (cf. 123, 124), although Kaler (124), unlike Peimbert (178), does not find any significant correlation between C and He (but note that C abundances obtained from lines in the visual are still in disagreement with those obtained from UV observations). Further comparisons of theoretical and observational PNe abundances are provided by Aller (5), Kaler (125, 126), and Peimbert & Torres-Peimbert (179).

A very nice demonstration of the connection between PNe and precursor AGB stars is the recent analysis of two very bright PNe in the LMC and one in the SMC (151, 228). In each case C not only exceeds O, thus showing that dredge up has occurred in the precursor star, but the absolute value of the C abundance is roughly the solar value, showing that the dredge-up mechanism has operated to approximately the same extent in the precursor star (151). Also, in each case an estimate of the brightness of the PNN (228) suggests that the PNN mass is on the order of or larger than $\sim 0.9\, M_\odot$, thus indicating that stars initially as massive as ~ 3–$6 M_\odot$ can become carbon stars.

5.1.4 POSSIBLE EFFECTS OF A THERMAL PULSE IN POST-AGB STARS A fraction $M_{eN}/\Delta M_H$ of hot post-AGB stars is expected to experience a final, strong pulse. This fraction is approximately 0.1, nearly independent of the value of M_H (114, 196). The development of a thermal pulse in a post-AGB star proceeds very differently from its development in an AGB star with a massive and extended convective envelope. In fact, the entropy barrier between the helium-burning convective shell and the H-rich layers above, which prevents contact mixing in AGB models, is much reduced in hot models with small envelope mass. Fujimoto (83) estimates that contact mixing should occur when $M_e \gtrsim 10^{-5}$, while Schönberner (218) and Iben (113) actually find contact mixing for a 0.6-$M_\odot$ model in which the pulse occurs when $M_e \lesssim 3 \times 10^{-4}$ (see Figure 5).

The ingestion of protons by the helium convective shell will most likely trigger a thermonuclear runaway, causing an expansion of the intershell, the almost complete destruction of the residual hydrogen through the

burning sequence $^{12}C(p,\gamma)^{13}N(e^+\nu)^{13}C(\alpha,n)^{16}O$, the ensuing production of *s*-process isotopes and perhaps also *r*-process isotopes, and a drastic disappearance of hydrogen from the stellar surface (218). We can reasonably anticipate the course of events following contact mixing. First, intershell expansion will drive C-rich materials to temperatures below $\sim 3 \times 10^6$ K, at which point carbon starts to recombine and opacity in the upper part of the He-C region increases. (At this stage, the H-rich skin may have already been swallowed.) Second, the opacity increase will assist the expansion through a thermal runaway (as more carbon cools below the recombination threshold, the high-opacity region becomes wider and further expansion becomes easier). Third, after the thermonuclear runaway has ceased (the flash quenched and the protons almost completely destroyed), helium burning will continue, just as after normal flashes. The postflash helium luminosity L_{He} is L_{max} as given by Equation 1, and burning persists at this luminosity for approximately 1/5 the interpulse time, which ranges from $\sim 4 \times 10^4$ yr for $M_H = 0.6$ to ~ 5 yr for $M_H = 1.4$.

In summary, stars experiencing a helium shell flash while on the hot side of the H-R diagram are expected to (*a*) traverse a wide loop in the H-R diagram, briefly reaching quite low effective temperatures, and then evolving at high effective temperatures for approximately one fifth of the interpulse time; (*b*) develop a He-C atmosphere whose composition is that of a typical intershell; and (*c*) show, occasionally, *s*-process and *r*-process enhancements, which result from a single burst of neutrons whose strength is proportional to the mass of the ingested hydrogen-rich envelope. (This mass can vary by orders of magnitude.)

It has been speculated that this series of events is responsible for the origin of some hydrogen deficient stars [e.g. R Cr B stars, some extreme helium stars, PNNi of type WC and WCN, some H-poor SdO stars, and non-DA white dwarfs (188, 193, 195)]. The presence of a C-rich envelope will most likely affect the stellar pulsation properties, thanks to the classical κ-mechanism now active in the various ionization stages of carbon (13, 57, 130, 227).

Following the actual course of all thermonuclear reactions occurring when hydrogen is ingested by the helium-burning convective shell presents formidable difficulties (connected in part with the treatment of simultaneous mixing and burning, as well as with the possible excitation of dynamic motions). These difficulties may be bypassed by simply neglecting the energy released in hydrogen-burning reactions. The evolution during the major portion of the subsequent quiescent helium-burning phase should in any case be largely independent of the precise details of the combined helium and hydrogen flash and may, therefore, be reliably followed via quasi-static calculations. Proceeding in this way, it is found explicitly (115, 116) that the PNN that experiences a helium flash in the

white dwarf configuration retraces during the quiescent helium-burning phase essentially the same path it followed during the preceding quiescent hydrogen-burning phase. Moreover, the fading time during helium burning is comparable with (but somewhat larger than) the fading time during hydrogen burning.

The implications of this result are that roughly 10–20% or more of all planetaries will be excited by energy produced by helium-burning reactions, and that (since they have grown considerably following their earlier excitation by energy produced by hydrogen-burning reactions) these nebulae should on average be much larger than those powered by hydrogen-burning reactions. This is consistent with recently uncovered evidence for a bimodal distribution of planetary sizes (116, 125), and in particular with the properties of the PNe A30 and A78, which are suggested to be typical examples of PNe whose central stars have recently experienced their final flash (116, 193, 196).

5.1.5 WHITE DWARFS The previous considerations indicate that at least 10% of post-AGB stars should produce a white dwarf of the various varieties called non-DA WDs, which share the common property of exposing a virtually hydrogen-free atmosphere. This figure is in remarkable agreement with the observed fraction of hot non-DA WDs ($\sim 15\%$; see 251).

As shown in Section 4.1, a relation between the final WD mass M_f and the initial mass M_i follows naturally from synthetic AGB models. Using such a relationship and using various stellar birth-rate histories for the Galaxy [i.e. various $\psi(M_i)$ functions; cf. Section 4.4] and theoretical white dwarf cooling times (230), Koester & Weidemann (135) obtain distribution functions for WD masses, and compare them with the observed mass spectrum of nearby WDs.

WDs can be sampled only in a small volume around the Sun. For instance, the sample analyzed by Koester et al. (134) begins to be severely incomplete beyond 20 pc. Correspondingly, a $\psi(M_i)$ weighting function that is appropriate for the Galaxy as a whole might not be appropriate for such a small portion. Large fluctuations in $\psi(M_i)$ for $M_i \gtrsim 2$ must be expected when considering small volumes, although WDs produced by stars with $M_i \lesssim 2$ could have reached the solar vicinity by diffusing from more distant birthplaces. Clearly, the ψ-function appropriate for the solar vicinity is very uncertain. Nevertheless, several authors (134, 135) argue that, from the study of nearby WDs, one can obtain information on the $M_f(M_i)$ relation, even for $M_i \gtrsim 2$ (see also 251, 252). We suggest that these studies have shown that old disk giants produce WD remnants with $M_f \cong 0.6$, but do not provide information about the contribution of more recent star formation.

A potentially more effective method of obtaining information about the

$M_f(M_i)$ relation, and about the very important critical mass M_w (cf. Section 4.1), is offered by the study of WDs in (young) clusters of known age, an approach first used by van den Heuvel (245) for the Hyades. Others (8, 9, 133, 205) have adopted this approach, and more effort in this direction would be welcome. For a recent review on WD stars, see Liebert (144).

5.2 *Carbon Ignition and Supernovae of Type I* $\frac{1}{2}$

It is possible that, at least for the initially most massive AGB stars, mass loss processes will not reduce the mass of the star below $\sim 1.4\,M_\odot$ before carbon is ignited in the core. It has become reasonably clear that, as the core mass approaches this value and carbon is ignited, a thermal runaway cannot be delayed long enough by the convective Urca process to prevent an explosion from disrupting the entire star.

Both Ergma & Paczyński (69) and Couch & Arnett (55) explore the efficiency of Urca processes in somewhat artificially constructed convective cores. They assume that (*a*) the time dependence of the density at the center of the core is obtained from a relationship between the central density and the total mass of the core, which grows at a rate given by synthetic AGB evolution; and (*b*) the size of the convective core is determined by demanding that the total rate of Urca neutrino losses exactly balances the rate at which energy is released by all nuclear and weak interaction processes and by the gravitational potential field (see also 236). The conclusions of Ergma & Paczyński are ambiguous. Couch & Arnett conclude that the convective Urca process involving ^{23}Na and ^{23}Ne will prevent a thermal runaway at least until the central density exceeds the threshold density for electron capture on ^{21}Ne ($\rho \sim 4 \times 10^9$ g cm^{-3}). They then assume that a new convective core is formed and that, in this core, the ^{21}Ne-^{21}F Urca pair plays the stabilizing role. The new core continues to evolve, with heating and cooling rates in balance, until central density reaches $\rho \sim 7 \times 10^9$ g cm^{-3}, at which point no self-consistent solution can be obtained and it is concluded that a thermal runaway will develop.

Iben (107, 108, 112) does a full quasi-static calculation of the entire core. The work done by convection in driving electrons inward against an adverse gradient in the Fermi energy, a process first appreciated by Couch & Arnett (54) and by Paczyński (169), is estimated locally, and it is not assumed that there is a balance between the Urca neutrino loss rate and heating rates. The quasi-static calculations show that the rate of electron capture by ^{23}Na near the base of the mixing region does not equal the rate of electron decay by ^{23}Ne near the outer edge of the mixing region and that this imbalance is a critical feature of the physics of the convective Urca process. It is primarily the energy released by the Fermi sea as a consequence of electron capture near the base of the mixing region that

drives turbulent convection. Convection in turn does the work to drive inward the electrons released near the outer edge of the convective region.

The quasi-static calculations show further that, soon after carbon is ignited, when the outer edge of the convective core has grown until the density there approaches the threshold density for electron capture on ^{23}Na, a series of thermal oscillations is initiated. These oscillations carry the star between two states of unstable equilibrium: a "cold" state, when heating exceeds the rate of Urca neutrino energy losses, and a "hot" state, at the end of which neutrino cooling exceeds heating.

When central density reaches and begins to exceed the threshold density for electron capture on ^{21}Ne ($\sim 3.8 \times 10^9$ g cm^{-3}), matter in a small central region cools dramatically, thanks to Urca neutrino losses from the ^{21}Ne-^{21}F pair, which are essentially in local equilibrium. The erstwhile convective core splits up into two parts, a small new convective core in which the ^{21}Ne-^{21}F pair controls behavior, and a large convective shell, at whose base the density remains fixed at about 3.8×10^9 g cm^{-3}. This latter circumstance is due to the intense cooling by the classical Urca process (local equilibrium) involving ^{21}Ne and ^{21}F.

From this point on, the density contrast between the base and the edge of the convective shell remains effectively fixed and, since the rate of energy release by carbon-burning reactions is much more sensitive to temperature than is the density-limited rate of energy loss by Urca neutrinos, temperatures in the convective shell climb monotonically higher. Further, the energy liberated by ^{12}C + ^{12}C reactions and by all additional reactions that potentially follow up to the formation of iron-peak elements (about 1 MeV per electron) is less than the energy needed to lift degeneracy in the core (electron Fermi energy at the center is $\varepsilon_F \sim$ 5–8 MeV), and "relief" by expansion is therefore not possible. It is thus evident that a thermal runaway must take place. The net result of this convoluted physics is that, in a single AGB star whose core reaches $\sim 1.4\, M_\odot$, the final thermal runaway begins in a convective shell when the central density reaches $\rho_c \sim 4 \times 10^9$ g cm^{-3}, rather than when it reaches $\rho_c \sim 7 \times 10^9$ g cm^{-3}, as found when events in the convective shell are ignored.

So a runaway occurs. But then what happens? Several authors (44, 121, 153, 163, 164) conclude that, although subsequent core evolution will be dynamic, a detonation, as envisioned first by Arnett (10) and explored by Bruenn (34, 35), will not grow, but, instead, a deflagration wave originating near the center will propagate outward. The net result is still total disruption of the star, but all of the matter in the core is not processed completely to iron-peak elements. Since the exploding star is a red supergiant with a mass in the H-rich envelope that increases with M_i, its spectrum and early light curve should closely resemble that of a supernova

of type II. However, a substantial amount of radioactive Ni and Co will be liberated by the exploding core, thus producing a late exponential luminosity decline, as in Arnett's (11) light curves for supernovae of type I. We propose the designation of "type I $\frac{1}{2}$" supernovae for these hypothetical objects.

Although the details of the deflagration are stated by Nomoto et al. (164) to be sensitive to the treatment of convection, these authors do not in fact explicitly treat convective transport, but simply assume that the speed of the deflagration front is some constant α times the local sound speed, supposing that the constant decreases with increasing efficiency of convection. Chechetkin et al. (44) also do not calculate convective transport explicitly, but argue that, because the rate at which the thermal runaways occurs is so large, such transport may be neglected. In both cases, convective Urca neutrino losses are ignored.

In approximating the energetics, Chechetkin et al. assume that carbon burning is followed immediately by conversion to iron-peak elements at the rate of the carbon-burning reactions. However, the maximum temperatures reached in their calculation are inconsistent with the assumption of total conversion, and they conclude that, over the whole core, conversion to iron-peak elements is only partial ("partial" being largely undefined).

The density-temperature history of the core is interesting. Nomoto et al. find that, for large α ($= 1.0$), all parts of the core move outward monotonically and reach escape velocity by the time that the deflagration front reaches $\sim 1\ M_\odot$; all of the matter behind the front has been processed to nuclear statistical equilibrium (NSE). For small α ($= 0.05$), expansion is followed by a brief contraction-and-cooling phase. The core bounces, and carbon burning in a convective shell provides enough energy to cause disruption of the whole star; only 11% of the original matter in the core reaches NSE.

In the Chechetkin et al. calculation, a unique value of $\alpha (\cong 0.1)$ falls out, apparently naturally, and a series of nine oscillations occurs. During the first eight oscillations, the mean overall density of the core increases, primarily as a consequence of electron capture on relevant iron-peak elements. The deflagration front remains approximately stationary in space as matter flows through it. However, when most of the matter in the core has passed through the front and the density at the front drops below $\sim 10^7$ g cm^{-3}, the deflagration develops into a detonation, as predicted by Mazurek et al. (153). The detonation propagates in both directions, and the heat released in the core leads to a final disruption. There is some confusion in this description in that, if matter behind the deflagration front is assumed to be in NSE, then there is no further energy to fuel a detonation. Thus, there are some rough edges to the calculation.

In summary, the authors of the two most recent calculations of the

dynamic event that follows the initial carbon-burning runaway conclude that the final outcome of this event is total disruption. However, the assumptions and approximations that have been made are in both cases incompletely justified, and one is not left with an overwhelming sense of confidence in the detailed results.

6. COMPARISON WITH THE OBSERVATIONS I. SURFACE COMPOSITION OF RED GIANTS AND CEPHEIDS

On comparing predicted with observed surface abundances for AGB stars, it is important to have first compared with the observations those surface abundance changes that are expected to occur prior to the AGB phase.

For example, if it could be established that, due to some form of "extramixing" during the main sequence phase or due to a second dredge up more extensive than exhibited by current theoretical models, the surface ratio of ^{14}N to ^{16}O is larger in the immediate (Cepheid) precursors of intermediate-mass AGB stars, then finding $N/O > 1$ in AGB stars could not of itself be taken as evidence for the operation of the EB process in the AGB stars.

6.1 *The First Dredge Up*

Canonical evolutionary models predict fairly precisely those surface abundance changes that should occur during the first dredge up: a substantial reduction of the abundances of Li, Be, and B; a decrease of the C abundance by $\sim 30\%$; a decrease in the $^{12}C/^{13}C$ ratio from ~ 90 to ~ 20–30; an increase of the N abundance by a factor $\sim 0.44(C/N)_0$, $(C/N)_0$ being the initial C to N ratio by number; and, finally, very little variation in the O abundance.

An observational check of predictions is relatively easy for Li and Be, both because the variations in these elements are rather large, and because several suitable lines are available in the optical. In contrast, B I and B II resonant lines are in the UV, and one will have to wait for the Space Telescope for a confirmation of the theoretical predictions. The determination of the $^{12}C/^{13}C$ ratio is also relatively easy, the main uncertainty coming from the estimate of the different degrees of saturation between the ^{12}CX and ^{13}CX molecular lines. On the other hand, the CNO abundances are much more difficult to derive.

The status of the theory vis a vis the observations for Li (e.g. 2, 7, 13) and Be (31, 32) has been most recently reviewed by Boesgaard (30) and by Lambert (141). Although there appears to be substantial agreement between predictions of the standard theory (mixing only in fully convective

regions), there are indications that some form of additional mixing ("extramixing") may have occurred during the main-sequence phase of some low-mass stars and led to a depletion of the light elements over a larger fraction of the interior than is given by standard theory. We do not embellish on these reviews, but instead limit our discussion to CNO elements and the $^{12}C/^{13}C$ ratio.

In cooler stars, most C is locked into CO, so that the C abundance derived from C atomic lines depends on the adopted O abundance. In a molecular equilibrium calculation, the abundance of atomic C increases if O is decreased. Therefore, for given equivalent widths of atomic C lines, a reduction in the adopted O means a decrease in the derived C abundance. Similarly, N abundances derived from CN features depend on the adopted C abundance, and one has

$$\frac{d \log \varepsilon(\mathrm{C})}{d \log \varepsilon(\mathrm{O})} \simeq +0.8, \frac{d \log \varepsilon(\mathrm{N})}{d \log \varepsilon(\mathrm{C})} = -1.0,$$

$$\text{and therefore,} \quad \frac{d \log \varepsilon(\mathrm{N})}{d \log \varepsilon(\mathrm{O})} \simeq -0.8, \quad 3.$$

where $\log \varepsilon(X)$ is the number abundance of the element X. The first derivative has been derived from Figure 5 in Luck (146) for $T_e \simeq 4000$–4250 K, and is a function of T_e vanishing around $T_e \simeq 5000$ K, when CO is totally unbound (Luck 1981, private communication). From these equations it follows that any random or systematic error in the O abundance generates a spurious correlation between C and O and a spurious anticorrelation between N and O. Similarly, random errors in C generate an anticorrelation between C and N. This perverse circulation of the errors can qualitatively (but not quantitatively) mimic the action of both the CN and ON cycles, a point to which we shall return.

In warmer stars, such as Cepheids, CO molecules are much less important, and the spurious C-O correlation almost vanishes. Similarly, the spurious anticorrelation between C and N is avoided when atomic N lines are used.

A check of theoretical predictions requires a knowledge of the initial CNO abundances. If evolved stars are members of a cluster, their initial CNO abundances can be inferred from observations of unevolved stars. More often, observed stars do not belong to a cluster; if $[\mathrm{C/Fe}]_0 \simeq [\mathrm{N/Fe}]_0 \simeq [\mathrm{O/Fe}]_0 \simeq 0$, as appears to be the case in main sequence stars with near-solar composition [cf. Clegg et al. (46)], the initial CNO abundances in evolved stars can be inferred from [Fe/H]. With this assumption, then, the variation in the number abundance of the element X is given by: $\delta(X) = \varepsilon(X) - \varepsilon(X)_\odot \, \mathrm{dex}\{[\mathrm{Fe/H}]\}$, where $\varepsilon(X)_\odot$ is the solar number abundance of the element X, while [Fe/H] and $\varepsilon(X)$ are the derived

abundances for the program star. Canonical first dredge-up theory predicts (if $[C/Fe]_0 = 0$) $\delta(C) = -\delta(N) \simeq 1.5 \times 10^8$ dex$\{[C/H]_0\} = 1.5 \times 10^8$ dex $\{[Fe/H]\}$, and $\delta(O) \cong 0.0$.

Conservation of CNO nuclei requires $\delta(C) = -\delta(N)$, if only CN-cycled material has been brought to the surface, or $\delta(N) = -\delta(C+O)$, if also ON-cycled material has been carried to the surface by some mixing process. These conditions allow an internal consistency check of observationally derived abundances: a violation of conservation constraints would imply that either initial or present abundances have been improperly estimated. In the former case, either the derived [Fe/H] could be wrong, or the assumption $[X/Fe]_0 = 0$ is not justified. Note that the propagation of the errors described by (3.) does not conserve nuclei. It is also clear that a relatively large sample of stars must be analyzed in this way, since (apart from systematic errors) internal errors are typically 0.1 to 0.3 dex, which implies large errors (by a factor of 2 or more) in the derived $\delta(X)$ values. Therefore, the unambiguous detection of evolutionary abundance changes is particularly difficult.

The motivation for this preliminary discussion has been to emphasize that CNO abundance analyses require assumptions that may or may not be justified, and that a critical examination of the data is required before drawing any conclusion about stellar mixing processes.

6.1.1 GIANTS In the case of $^{12}C/^{13}C$ ratios, there is only partial agreement with the observations (see, for example, 141). While the majority of stars appear to have $^{12}C/^{13}C$ values consistent with the standard theory, a nonnegligible minority ($\sim 30\%$) appear to have $^{12}C/^{13}C$ values considerably lower (cf. 60, 95). A few stars with $^{12}C/^{13}C \lesssim 30$ are possibly currently experiencing the third dredge-up phase. The origin of the ^{13}C-rich stars is still unclear, and the most likely possibilities include (*A*) a nonsolar initial $^{12}C/^{13}C$ ratio, (*B*) extra CN-cycling produced by some sort of "extramixing," and (*C*) mass exchange in binary systems.

A. Primordial inhomogeneities The $^{12}C/^{13}C$ ratio in the interstellar medium is still quite uncertain. The most recent determinations give a value around 70 (244), with an indication of variations from one molecular complex to another. However, these variations are of the same order as the errors, and a universal $^{12}C/^{13}C$ ratio equal to the solar ratio cannot be ruled out. At any rate, while at least some stars with a ratio around 15 may have been ^{13}C-rich at formation, primordial inhomogeneities are very unlikely to be the origin of the most extreme ^{13}C-rich stars for which $^{12}C/^{13}C \gtrsim 10$.

B. Extramixing Owing to the uncertainties in the physics of hypothetical extramixing, it is clear that the theory needs to be guided by the

observations. It is important to observe ^{13}C as well as ^{12}C, N, O, and the light elements (Li, Be, and B) in the same stars, thus having information on the depth at which extramixing has occurred (if at all).

The study of Lambert & Ries (142) moves in this direction: using their data, one derives $\langle\delta(O)\rangle \simeq 0.0$, $\langle\delta(C)\rangle = -(1.35 \pm 1.31) \times 10^8$, and $\langle\delta(N)\rangle = +(1.18 \pm 0.80) \times 10^8$ for 31 giants (excluding the extreme case of 37 Com). These figures are quite consistent with canonical mixing alone. The agreement is particularly good for the Hyades giants, which also exhibit "canonical" $^{12}C/^{13}C$ ratios. However, ^{13}C-rich giants also appear richer in N and poorer in C compared with canonical predictions.

C. Duplicity Membership in a binary can affect in various ways the $^{12}C/^{13}C$ ratio of giants. We distinguish three cases: (*a*) A merged low-mass companion (233). A low-mass and fully convective companion ($M \lesssim 0.4$) is homogeneous and has a very low $^{12}C/^{13}C$ ratio. When the primary fills its Roche lobe, the companion can merge with the primary and the system degenerates to a single star (250). Clearly, a ^{13}C-rich star is produced, and this property is preserved during its subsequent evolution. (*b*) A double first dredge up. A more-massive companion can fill its Roche lobe after completion of its first dredge-up phase. In this way the accreting star acquires an envelope with $^{12}C/^{13}C \simeq 20$. The primary star then becomes a white dwarf. Subsequently, the secondary evolves to the giant branch and suffers its own first dredge up, further reducing the surface $^{12}C/^{13}C$ ratio. (*c*) A companion with envelope burning. A more-massive companion can fill its Roche lobe during its AGB phase. If it is massive enough [at least more massive than about 3 $M_\odot$ (197)], the EB process may have reduced its envelope $^{12}C/^{13}C$ ratio to the equilibrium value (~ 3.5). In this way the secondary star acquires an extremely ^{13}C-rich envelope. The primary star then becomes a C-O white dwarf. After exhausting hydrogen at its center, the secondary star will evolve to the giant branch and, on experiencing its first dredge up, will display a slight increase in the $^{12}C/^{13}C$ ratio at its surface!

An observational check of possibilities (*b*) and (*c*) appears feasible. Small radial velocity variations should be detectable as a result of the orbital motion of the red giant, as in the case of the Ba II stars (154). The WD companion might be detected in the UV, as in the case of the Ba II star ζ Cap (33).

6.1.2 CEPHEIDS AND SUPERGIANTS With very few exceptions, classical Cepheids have experienced the first dredge-up phase and are in the phase of core helium-burning. The same is true of G and K supergiants, which, together with Cepheids, are for the most part intermediate-mass stars. What makes them particularly interesting in the context of composition

changes is that their main sequence progenitors are typically rotating rapidly enough that extramixing processes in them, if they are effective anywhere, should be optimally active. Further, since they have been on the red giant branch, still other mixing processes operating during this phase may have had an opportunity to bring processed matter to the surface.

A recent study by Luck & Lambert (148, hereinafter LL) has come to the startling conclusion that the distribution of the CNO elements at the surfaces of Cepheids has been achieved by the mixing to the surface of matter in which considerable O (as well as C) has been processed into N. The LL study, which also provides CNO abundances for a few nonvariable (NV) supergiants, is complemented by an earlier study by Luck (146) of CNO abundances in a fairly extended sample of late-type (G and K) supergiants (luminosity class Ib). If taken at face value, the Lambert (141) and LL interpretations of the observational data imply that substantial extramixing has occurred either during the main sequence phase or during the brief red giant phase prior to the ignition of helium. This has such important implications for the theory of stellar evolution that we have taken the liberty of rediscussing the data.

Using $\delta(X) = \varepsilon(X) - \varepsilon(X)_{\odot} \cdot \mathrm{dex}\{[\mathrm{Fe/H}]\}$, we have obtained $\delta(X)$ values for $X = \mathrm{C}$, N, and O by taking the individual values of $\varepsilon(X)$ and [Fe/H] given by the quoted authors. On plotting $\delta(\mathrm{N})$ vs. $\delta(\mathrm{C+O})$ for LL Cepheids and NVs we find that (*a*) there is no correlation whatsoever between the N enhancement, $\delta(\mathrm{N})$, and C + O depletion, $\delta(\mathrm{C+O})$; (*b*) the C + O depletion is systematically larger than the enhancement of N, with $|\langle\delta(\mathrm{C+O})\rangle|$ being larger than $\langle\delta(\mathrm{N})\rangle$ by a factor ranging from ~ 3 for Cepheids up to ~ 11 for Luck's NVs; and (*c*) NVs are, on the average, more discrepant than are the Cepheids with respect to the $\delta(\mathrm{N}) = -\delta(\mathrm{C+O})$ conservation constraint. We conclude that some systematic error may be affecting some of the present and/or initial CNO abundances. Owing to the large O underabundances found by Luck and LL, we suspect that O may have been systematically underestimated in the program stars. From Figure 8, which gives $\delta(\mathrm{N})$ vs. $\delta(\mathrm{C})$ for the whole Luck and LL sample, we see that $\langle\delta(\mathrm{N})\rangle \simeq -\langle\delta(\mathrm{C})\rangle$ for the Cepheids (but still the scatter is rather large) and that the NVs continue to exhibit systematic overdepletions of C with respect to the N enhancements.

This different behavior of Cepheids and NVs provides a strong hint that O has been, in fact, systematically underestimated. This is so because, while a good fraction of NVs suffer from the systematic errors described by (3.), this is not the case for the Cepheids. Correspondingly, only for NVs does an underestimate of O generate an overestimate of $|\delta(\mathrm{C})|$. This conclusion is reinforced by the fact that the C-O correlation shown in LL Figures 6 and 7 has almost exactly the same slope as that of the spurious correlation given

by (3.). We infer that most of the apparent C depletion in NVs is, possibly, solely a consequence of a systematic underestimation of O.

Assuming [O/Fe] = 0 for all NVs and using (3.), one can generate a new set of C and N abundances consistent with Luck and LL data, thus obtaining new values for δ(C) and δ(N). Unfortunately, most δ(N)s obtained in this way turn out to be negative, indicating an unphysical N depletion. We conclude that not only the present abundances, but also the initial abundances, may have been improperly estimated. Assuming $[C/H]_0 = [N/H]_0 = [O/H]_0 = 0$ (or, equivalently, [Fe/H] = 0) and [O/H] = 0 for all NV stars, and computing new $\delta(X)$s using (3.) and the $\delta(X)$, $\varepsilon(X)$, and [Fe/H] relationships, one obtains $\langle\delta(C)\rangle = -1.9 \times 10^8$ and $\langle\delta(N)\rangle = +2.2 \times 10^8$, which is in reasonable agreement with canonical first dredge-up predictions [$\delta(N) = -\delta(C) = 1.5 \times 10^8$]. By assuming solar initial abundances, without changing the present CN (these abundances having been derived by a different method in LL), one can also obtain revised δ(C) and δ(N) values for the LL Cepheids. The new $\delta(X)$ values obtained in this way show that (*a*) systematic departures from the $\delta(N) = -\delta(C)$ line have almost completely disappeared, (*b*) the scatter for Cepheids has been greatly

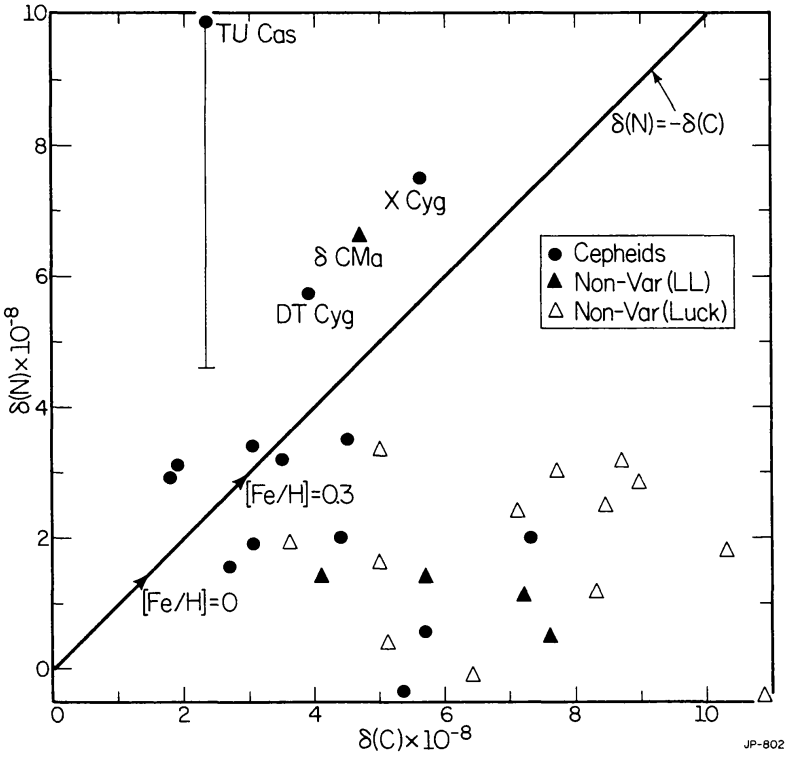

Figure 8 The abundance variation δ(N) vs. δ(C) taking the Luck (146) and Luck & Lambert (148) abundances at face value, and assuming $[CNO/Fe]_0 = 0$. CN processing would imply $\delta(N) = -\delta(C)$, on average. The effect of the 0.3-dex uncertainty in the nitrogen determination is shown for TU Cas. The expected effect of the standard first dredge up is shown for two values of [Fe/H].

reduced, and (*c*) the LL NVs have δ(N) values that are systematically larger than those of Luck's stars.

Point (*a*) further strengthens our suspicion that O has been systematically underestimated in all stars, and indicates that, conversely, [Fe/H] has been systematically overestimated by Luck (146); indeed, this is confirmed by recent redeterminations (147). Point (*b*) suggests that the scatter in [Fe/H] among LL Cepheids (from -0.13 to 0.34) is primarily due to observational errors, and point (*c*) indicates that, in LL NVs, N has been obtained from N I lines rather than from CN lines [and in this case (3.) does not apply]. In fact, two NVs (α Aqr and β Dra) have been analyzed both by Luck and by LL, and, while C is in very close agreement, N is systematically lower by an average of 0.2 dex in LL, suggesting that N I rather than CN has been used for the LL analysis (confirmed by Luck, private communication). We note that the 0.2-dex difference is almost precisely what one expects as a result of the O (and induced C) underestimation. Thus, the cases of α Aqr and β Dra provide an independent indication that, quite possibly, O has been underestimated. Moreover, when the LL nitrogen abundances for the NVs are used, the corresponding δ(N) values cease to be exceptional.

Whatever abundances are adopted, four stars (δ CMa, TU Cas, X Cyg, and DT Cyg) are distinctly apart from the others, in spite of the "data-massaging" to which they have been subjected. They appear to be much richer in N than all other stars. However, the typical LL 1σ internal error is $\sim$0.3 dex, and therefore these few cases need not be considered as established deviants. Excluding the four anomalous stars, one obtains $\langle\delta(\mathrm{C})\rangle = -(2.1 \pm 0.7) \times 10^8$ and $\langle\delta(\mathrm{N})\rangle = (1.8 \pm 1.1) \times 10^8$ for the remaining 27 variable and NV objects. Hence there is only very marginal evidence for mixing beyond canonical first dredge-up predictions.

These considerations show how small random and systematic errors in both the derived present abundances and in the guessed initial abundances can generate spurious correlations hiding any real effect. Disappointingly enough, it appears that a substantial improvement in the accuracy of abundance determinations is required before drawing any firm conclusion about CNO processing in intermediate-mass stars.

Our final conclusions, which disagree with those of Lambert (141) and LL, are that (*a*) there is no evidence that ON-cycled materials have been brought to the surface of the studied stars, and (*b*) there is some evidence for CN-cycled materials being present, but the abundance changes are, within the observational errors, consistent with canonical first dredge-up predictions. These conclusions suggest that, in main sequence intermediate-mass stars at least, μ-gradients prevent extramixing processes from significantly altering the ^{12}C, N, and O distributions established locally by nuclear processing.

7. COMPARISON WITH THE OBSERVATIONS II. THE SURFACE COMPOSITION OF AGB STARS

The variety of composition "peculiarities" exhibited by red giant stars has been recently reviewed by Scalo (214). Basically, three types of peculiarities are found (often in the same star): (*a*) nonsolar C/O ratios (carbon stars, MS, and S stars), sometimes accompanied by a low $^{12}C/^{13}C$ ratio; (*b*) enhancement of *s*-process isotopes (notably Tc); and (*c*) very large Li overabundances (in a few stars). Qualitatively, all of these peculiarities are produced by existing AGB models, thanks to the combined effect of the third dredge-up process and of the EB process. The problem is to establish whether theoretical models can also quantitatively account for the observations and to derive inspiration from possible failures as to how model deficiencies may be remedied. Our task is not a trivial one. On the one hand, theoretical predictions depend on a large variety of assumptions [here parameterized as η, M_{PN}, ℓ/H, $\psi(M_i)$, and the like]. On the other hand, the observational material is extensive, is scattered in an enormous number of papers, is subject to a variety of selection effects, and is very rarely in a quantitative format (particularly as far as abundances are concerned).

To complicate matters still further, perhaps some 50% of all intermediate-mass stars are born in binary systems. After developing their own chemical peculiarities, some of these will fill their Roche lobes and transfer their pecularities to their companions. The final surface abundance of a companion will of course depend not only on the composition of the accreted material, but also on the amount of dilution with the envelope of the secondary. Clearly, "binarism" will further magnify the variety of composition patterns already present in single AGB models. Altogether, current AGB theory is able to generate a stellar zoo at least as variegated as that found in the observational literature.

Low-mass evolved secondaries with surface peculiarities can spend several times 10^8 yr during their first red giant phase. Thus, if only one percent of all low-mass giant branch stars were to develop peculiar surface compositions by virtue of accretion from a short-lived AGB star of peculiar surface composition, such stars would easily outnumber single peculiar AGB stars, which live only $\sim 10^6$ yr. The two groups of peculiar stars are expected to be distinguishable according to luminosity. Single stars can develop their own peculiarities only after they become brighter than at least $M_{bol} \sim -3.5$. Hence, peculiar red giants fainter than $M_{bol} \cong -3.5$ are very likely secondaries in the first red giant branch phase of evolution rather than single stars in the AGB phase. They include Ba II stars, most R-type carbon stars, and CH stars. Radial-velocity measurements of Ba stars by

McClure et al. (154) demonstrate that many Ba stars are indeed binaries, and give welcome support to the idea that the chemical peculiarities of giants of low luminosity are the result of mass transfer.

We first emphasize that, of the two basic observables (M_{bol} and T_e), only the first one is accurately predicted by AGB models. As is well known, model T_e values are extremely sensitive to the treatment of convection, and also depend on (generally unavailable) molecular and even perhaps grain opacities. Furthermore, current theoretical AGB stars of all masses span a quite restricted range in T_e so that, at any T_e, one may expect to encounter stars of a variety of initial masses and luminosities, and a tight correlation between T_e and chemical peculiarities is not to be expected unless, of course, the development of peculiarities leads to large changes in surface opacities and therefore in stellar radius.

In contrast, as discussed in Section 2, current AGB models suggest that a threshold luminosity exists for every process affecting the surface composition: (*a*) dredge up of carbon occurs above a quiescent luminosity $L = L(M_H^{min}) = L_D$, M_H^{min} being the minimum core mass for which the third dredge-up process operates, and surface C exceeds surface O when $L > L_C > L_D$; (*b*) dredge up of *s*-process isotopes in the solar-system distribution will occur for $L \gtrsim L(M_H \sim 1.0) = L_{ss}$; and (*c*) envelope burning converts ^{12}C into ^{13}C and ^{14}N when $L > L_{EB}$. All of these critical luminosities are mass and initial-composition-dependent, and only the second one does not depend on ℓ/H. Finally, since low-level *s*-process production is expected to occur in all AGB stars that experience dredge up, it is expected that, once $C \cong O$ at the surface, a star will be seen as an S star. This will occur at a mean $L = L_S = L_C$. For all of these reasons, bolometric magnitudes of peculiar giants represent the most important quantity in comparing theory with observations.

Unfortunately, the distance of most galactic peculiar giants is very poorly known, and any sample is likely to be somewhat contaminated by low-luminosity stars with externally acquired peculiarities and to be distorted by selection effects (particularly in the case of samples that are apparent-magnitude-limited). We therefore avoid any further discussion of field stars in our Galaxy (except for stars showing *s*-process enhancements), but stress that it would be very useful for future comparisons to have reliable bolometric magnitudes (via IR photometry) for the few galactic C stars of known distance (cf. 91).

7.1 *Carbon Stars in Magellanic Cloud Globular Clusters*

C stars have been found in several Cloud clusters (3, 24, 78, 80, 157, 158). In all studied C-star-containing clusters but one (NGC 1651), every C star is brighter than the brightest M star in the same cluster. As some 20–50% of all

low-mass TP-AGB stars are expected to be within a (one-half to one magnitude deep) postflash luminosity dip (see Section 2) and roughly half of the stars that pulsate dynamically will be in the low-luminosity phase of the light curve, it is in fact surprising that there are not more cases in which a C star is less bright than several M stars. We conclude that the available evidence from Cloud clusters is qualitatively in agreement with the third dredge-up theory, which predicts that AGB stars become C stars when the quiescent luminosity exceeds a critical value.

The data suggest that, for low-mass stars, this critical luminosity is around $M_{\rm bol} \cong -5.0 \pm 0.2$, with C stars that are in the range $\sim -5.0 < M_{\rm bol} < \sim -4.2$ ($\sim 25\%$ of the entire sample) being in a postflash dip and/or around a light curve minimum. In turn, this argues that fresh carbon begins to be injected into the stellar envelope when the core mass reaches a value somewhere between 0.60 and 0.65 $M_\odot$. If the third dredge-up process is responsible for the appearance of carbon at the surface, then $M_{\rm H}^{\rm min}$ must be in this range. Smaller values of $M_{\rm H}^{\rm min}$ would indeed produce too many C stars fainter than $M_{\rm bol} \cong -4.0$. The fact that dredge up at $M_{\rm H} \simeq 0.6$ has actually been found in several low-Z, low-M models (115, 118) should encourage further intensive theoretical work on low-mass AGB stars, with a fairly extended coverage of the parameter space ($M_{\rm i}$, ℓ/H, and composition), and application of refinements in the pertinent input physics (in particular, in the intermediate temperature opacities of carbon-rich mixtures).

Frogel & Blanco (76) have examined 32 Cloud clusters to determine the M-star to C-star transition luminosity as a function of cluster age [using the classification scheme in (224)]. They find a convincing correlation between the transition luminosity and youth, with the average $M_{\rm Bol}^{\rm transition}$ decreasing from about -3.7 for class VII clusters ($\sim 10^{10}$ yr) to about -5.5 for class II clusters ($\sim$ few 10^8 yr). This is qualitatively in accord with theoretical predictions (see Figure 7), which show that the initial interpulse magnitude at which the TP-AGB phase begins decreases from about -4 to -6 as the progenitor main sequence lifetime decreases from $\sim 10^{10}$ yr to $\sim 10^8$ yr.

The absence of C stars in the very youngest clusters ($< 10^8$ yr) suggests that either dredged-up carbon is efficiently converted into nitrogen or that a superwind terminates the AGB phase when (or before) C exceeds O and $M_{\rm Bol} \gtrsim -6$.

7.2 *Observations of Field Carbon Stars in the Magellanic Clouds*

Extensive surveys of field C stars in the Clouds are now available in the literature. Recognition of C stars is achieved by using objective prism or grism plates, and by noting the presence either of the C_2 Swan bands in the

blue-green (212, for LMC, hereinafter SP), or the CN bands in the near-IR (257, for LMC, hereinafter WORC; and 28, for both SMC and LMC, hereinafter BMB). Westerlund (256) has remarked that in the blue-green surveys about 400 stars not identified in his near-IR surveys were found. In the BMB surveys of selected regions, however, the stars from the blue-green survey falling in the regions were picked independently. Nevertheless, the stars found in the blue-green survey may include hotter C stars, and some of them (but not all) are hydrogen deficient (201). Such hotter stars may have weak near-infrared CN bands, and, as emphasized by BMB, would be missed in their survey. Apart from this limitation, the BMB survey appears fairly complete.

As far as oxygen stars are concerned, the BMB survey includes only stars of spectral type later than M5, implying that only a small minority of E-AGB and a fraction of TP-AGB oxygen stars have been detected. Spectral types for the M stars in the SP survey are not available. A survey of oxygen stars in the LMC has been recently published by Westerlund et al. (258, hereinafter WOH). It includes stars later than M0, with the somewhat artificial grouping into "supergiants" (earlier than M5) and "giants" (M5 or later). Since many of the SP stars do not appear in the WOH survey, they are probably K giants (supergiants). We conclude that reasonably complete LFs for E-AGB and TP-AGB oxygen stars are not yet available.

As noted by Blanco et al. (25) and by Blanco & McCarthy (27), the number ratio of C- to M-type stars (later than M5!) exhibits enormous variations in going from the galactic bulge (C/M $\cong$ 0.002), to the solar neighborhood ($\sim$0.01), to the LMC ($\sim$1.7), and to the SMC ($\sim$25). The existence of a C/M gradient in the galactic disk has also been established (26, 255). Metallicities and age variations are presumably responsible for these large differences in C/M. In fact, theory indicates that (*a*) for decreasing metallicity the fraction of AGB stars becoming C stars increases, as does the fraction of the AGB phase during which a star is C-type; (*b*) for decreasing metallicity, the AGB tracks shift to higher temperatures and the fraction of AGB stars later than M5 rapidly drops [e.g. all AGB stars in galactic globular clusters are K-type, and all oxygen stars in the MC clusters containing C stars are earlier than M5 (cf. 32, 78)]; and (*c*) if a population is sufficiently old (the precise age depends on $M_{\rm H}^{\rm min}$ and Z), no star becomes C-type, simply because the stellar envelope "evaporates" before $M_{\rm H} = M_{\rm H}^{\rm min}$. Note that, given the current limitation on M star identification (none earlier than M5), point (*b*) is at least as important as point (*a*) in producing C/M changes with metallicity.

Further, theoretical C/M values, homogeneous with the observational ones, cannot be reliably computed, as one does not know how to reliably assign spectral types to model oxygen stars. Nevertheless, we are hopeful

that the observed differences can be entirely accounted for by current theory, once it has been worked out in sufficient detail. Scalo (214) reaches the opposite conclusion, comparing theoretical C/O-rich ratios for synthetic TP-AGB stars from Renzini & Voli (197) with observed C/M values (M later than M5!). From the close resemblance of the observed M- and C-type (partial) LFs in the LMC, Scalo also concludes that the production of C star characteristics is due to a stochastic process that, for a given mean luminosity and initial composition, works in some stars and not in others. The distributions constructed here (see Section 7.3) and by Iben (109) show that, in fact, overlap and even close resemblance of the two distributions follows quite naturally from the third dredge-up theory, given an appropriate dredge-up law. Thus, the distributions of field C stars and M stars are not evidence for a stochastic dredge-up process. In conclusion, although a definitive quantitative comparison between theoretical and observational C/O ratios in various stellar populations must be postponed until complete LFs for oxygen stars (K- and M-type) in various populations are available, the prognosis for a reasonably satisfactory match between theory and observation is bright.

We note finally that the larger proportion of C stars in the SMC compared with that in the LMC, and in the LMC compared with that in the Galaxy, should immediately translate into a different relative proportion of carbon and silicate grains in the interstellar medium of the three galaxies. It is therefore no surprise that the UV extinction curve is indeed quite different in these galaxies (204) and that the differences correlate with the frequency of C stars.

7.3 *A Comparison of Theoretical and Observed Distributions*

Bolometric magnitudes of C stars from the BMB survey have been obtained for the so-called BMB Bar West field in the LMC, (199, 200) and for various BMB fields in both the LMC and the SMC (48, 79). The observed LFs confirm that Cloud C stars are TP-AGB objects ($M_{\rm bol} < -3.5$), but they look remarkably different from theoretical LFs (48, 79, 109, 200) prepared prior to the very recent discovery of dredge up for small $M_{\rm H}$ (117, 118). More specifically, the observed LF peaks at $M_{\rm bol} \cong -5.0$, with very few stars fainter than $M_{\rm bol} = -4.0$ or brighter than $M_{\rm bol} = -6.0$, while the theoretical LFs peak at $M_{\rm bol} \cong -6$, with very few stars fainter than $M_{\rm bol} = -5.0$, and extend to $M_{\rm bol} \cong -7.3$. That is, faint C stars ($M_{\rm bol} \gtrsim -5.0$) are not produced by the models, while bright theoretical C stars ($M_{\rm bol} \lesssim -6.0$) have far too few observed counterparts. The ramifications of these discrepancies are discussed extensively by Iben (109). New calculations that take opacities for low-temperature carbon-rich matter properly into

account (117, 118) remove the discrepancies at low luminosity. Unfortunately, time does not permit the construction of theoretical LFs that incorporate the new model results.

In constructing all of the LFs shown in Figure 9, the following assumptions have been made: (*a*) $\psi(M_i) \propto M_i^{-2.35}$ (if not specified otherwise); (*b*) $Z = 0.004$ for $M_i < 2$ and $Z = 0.012$ for $M_i > 2.5$, so as to roughly mimic a chemical evolution of the LMC; (*c*) initial C and O abundances as in Renzini & Voli (197); (*d*) "Case A" for the PN ejection, if not specified otherwise; (*e*) $M_H^{min} = 0.5$; (*f*) $\delta M_{bol} = 0.5$, for the postflash dip, with a "recovery" time $0.2\Delta t_{ip}$; and (*g*) $L(M_H, M)$ as given by (1′.). We emphasize that the last three assumptions are somewhat inconsistent with several of our previous conclusions. A choice such as $M_H^{min} \cong 0.6$, $\delta M_{bol} \cong 1.0$, and an interpulse recovery time $\sim 0.4\Delta t_{ip}$ would have been more appropriate for the lowest-mass stars. Further, (1′.) somewhat overestimates the maximum quiescent stellar luminosity as a function of M_H for the lowest-mass stars. Correspondingly, the low-luminosity part of each LF is to be viewed only as suggestive, and we here concentrate on the behavior of the high-luminosity side. Moreover, our LFs apply only to TP-AGB stars, E-AGB stars not having been taken into account.

Figure 9*a* shows that $\sim 29\%$ of model C stars are brighter than $M_{bol} = -6.0$ ($f_6 = 0.29$, f_6 being the fraction of C stars brighter than $M_{bol} = -6.0$). This is clearly at variance with the observations, where very few stars (later than M5 or C2!) are brighter than $M_{bol} = -6$. The model stars with $M_i \lesssim 2$ have total nuclear-burning lifetimes of less than 10^9 yr, and one easy way to resolve the discrepancy with the observations is to assume that appreciable star formation has not occurred in the surveyed fields during the last 10^9 yr or so (109, 110, 191). Actually, there are indications that the bulk of star formation in the LMC occurred (3–5) $\times 10^9$ yr ago (38). However, in Cepheid and C star surveys that cover the entire LMC, over 1000 Cepheids have been identified (174), but only a handful of C stars brighter than $M_{bol} = -6.0$ have been found (cf. 201, 223). Typical LMC Cepheids are progeny of intermediate-mass stars with main sequence lifetimes less than a few times 10^8 yr, and bright ($M_{bol} < -6$) AGB stars are progeny of Cepheids. Since the lifetime of a typical Cepheid is comparable to the expected lifetime of a bright AGB C star ($\sim 10^6$ yr), one expects comparable numbers of Cepheids and bright C stars, in contrast to the situation in the LMC as a whole. Thus, the "bright C star" discrepancy applies to the LMC as a whole, and one cannot invoke the "old age solution" to resolve it. More recently, Becker (19) finds at least 9 Cepheids in the Bar West field! So, even in the case of the BMB fields, there is no escaping embarrassment by invoking ages $> 10^9$ yr. The presently available data thus strongly indicate that there may be some cause preventing AGB stars from appearing as bright C stars.

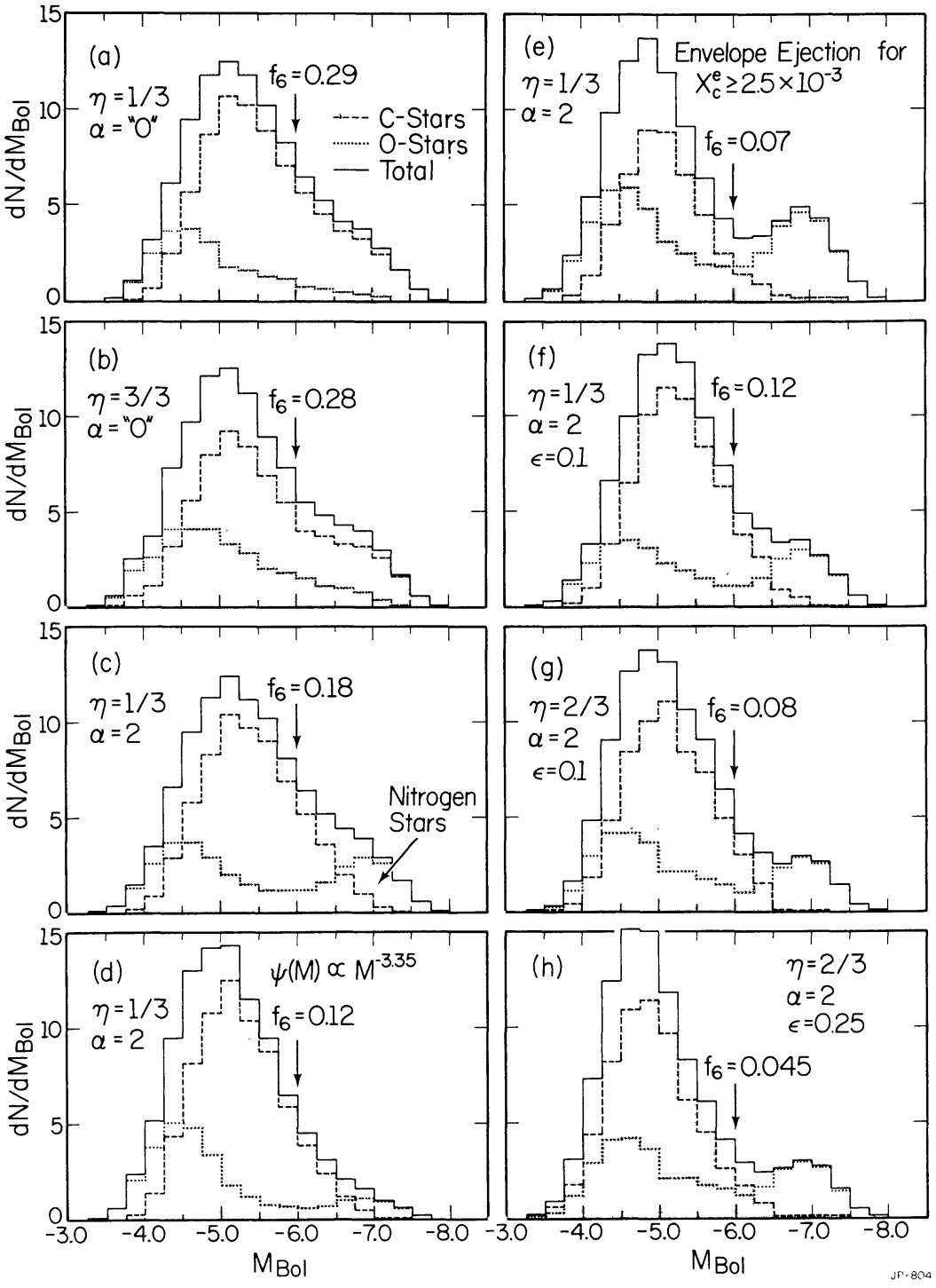

Figure 9 Luminosity functions for TP-AGB stars, as resulting from a variety of assumptions (see text). The cases with $\alpha =$ "0" (panels *a* and *b*) result from neglecting the envelope-burning process. For all other cases, $\alpha = \ell/H = 2$. The high-luminosity peak in the LFs for O-rich stars is produced by the inclusion of the envelope-burning process, and represents the expected LF of nitrogen-rich stars.

This conclusion can be avoided only if the bright C stars are either too red or too blue to have been detected in the near-infrared.

Fortunately there are other possible ways of alleviating the problem of the missing bright C stars. Figure 9*b* shows that increasing the normal MLR by increasing η from 1/3 to 1 has essentially no effect (f_6 decreases from 0.29 to 0.28!). This is so because the TP-AGB lifetime is almost equally affected for all values of M_i (cf. Figure 7). A more substantial improvement is obtained when envelope burning is included in the calculations (f_6 drops to 0.18 for $\ell/H = 2$; cf. Figure 9*c*). This is because for large ℓ/H and large M_i, dredged-up carbon is efficiently converted into nitrogen, thereby preventing C/O from growing beyond unity; the very brightest AGB stars are now oxygen stars very rich in nitrogen, with N/O up to 10 (197), and if they have a spectrum earlier than M5, they would not appear in the survey by BMB. If, further, they are of the type WOH call "supergiants" (*Sp.* $\leq$ M4), most of them should show *s*-process isotopes in nearly the solar-system distribution. Bright, long-period variables ($-6.0 \gtrsim M_{bol} \gtrsim -7.3$) that are not C stars have been actually identified in the field by Wood et al. (269), and these variables show strong ZrO bands. These stars thus may provide evidence that AGB stars with $M_i \gtrsim 3$ (*a*) dredge up carbon; (*b*) process this carbon into nitrogen; and (*c*) produce and dredge up neutron-rich isotopes.

Nevertheless, there are still rough spots in the theoretical models that are not inconsequential. Figure 10 shows AGB evolutionary lines in the M_{bol}-log(C/O) plane, and a comparison with Figure 9*c* indicates that C stars brighter than $M_{bol} = -6.0$ are still produced by stars in the mass range $2 \lesssim M_i \lesssim 3$, for which envelope burning does not occur or is not efficient enough to prevent the development of C star characteristics. Figure 9*d* shows that adopting a steeper weighting function, $\psi(M_i) \propto M_i^{-3.35}$, does not help much: f_6 decreases only to 0.12. Clearly, some other mechanism must be invoked to prevent stars with $2 \lesssim M_i \lesssim 3$ from becoming brighter than $M_{bol} = -6.0$. Figure 10 shows that these model AGB stars develop extremely high surface carbon abundances (C/O greater than 10!), and it would be quite surprising if such extreme surface compositions would not have direct consequences for mass-loss processes and/or for circumstellar (CS) absorption. For illustrative purposes, we have assumed that envelope ejection occurs as soon as the abundance of excess carbon exceeds 2.5×10^{-3} by mass (a catastrophic condensation of graphite grains in the atmosphere?). Asterisks in Figure 10 mark the points where this is assumed to occur. The corresponding LF is shown in Figure 9*e*, and now one has $f_6 = 0.07$.

Absorption by CS graphite must also be considered. The absolute bolometric magnitude of C stars in the Clouds and in other stellar systems is currently most accurately determined from near-IR (JHK) photometry

(Frogel et al. (80)). However, the M_{bol} estimated from near-IR photometry may not reflect the actual bolometric luminosity of a C star if substantial CS reddening occurs (49, 109, 110, 191). Actually, C stars have high MLRs, and C-rich grains are likely to form in the expanding CS envelope. In turn, these carbon grains could efficiently absorb the near-IR stellar radiation, redistributing it to longer wavelengths. Direct observational evidence of substantial CS absorption and reemission does indeed exist for many galactic C stars (e.g. CW Leo, but see also 49, 90, 131). Assuming that grains are in the form of clean graphite, and using the absorption coefficient of small graphite grains (156), we can estimate the optical depth of the CS envelope: $\tau_\lambda = 2.35 \times 10^{12} \varepsilon (2.2\mu/\lambda)^{1.5} Y_{FC} \dot{M}/R$, where Y_{FC} is the number abundance of excess carbon, λ is the wavelength in microns, and ε is an efficiency parameter, which we write as $\varepsilon = f(10/v_{exp})/(R_g/2R)$. Here, f is the fraction of excess carbon that actually condenses into graphite grains, R_g is the condensation radius in solar units, and v_{exp} is the wind velocity in km s^{-1} at $r = R_g$. For simplicity we have assumed that v_{exp} is constant even beyond $r = R_g$. Obviously, τ_λ depends on a combination of parameters, each of which is poorly known. We will treat ε as a free parameter, while the other quantities appearing in τ_λ follow directly from the evolutionary calculations. From our expression for τ_λ we can derive the reddening

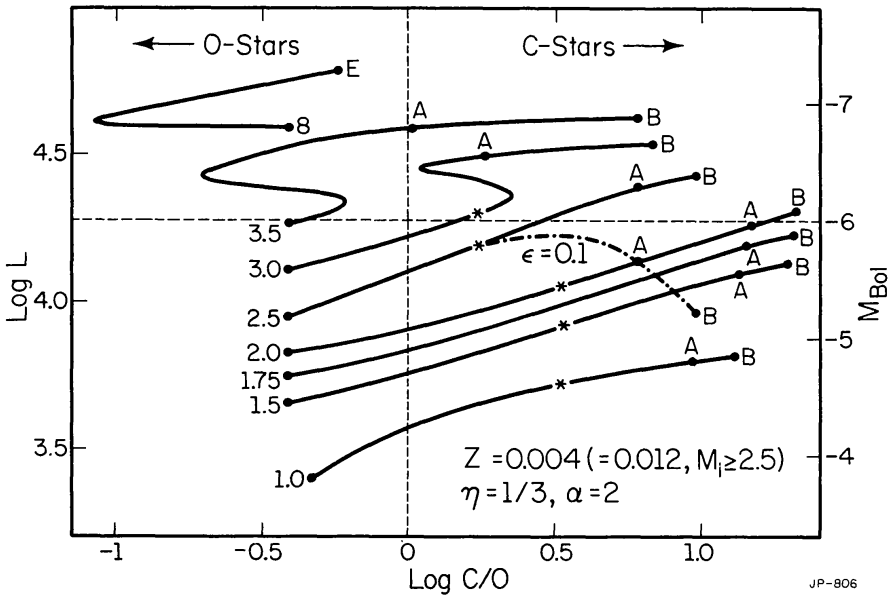

Figure 10 TP-AGB evolutionary lines in the log L vs. C/O plane. Each line is labeled with the value of the initial mass M_i. Stars with $M_i > 3$ experience the envelope-burning process. The effect of circumstellar graphite absorption is shown for the case $M_i = 2.5$ (dot-dashed line). Points A and B correspond to the envelope ejection, respectively, for "Case A" and "Case B." Point E marks the termination of the TP-AGB phase for the star with $M_i = 8$. The asterisks indicate the point where a surface abundance of excess carbon $X_c^e = 2.5 \times 10^{-3}$ is reached.

relation between near-IR colors: $E(J-K) \cong 2.4E(H-K)$. Since this reddening relationship runs almost exactly parallel to the observed locus that may be inferred from the IR colors of Magellanic Cloud C stars (47) and of galactic C stars (162), it becomes clear that CS absorption may substantially affect the observed JHK colors.

Although there is no a priori guarantee that ε remains constant in the course of the evolution of a C star (or has the same value for stars of different initial mass and composition), we have nevertheless assumed it to be so in computing AGB LFs. We define a fictitious bolometric magnitude $M'_{\rm bol} = M_{\rm bol} + \delta K$, with $\delta K = 1.086\tau_K$, which is the "bolometric magnitude" as obtained from near-IR photometry (80) if the CS envelope of a C star has an optical depth τ_K.

Following these prescriptions, we estimate the effect of CS graphite absorption, and the result for a star of $M_i = 2.5$ and $\varepsilon = 0.1$ is shown in Figure 10 ($M'_{\rm bol}$ is plotted instead of $M_{\rm bol}$). The corresponding LF is shown in Figure 9*f*, which compared with the analogous case having no CS absorption (Figure 9*c*) indicates that f_6 has decreased from 0.18 to 0.12. Increasing η to 2/3, f_6 further decreases to 0.08 (Figure 9*g*), and, finally, on increasing ε to 0.25, f_6 drops to 0.045 (Figure 9*h*). We conclude that a combination of all these effects may be responsible for the lack of bright C stars in the Clouds. The problem is to find their individual importance; this can be achieved only with the help of new observations.

We now list crucial future observations that bear on these matters: (*a*) far-IR photometry (4–20 μ) of galactic and Magellanic Cloud C stars to assess the presence of CS absorption; (*b*) determination of the bolometric magnitude of the SP warm C stars, most of which are not included in current IR surveys; (*c*) a careful study of the stellar populations in the various Cloud fields (Cepheid and main sequence LFs); (*d*) a search for "nitrogen stars," i.e. AGB stars earlier than M5, with strong ^{13}CN bands, and with $-6.0 \gtrsim M_{\rm bol} \gtrsim -7.3$; and (*e*) C/O determinations for Cloud C stars.

These observations should eventually provide a decisive test of the theory of AGB stars. In the meantime, the most important theoretical problems remain the complete understanding of mixing processes in AGB stars and the determination of the dredge-up law when core mass is small.

7.4 *Neutron-Rich Isotopes in Red Giant Atmospheres*

The classification of a star as MS, S, or SC has sometimes been interpreted as evidence of *s*-process enrichment, thanks to the strength of the ZrO bands. (Zr is an *s*-process element.) However, molecular equilibrium calculations have shown that the relative intensity of TiO and ZrO bands is primarily a function of the C/O ratio (cf. 4, 129, 216, 235). Therefore, direct

abundance determinations from atomic lines are required to assess whether or not *s*-process isotopes are actually enhanced. Unfortunately, only a few such abundance analyses have been completed so far. In particular, see Boesgaard (29) for the Ti/Zr ratio and Little-Marenin & Little (145, LML) for the presence of Tc.

In the framework of the third dredge-up theory, every star has to pass through an S-type phase (C/O $\cong$ 1) before becoming a C star (C/O > 1). The stellar luminosity during the S star phase is expected to increase monotonically with M_i, as is the abundance of *s*-process isotopes (109, 110, 120). Similarly, the neutron exposure parameter Λ (describing the relative abundances of *s*-process isotopes) is predicted to vary systematically with M_i [for example, decreasing from $\sim$13 for $M_i = 2.5$, to $\sim$5 for $M_i \gtrsim 4$ (120)]. Much larger values of Λ are expected to be produced in models with low core mass, and, indeed, Λ is a poor parameter for the description of the neutron-rich isotope distributions expected in such stars. These theoretical predictions are in qualitative agreement with the Ti/Zr determinations (29), which show that, compared with its abundance in M stars, Zr appears to be genuinely enhanced in a sample of nine S stars.

The nucleosynthetic characteristics of the most relevant models ($M_i \gtrsim 2.5$) are just now beginning to be explored. The bulk of observed S stars are probably low-mass objects for which $M_i < 2.5$, and their neutron-rich isotopic distributions are not expected to resemble the solar-system *s*-process distribution ($\Lambda \cong 5.5$), which is so nicely reproduced and brought to the surface by more-massive models. The apparent absence of observational counterparts of these more-massive AGB stars, as emphasized in several reports (109–111) may be a chimera, as detailed in Section 7.3. Since, as discussed in Section 2.5, the neutron-rich isotope distribution formed in low-mass stars is expected to vary considerably from one low-mass AGB star to another, the characteristics of at least some of the variations in neutron-rich distributions found among "peculiar" giants (37, 56, 58, 181, 240) are understandable, especially if one excludes stars that may have achieved their abundance anomalies as a consequence of being in a binary system. The occurrence of neutron-rich isotope distributions flatter than the solar-system distribution of *s*-process isotopes (59) suggests much larger exposures than can be produced by the ^{22}Ne source and confirms that another source (presumably the ^{13}C source) is required, at least in some stars. Once again, a more detailed comparison has to be postponed until more models with $M_i \gtrsim 2.5$ and more-complete physics become available.

In more-massive stars ($M_i \gtrsim 5$, for solar initial abundance), envelope burning can prevent C/O from approaching unity. However, envelope burning does not tamper with the results of neutron capture processing, and, correspondingly, *s*-process enhancements are not necessarily confined

to S or C stars: some M stars, particularly the nitrogen-rich ones, may exhibit large *s*-process overabundances (in this case with a nearly solar distribution, as these stars must have fairly massive progenitors). The LML study shows indeed that Tc is present in quite a few M stars. If some of these objects are actually nitrogen-rich stars, they should also exhibit a low $^{12}C/^{13}C$ ratio, and, occasionally, strong CN bands.

The high proportion of Tc stars among late-type giants (spectral type S or later than M5) found by LML has been used by Scalo (214) and Scalo & Miller (215, SM) as evidence against the ^{22}Ne source. However, their argument suffers from the fact that the LML sample is magnitude limited ($B < 9.5$), thus including a larger proportion of brighter (more-massive) AGB stars. Since model TP-AGB luminosities range from $\log L \cong 3.3$ up to $\cong 4.8$, the brightest AGB stars (more *s*-process-enhanced, thanks to increased neutron production by the ^{22}Ne source) have been sampled in a volume some 30 times larger than that for the faintest (less *s*-process-enhanced) AGB stars. Note that the Galaxy is flat, so sampled volumes go roughly as the square of the limiting distance. This obvious selection effect is not considered by SM.

Population simulations of the Tc enhancement against effective temperature are also used by SM to infer that dredge up of *s*-process elements should only occur in AGB stars with core mass in a quite restricted range (e.g. $0.6 \lesssim M_H \lesssim 0.9$). However, their simulation is totally dependent on the adopted $T_e(L, M, Z)$ relation. For instance, using the Iben & Truran (120) relation, rather than the Becker & Iben (20) relation adopted by SM, just the opposite conclusion would have been reached; using the first relation, and the SM dredge-up assumptions, the degree of *s*-process enhancement at fixed T_e decreases with increasing luminosity (or M_i), while the opposite trend is found using the second relation. This underlines the fact that the temperatures of the models are uncertain, and that correlation with other observables (particularly luminosity) is less ambiguous, and should be preferred in comparing with the observations. LML note that the fraction of Tc stars is larger, the larger the pulsation period. Since the pulsation period is expected to increase with luminosity, there is an indication that the presence of Tc is more likely in brighter stars, as is expected when ^{22}Ne is the major provider of neutrons.

SM state that $\sim 30\%$ of the AGB stars in the LML sample that have enhanced *s*-process elements do not have Tc. This figure is based on the unverified assumption that all MS, S, and SC stars have high *s*-process abundances (not just strong ZrO bands). Out of the 9 such stars in the LML sample that do not show Tc, none have been checked for the Zr abundance [that is, they are not in the Boesgaard (29) sample]. However, two Boesgaard high Zr stars (HD 35155 and HR 1105) do not have Tc (175). The

C star UU Aur is also Zr-rich but does not have Tc (247). An additional distinctive property of these three stars is that they are nonvariable, contrary to all other stars with Tc (cf. LML, 175). This may indicate that the three stars are not in the AGB phase. The absence of Tc in them could be explained by assuming that each star is a binary that received *s*-process isotopes from an AGB primary some time in the past. The fact that they do not pulsate gives some support to this interpretation. Alternatively, we also note that the Tc/Zr ratio is expected to vary appreciably as a function of the stellar core mass. For instance, the number of flashes during one terrestrial half-life of ^{99}Tc ($\sim 2 \times 10^5$ yr) increases from less than 1 for $M_H = 0.6$, to ~ 80 for $M_H = 1.0$. Clearly, high Tc/Zr ratios can never be achieved in low-mass model AGB stars, whereas, in high-mass AGB stars, any Tc present will be the cumulative result of many previous pulses. These considerations indicate that the interpretation favored by SM does not preclude alternative sites for the origin of Tc-deprived stars.

Another relevant characteristic of Tc that has been overlooked in the SM argument is that, whereas an isotope such as ^{99}Tc will live for about 2×10^5 yr at the surface of a giant star, its lifetime at the high temperatures found in helium convective shells during thermal pulses can be considerably smaller (64). This is because several low-lying nuclear levels of such an isotope are populated at high temperatures, and the lifetime of these levels against β-decay can be estimated to be many orders of magnitude smaller than the lifetime (terrestrial) of the lowest state (53). In fact, under conditions found in convective shells during the peak of a pulse (for $M_H = 0.6 \rightarrow 1.4$), estimates (64) show the lifetime of ^{99}Tc to be comparable to the lifetime of the convective shell following pulse peak, rather than orders of magnitude larger, as is the case when the terrestrial lifetime is assumed. The full ramifications of these results have yet to be explored, but it is clear that arguments based on a large and constant lifetime for Tc are no longer tenable.

We conclude that, although challenged from many sides, the third dredge-up theory for the origin of peculiar giants, with the ^{22}Ne source for *s*-processing in the more-massive and the ^{13}C source for neutron capture processing in the less-massive intermediate-mass stars and in low-mass stars, is still the most useful tool in interpreting the advanced AGB evolution of low- and intermediate-mass stars. By this, we do not mean to imply that the theory as we present it is complete or even correct, recognizing that there are several physical processes that have not been taken into account. The most crucial observations for a conclusive check of the theory will be spectroscopic studies of complete and unbiased samples of AGB stars in the Magellanic Clouds.

ACKNOWLEDGMENTS

We are indebted to a number of scientists who have generously given of their time and advice: Gordon Baym, Steven Becker, Victor Blanco, Jay Frogel, Jay Gallagher, Susan Lamb, Earle Luck, André Maeder, Nino Panagia, Detlef Schönberner, James Truran, Volker Weidemann, and Peter Wood. We are particularly grateful to Jay Frogel, both for discussions and for a careful reading of the manuscript, which resulted in substantial improvements in organization. One of us (AR) acknowledges the support of the Italian Ministry of Foreign Affairs for a travel grant, and the other (I^2, Jr) reiterates his indebtedness to the US National Science Foundation for continued support. Finally, many, many thanks to Deana Griffin for her cheerful mien during many hectic days and for her competent typing of the large number of successive versions of the manuscript, and many thanks to Janus Wehmer for pinch-hitting at crucial moments.

A longer version of this paper appeared as a University of Illinois Astrophysics Preprint (IAP-82-2), and it may be obtained from the authors by direct request.

Literature Cited

1. Aaronson, M., Liebert, J., Stocke, J. 1982. *Ap. J.* 254:507
2. Aaronson, M., Mould, J. 1980. *Ap. J.* 240:804
3. Aaronson, M., Mould, J. 1982. *Ap. J. Suppl.* 48:161
4. Ake, T. B. 1979. *Ap. J.* 234:538
5. Aller, L. H. 1983. In *Planetary Nebulae*, ed. D. R. Flower, p. 1. Dordrecht: Reidel
6. Almeida, J., Käppeler, F. 1983. *Ap. J.* 265:417
7. Alschuler, W. R. 1975. *Ap. J.* 195:649
8. Anthony-Twarog, B. J. 1981. *Ap. J.* 245:247
9. Anthony-Twarog, B. J. 1982. *Ap. J.* 255:245
10. Arnett, W. D. 1969. *Astrophys. Space Sci.* 5:180
11. Arnett, W. D. 1982. In *Supernovae, A Survey of Current Research*, ed. M. J. Rees, R. J. Stoneham, p. 221. Dordrecht: Reidel
12. Arnould, M., Nørgaard, H. 1981. *Comments Astrophys.* 9:145
13. Bartolini, C., Bonifazi, A., D'Antona, F., Fusi-Pecci, F., Oculi, L., et al. 1982. *Astrophys. Space Sci.* 83:287
14. Baud, B., Habing, H. J. 1983. In *Planetary Nebulae*, ed. D. R. Flower, p. 530. Dordrecht: Reidel
15. Baud, B., Habing, H. J., Mathews, H. E., Winneberg, A. 1981. *Astron. Astrophys.* 95:156
16. Becker, S. A. 1979. PhD thesis. Univ. Ill.
17. Becker, S. A. 1981. *Ap. J. Suppl.* 45:475
18. Becker, S. A. 1981. In *Physical Processes in Red Giants*, ed. I. Iben Jr., A. Renzini, p. 141. Dordrecht: Reidel
19. Becker, S. A. 1981. *Ap. J.* 248:298
20. Becker, S. A., Iben, I. Jr. 1979. *Ap. J.* 232:831
21. Becker, S. A., Iben, I. Jr. 1980. *Ap. J.* 237:111
22. Becker, S. A., Iben, I. Jr., Tuggle, R. S. 1977. *Ap. J.* 218:633
23. Beer, H., Käppeler, F. 1980. *Phys. Rev. C* 21:534
24. Bessel, M. S., Wood, P. R., Lloyd-Evans, T. 1982. Preprint
25. Blanco, B. M., McCarthy, M. F., Blanco, V. M. 1978. *Nature* 271:638
26. Blanco, V. M. 1965. In *Stars and Stellar Systems*, ed. A. Blaauw, M. Schmidt, 5:241. Univ. Chicago Press
27. Blanco, V. M., McCarthy, M. F. 1981. In *Physical Processes in Red Giants*, ed.

I. Iben Jr., A. Renzini, p. 147. Dordrecht: Reidel
28. Blanco, V. M., McCarthy, M. F., Blanco, B. M. 1980. *Ap. J.* 242:938
29. Boesgaard, A. M. 1970. *Ap. J.* 161:163
30. Boesgaard, A. M. 1976. *Publ. Astron. Soc. Pac.* 88:353
31. Boesgaard, A. M. 1976. *Ap. J.* 210:466
32. Boesgaard, A. M., Chesley, S. E. 1976. *Ap. J.* 210:475
33. Böhm-Vitense, E. 1980. *Ap. J. Lett.* 238:L35
34. Bruenn, S. W. 1971. *Ap. J.* 168:203
35. Bruenn, S. W. 1972. *Ap. J. Suppl.* 24:283
36. Burbidge, E. M., Burbidge, G. R., Fowler, W. A., Hoyle, F. 1957. *Rev. Mod. Phys.* 29:547
37. Butcher, H. R. 1976. *Ap. J.* 210:489
38. Butcher, H. R. 1977. *Ap. J.* 216:372
39. Cameron, A. G. W. 1955. *Ap. J.* 121:144
40. Cameron, A. G. W. 1960. *Astron. J.* 65:485
41. Cassinelli, J. P. 1979. *Ann. Rev. Astron. Astrophys.* 17:275
42. Castellani, V., Giannone, P., Renzini, A. 1973. In *Variable Stars in Globular Clusters and Related Systems*, ed. J. D. Fernie, p. 197. Dordrecht: Reidel
43. Castor, J. I. 1981. In *Physical Processes in Red Giants*, ed. I. Iben Jr., A. Renzini, p. 285. Dordrecht: Reidel
44. Chechetkin, V. M., Gershtein, S. S., Imshennik, V. S., Ivanova, L. N., Khlopov, M. Yu. 1980. *Astrophys. Space Sci.* 67:61
45. Clayton, D. D., Fowler, W. A., Hull, T. C., Zimmerman, B. A. 1961. *Ann. Phys.* 12:121
46. Clegg, R. E. S., Lambert, D. L., Tomkin, J. 1981. *Ap. J.* 250:262
47. Cohen, J. G. 1982. *Ap. J.* 258:143
48. Cohen, J. G., Frogel, J. A., Persson, S. E., Elias, J. H. 1981. *Ap. J.* 249:481
49. Cohen, M. 1979. *MNRAS* 186:837
50. Cohen, M. 1980. *Ap. J. Lett.* 238:L81
51. Cohen, M., Schmidt, G. D. 1982. *Ap. J.* 259:693
52. Cosner, K., Iben, I. Jr., Truran, J. W. 1980. *Ap. J. Lett.* 238:L91
53. Cosner, K., Truran, J. W. 1981. *Astrophys. Space Sci.* 78:85
54. Couch, R. G., Arnett, W. D. 1973. *Ap. J. Lett.* 180:L101
55. Couch, R. G., Arnett, W. D. 1975. *Ap. J.* 196:791
56. Cowley, A. P., Downs, P. L. 1980. *Ap. J.* 236:648
57. Cox, J. P., King, D. S., Cox, A. N., Wheeler, J. C., Hansen, C. J., Hodson, S. W. 1980. *Space Sci. Rev.* 27:529
58. Danziger, I. J. 1965. *MNRAS* 130:199
59. Danziger, I. J. 1966. *Ap. J.* 143:527
60. Dearborn, D. S. P., Eggleton, P. P. 1977. *Ap. J.* 213:448
61. DeGioia-Eastwood, K., Hackwell, J. A., Grasdalen, G. L., Gehrz, R. D. 1981. *Ap. J. Lett.* 245:L75
62. De Jong, T. 1983. *Ap. J.* In press
63. Despain, K. H. 1980. *Ap. J. Lett.* 236:L165
64. Despain, K. H., Cosner, K., Truran, J. W. 1983. Preprint
65. Donn, B., Wickramasinghe, N. C., Stecher, T. P. 1968. *Ap. J.* 153:451
66. Eberhardt, P., Jungck, M. H. A., Meier, F. O., Niederer, F. 1979. *Ap. J. Lett.* 234:L169
67. Elitzur, M. 1981. In *Physical Processes in Red Giants*, ed. I. Iben Jr., A. Renzini, p. 363. Dordrecht: Reidel
68. Engels, D., Schultz, G. V., Sherwood, W. A. 1981. In *Physical Processes in Red Giants*, ed. I. Iben Jr., A. Renzini, p. 401. Dordrecht: Reidel
69. Ergma, E., Paczyński, B. 1974. *Acta Astron.* 24:1
70. Feast, M. W. 1981. In *Physical Processes in Red Giants*, ed. I. Iben Jr., A. Renzini, p. 193. Dordrecht: Reidel
71. Feast, M. W., Catchpole, R. M., Carter, B. S., Roberts, G. 1980. *MNRAS* 193:377
72. Fowler, W. A., Caughlan, G. R., Zimmerman, B. A. 1975. *Ann. Rev. Astron. Astrophys.* 13:69
73. Fox, N. W., Wood, P. R. 1982. *Ap. J.* 259:198
74. Freeman, K. C. 1980. In *Star Clusters*, ed. J. E. Hesser, p. 317. Dordrecht: Reidel
75. Frogel, J. A. 1981. In *Physical Processes in Red Giants*, ed. I. Iben Jr., A. Renzini, p. 63. Dordrecht: Reidel
76. Frogel, J. A., Blanco, V. M. 1983. In press
77. Frogel, J. A., Blanco, V. M., McCarthy, M. F., Cohen, J. G. 1982. *Ap. J.* 252:133
78. Frogel, J. A., Cohen, J. G. 1982. *Ap. J.* 253:580
79. Frogel, J. A., Cohen, J. G., Persson, S. E., Elias, J. H. 1981. In *Physical Processes in Red Giants*, ed. I. Iben Jr., A. Renzini, p. 159. Dordrecht: Reidel
80. Frogel, J. A., Persson, S. E., Cohen, J. G. 1980. *Ap. J.* 239:495
81. Frogel, J. A., Persson, S. E., Cohen, J. G. 1981. In *Physical Processes in Red Giants*, ed. I. Iben Jr., A. Renzini, p. 55. Dordrecht: Reidel
82. Frogel, J. A., Whitford, A. E. 1982. *Ap. J. Lett.* 259:L7
83. Fujimoto, M. Y. 1977. *Publ. Astron. Soc. Jpn.* 29:331
84. Fujimoto, M. Y., Nomoto, K.,

Sugimoto, D. 1976. *Publ. Astron. Soc. Jpn.* 28:89
85. Fujimoto, M. Y., Sugimoto, D. 1979. *Publ. Astron. Soc. Jpn.* 31:1
86. Fusi-Pecci, F., Renzini, A. 1976. *Astron. Astrophys.* 46:447
87. Gerola, H., Carnevali, L., Salpeter, E. E. 1982. Preprint
88. Gingold, R. A. 1974. *Ap. J.* 193:177
89. Gingold, R. A. 1975. *Ap. J.* 198:425
90. Goebel, J. H., Bregman, J. D., Witteborn, F. C., Taylor, B. J., Willner, S. P. 1981. *Ap. J.* 246:455
91. Gordon, C. P. 1968. *Publ. Astron. Soc. Pac.* 80:597
92. Härm, R., Schwarzschild, M. 1975. *Ap. J.* 200:324
93. Herman, J., Habing, H. J. 1981. In *Physical Processes in Red Giants*, ed. I. Iben Jr., A. Renzini, p. 383. Dordrecht: Reidel
94. Hill, S. J., Willson, L. A. 1979. *Ap. J.* 229:1029
95. Hinkle, K. H., Lambert, D. L., Snell, R. L. 1976. *Ap. J.* 210:864
96. Hodge, P. W. 1961. *Ap. J.* 133:413
97. Hodge, P. W. 1971. *Ann. Rev. Astron. Astrophys.* 9:35
98. Hodge, P. W. 1982. *Ap. J.* 256:447
99. Iben, I. Jr. 1967. *Ann. Rev. Astron. Astrophys.* 5:571
100. Iben, I. Jr. 1974. *Ann. Rev. Astron. Astrophys.* 12:215
101. Iben, I. Jr. 1974. *Bull. Am. Astron. Soc.* 6:316
102. Iben, I. Jr. 1975 *Ap. J.* 196:525
103. Iben, I. Jr. 1975. *Ap. J.* 196:549
104. Iben, I. Jr. 1976. *Ap. J.* 208:165
105. Iben, I. Jr. 1977. *Ap. J.* 217:788
106. Iben, I. Jr. 1977. In *Advanced Stages in Stellar Evolution*, ed. P. Bouvier, A. Maeder, p. 1. Geneva: Geneva Obs.
107. Iben, I. Jr. 1978. *Ap. J.* 219:213
108. Iben, I. Jr. 1978. *Ap. J.* 226:996
109. Iben, I. Jr. 1981. *Ap. J.* 246:278
110. Iben, I. Jr. 1981. In *Physical Processes in Red Giants*, ed. I. Iben Jr., A. Renzini, p. 3. Dordrecht: Reidel
111. Iben, I. Jr. 1981. In *Effects of Mass Loss on Stellar Evolution*, ed. C. Chiosi, R. Stalio, p. 373. Dordrecht: Reidel
112. Iben, I. Jr. 1982. *Ap. J.* 253:248
113. Iben, I. Jr. 1982. *Ap. J.* 260:821
114. Iben, I. Jr. 1983. *Ap. J.* Submitted for publication
115. Iben, I. Jr. 1983. *Ap. J.* Submitted for publication
116. Iben, I. Jr., Kaler, J. M., Truran, J. W., Renzini, A. 1983. *Ap. J.* 264:605
117. Iben, I. Jr., Renzini, A. 1982. *Ap. J. Lett.* 259:L79
118. Iben, I. Jr., Renzini, A. 1982. *Ap. J. Lett.* 263:L188
119. Iben, I. Jr., Rood, R. T. 1970. *Ap. J.* 161:587
120. Iben, I. Jr., Truran, J. W. 1978. *Ap. J.* 220:980
121. Imshennik, D. K., Nadyozhin, D. K., Utrobin, V. P. 1981. *Astrophys. Space Sci.* 78:105
122. Jones, T. J., Hyland, A. R., Gatley, I. 1982. Preprint
123. Kaler, J. B. 1979. *Ap. J.* 228:163
124. Kaler, J. B. 1981. *Ap. J.* 249:201
125. Kaler, J. B. 1983. *Ap. J.* In press
126. Kaler, J. B. 1983. In *Planetary Nebulae*, ed. D. R. Flower, p. 245. Dordrecht: Reidel
127. Kaler, J. B., Iben, I. Jr., Becker, S. A. 1978. *Ap. J. Lett.* 224:L63
128. Käppeler, F., Beer, H., Wisshak, K., Clayton, D. D., Macklin, R. L., Ward, R. A. 1982. *Ap. J.* 257:821
129. Keenan, P. C., Boeshaar, P. C. 1980. *Ap. J. Suppl.* 43:379
130. King, D. S. 1980. *Space Sci. Rev.* 27:519
131. Kleinmann, S. G., Gillett, F. C., Joyce, R. R. 1981. *Ann. Rev. Astron. Astrophys.* 19:411
132. Knapp, G. R., Phillips, T. G., Leighton, R. B., Lo, K. Y., Wannier, P. G., et al. 1982. *Ap. J.* 252:616
133. Koester, D., Reimers, D. 1981. *Astron. Astrophys.* 99:L8
134. Koester, D., Schultz, H., Weidemann, V. 1979. *Astron. Astrophys.* 76:262
135. Koester, D., Weidemann, V. 1980. *Astron. Astrophys.* 81:145
136. Kunkel, W. E. 1979. *Ap. J.* 228:718
137. Kwok, S. 1981. In *Physical Processes in Red Giants*, ed. I. Iben Jr., A. Renzini, p. 421. Dordrecht: Reidel
138. Kwok, S. 1981. In *Effects of Mass Loss on Stellar Evolution*, ed. C. Chiosi, R. Stalio, p. 347. Dordrecht: Reidel
139. Kwok, S. 1982. *Ap. J.* 258:280
140. Kwok, S., Purton, G. R., Fitzgerald, P. M. 1978. *Ap. J. Lett.* 219:L125
141. Lambert, D. L. 1981. In *Physical Processes in Red Giants*, ed. I. Iben Jr., A. Renzini, p. 115. Dordrecht: Reidel
142. Lambert, D. L., Ries, L. M. 1981. *Ap. J.* 248:228
143. Lewis, R. S., Alaerts, L., Matsuda, J.-L., Anders, E. 1979. *Ap. J. Lett.* 234:L165
144. Liebert, J. 1980. *Ann. Rev. Astron. Astrophys.* 18:363
145. Little-Marenin, I. R., Little, S. J. 1979. *Astron. J.* 84:1374
146. Luck, R. E. 1978. *Ap. J.* 219:148
147. Luck, R. E. 1982. *Ap. J.* 256:177
148. Luck, R. E., Lambert, D. L. 1981. *Ap. J.* 245:1018
149. Lucy, L. B. 1967. *Astron. J.* 72:813
150. Lynden-Bell, D. 1976. *MNRAS* 174:695

151. Maran, S. P., Aller, L. H., Gull, T. R., Stecher, T. P. 1982. *Ap. J. Lett.* 253: L43
152. Mathews, W. G. 1978. In *Planetary Nebulae*, ed. Y. Terzian, p. 251. Dordrecht: Reidel
153. Mazurek, T. J., Meier, D. L., Wheeler, J. C. 1977. *Ap. J.* 213: 518
154. McClure, R. D., Fletcher, J. M., Nemec, J. M. 1980. *Ap. J. Lett.* 238: L35
155. Mengel, J. G. 1976. *Astron. Astrophys.* 48: 33
156. Mezger, P. G., Mathis, J. S., Panagia, N. 1982. *Astron. Astrophys.* 105: 372
157. Mould, J. R., Aaronson, M. 1979. *Ap. J.* 232: 421
158. Mould, J. R., Aaronson, M. 1980. *Ap. J.* 240: 464
159. Mould, J. R., Aaronson, M. 1982. *Ap. J.* 263: 629
160. Mould, J. R., Cannon, R. D., Aaronson, M., Frogel, J. A. 1982. *Ap. J.* 254: 500
161. Neugebauer, G., Leighton, R. B. 1969. *Two Micron Sky Survey: A Preliminary Catalogue, NASA SP-3047*
162. Noguchi, K., Kawara, K., Kabayashi, Y., Okuda, H., Sato, S. 1981. *Publ. Astron. Soc. Jpn.* 33: 373
163. Nomoto, K. 1981. In *Fundamental Problems in the Theory of Stellar Evolution*, ed. D. Sugimoto, D. Q. Lamb, D. N. Schramm, p. 295. Dordrecht: Reidel
164. Nomoto, K., Sugimoto, D., Neo, S. 1976. *Astrophys. Space Sci.* 39: L37
165. Nørgaard, H. 1980. *Ap. J.* 236: 895
166. Olnon, F. M. 1981. In *Physical Processes in Red Giants*, ed. I. Iben Jr., A. Renzini, p. 237. Dordrecht: Reidel
167. Paczyński, B. 1970. *Acta Astron.* 20: 47; 20: 287
168. Paczyński, B. 1971. *Acta Astron.* 21: 417
169. Paczyński, B. 1973. *Astrophys. Lett.* 15: 147
170. Paczyński, B. 1975. *Ap. J.* 202: 558
171. Paczyński, B. 1977. *Ap. J.* 214: 812
172. Paczyński, B., Ziolkowski, J. 1968. *Acta Astron.* 18: 255
173. Deleted in proof
174. Payne-Gaposchkin, C. H. 1971. *Smithsonian Contrib. Astrophys.* 13: 1
175. Peery, B. F. Jr. 1971. *Ap. J. Lett.* 163: L1
176. Peimbert, M. 1973. *Mem. Soc. R. Sci. Liege, 6e Ser.* 5: 307
177. Peimbert, M. 1980. *The Universe at Ultraviolet Wavelength*, ed. R. D. Chapman, p. 557. NASA
178. Peimbert, M. 1981. In *Physical Processes in Red Giants*, ed. I. Iben Jr., A. Renzini, p. 409. Dordrecht: Reidel
179. Peimbert, M., Torres-Peimbert, S. 1983. In *Planetary Nebulae*, ed. D. R. Flower, p. 233. Dordrecht: Reidel
180. Perinotto, M., Renzini, A. 1979. In *Astronomical Uses of the Space Telescope*, ed. F. Macchetto, F. Pacini, M. Tarenghi, p. 147. ESO
181. Peterson, R. 1976. *Ap. J.* 206: 800
182. Prialnik, D., Shaviv, G., Kovetz, A. 1981. *Ap. J.* 247: 225
183. Price, S. D., Walker, R. G. 1976. *The AFGL Four Color Infrared Sky Survey. AFCL-TR-76-0208*. Hanscomb AFB, Mass: Air Force Geophys. Lab.
184. Reimers, D. 1975. *Mem. Soc. R. Sci. Liege, 6e Ser.* 8: 369
185. Reimers, D. 1975. In *Problems in Stellar Atmospheres and Envelopes*, ed. B. Baschek, W. H. Kegel, G. Traving, p. 229. Berlin/Heidelberg: Springer
186. Reimers, D. 1981. In *Physical Processes in Red Giants*, ed. I. Iben Jr., A. Renzini, p. 269. Dordrecht: Reidel
187. Renzini, A. 1977. In *Advanced Stages of Stellar Evolution*, ed. P. Bouvier, A. Maeder, p. 151. Geneva: Geneva Obs.
188. Renzini, A. 1979. In *Stars and Star Systems*, ed. B. E. Westerlund, p. 155. Dordrecht: Reidel
189. Renzini, A. 1980. In *Variability in Stars and Galaxies*, p. E.3.1. Liege Univ. Press
190. Renzini, A. 1980. *Mem. Soc. Astron. Ital.* 51: 749
191. Renzini, A. 1981. In *Physical Processes in Red Giants*, ed. I. Iben Jr., A. Renzini, p. 165. Dordrecht: Reidel
192. Renzini, A. 1981. In *Physical Processes in Red Giants*, ed. I. Iben Jr., A. Renzini, p. 431. Dordrecht: Reidel
193. Renzini, A. 1981. *Effects of Mass Loss on Stellar Evolution*, ed. C. Chiosi, R. Stalio, p. 319. Dordrecht: Reidel
194. Renzini, A. 1981. *Ann. Phys.* (*Paris*) 6: 87
195. Renzini, A. 1982. In *Wolf-Rayet Stars*, ed. C. de Loore, A. J. Willis, p. 413. Dordrecht: Reidel
196. Renzini, A. 1983. In *Planetary Nebulae*, ed. D. R. Flowers, p. 267. Dordrecht: Reidel
197. Renzini, A., Voli, M. 1981. *Astron. Astrophys.* 94: 175
198. Renzini, A., Mengel, J. G., Sweigart, A. V. 1977. *Astron. Astrophys.* 56: 369
199. Richer, H. B. 1981. *Ap. J.* 243: 744
200. Richer, H. B. 1981. In *Physical Processes in Red Giants*, ed. I. Iben Jr., A. Renzini, p. 153. Dordrecht: Reidel
201. Richer, H. B., Olander, N., Westerlund, B. E. 1979. *Ap. J.* 230: 724
202. Richer, H. B., Westerlund, B. E. 1983. *Ap. J.* 264: 114
203. Ridgway, S. T., Hall, D. N. B. 1980. In *Interstellar Molecules*, ed. B. H. Andrew, p. 509. Dordrecht: Reidel
204. Rocca-Volmerange, B., Prevot, L.,

Ferlet, R., Lequeux, J., Prevot-Burnichon, M. L. 1981. *Astron. Astrophys.* 99:L5
205. Romanishin, W., Angel, J. R. P. 1980. *Ap. J.* 235:992
206. Rood, R. T. 1972. *Ap. J.* 177:681
207. Rosino, L. 1973. *Astron. Astrophys. Suppl.* 9:347
208. Sackman, I.-J. 1977. *Ap. J.* 212:159
209. Sackman, I.-J. 1980. *Ap. J.* 235:554
210. Sackman, I.-J. 1980. *Ap. J. Lett.* 241:L37
211. Sackman, I.-J., Smith, R. L., Despain, K. H. 1974. *Ap. J.* 187:555
212. Sanduleak, N., Philip, A. G. D. 1977. *Publ. Warner & Swasey Obs.* 2:5
213. Scalo, J. M. 1976. *Ap. J.* 206:215
214. Scalo, J. M. 1981. In *Physical Processes in Red Giants*, ed. I. Iben Jr., A. Renzini, p. 77. Dordrecht: Reidel
215. Scalo, J. M., Miller, G. E. 1981. *Ap. J.* 246:251
216. Scalo, J. M., Ross, J. E. 1976. *Astron. Astrophys.* 48:219
217. Scalo, J. M., Ulrich, R. K. 1973. *Ap. J.* 183:151
218. Schönberner, D. 1979. *Astron. Astrophys.* 79:108
219. Schönberner, D. 1981. *Astron. Astrophys.* 103:119
220. Schönberner, D., Weidemann, V. 1981. In *Physical Processes in Red Giants*, ed. I. Iben Jr., A. Renzini, p. 463. Dordrecht: Reidel
221. Schönberner, D., Weidemann, V. 1983. In *Planetary Nebulae*, ed. D. R. Flower, p. 359. Dordrecht: Reidel
222. Schramm, D. N. 1977. In *Advanced Stages in Stellar Evolution*, ed. P. Bouvier, A. Maeder, p. 284. Geneva: Geneva Obs.
223. Schwarzschild, M., Härm, R. 1967. *Ap. J.* 150:961
224. Searle, L., Wilkinson, A., Bagnuolo, W. G. 1980. *Ap. J.* 239:803
225. Shklovski, I. S. 1956. *Astron. Zh.* 33:315
226. Srinivasan, B., Anders, E. 1978. *Science* 201:51
227. Starrfield, S. J., Cox, A. N., Hodson, S. W. 1980. *Space Sci. Rev.* 27:621
228. Stecher, T. P., Maran, S. P., Gull, T. R., Aller, L. H., Savedoff, M. P. 1982. *Ap. J. Lett.* 262:L41
229. Sugimoto, D., Nomoto, K. 1975. *Publ. Astr. Soc. Jpn.* 27:197
230. Sweeny, M. A. 1976. *Astron. Astrophys.* 49:375
231. Sweigart, A. V., Gross, P. G. 1978. *Ap. J. Suppl.* 36:405
232. Tinsley, B. M. 1980. *Fundam. Cosmic Phys.* 5:287
233. Tomkin, J., Luck, R. E., Lambert, D. L. 1976. *Ap. J.* 210:694
234. Truran, J. W., Iben, I. Jr. 1977. *Ap. J.* 216:797
235. Tsuji, T. 1965. *Ann. Tokyo Astron. Obs. Ser. 2* 9:1
236. Tsuruta, S., Cameron, A. G. W. 1976. *Astrophys. Space Sci.* 39:397
237. Tuchman, Y., Sack, N., Barkat, Z. 1979. *Ap. J.* 234:217
238. Tuggle, R. S., Iben, I. Jr. 1972. *Ap. J.* 178:455
239. Ulrich, R. K. 1973. In *Explosive Nucleosynthesis*, ed. D. N. Schramm, W. D. Arnett, p. 139. Austin: Univ. Texas
240. Utsumi, K. 1970. *Publ. Astron. Soc. Jpn.* 22:93
241. Uus, U. 1970. *Nauch. Inform. Acad. Nauk.* 17:3
242. Van Agt, S. L. Th. J. 1978. *Publ. DDO Obs.* 3:205
243. van den Bergh, S. 1973. *Astron. Astrophys.* 28:469
244. Vanden Bout, P. A., Snell, R. L. 1980. *Ap. J.* 236:460
245. van den Heuvel, E. P. J. 1975. *Ap. J. Lett.* 196:L121
246. Walker, R. G., Price, S. D. 1975. *AFCRL Infrared Sky Survey, Vol. 1. AFCRL-TR-75-0373.* Hanscomb AFB, Mass: Air Force Geophys. Lab.
247. Wallerstein, G. 1973. *Ann. Rev. Astron. Astrophys.* 11:115
248. Wannier, P. G., Redman, R. O., Phillips, T. G., Leighton, R. B., Knapp, G. R., Huggins, P. J. 1980. In *Interstellar Molecules*, ed. B. H. Andrew, p. 487. Dordrecht: Reidel
249. Ward, R. A. 1977. *Ap. J.* 216:540
250. Webbink, R. F. 1976. *Ap. J.* 209:829
251. Weidemann, V. 1980. In *White Dwarfs and Variable Degenerate Stars*, ed. H. M. Van Horn, V. Weidemann, p. 206. Univ. Rochester
252. Weidemann, V. 1981. In *Effects of Mass Loss on Stellar Evolution*, ed. C. Chiosi, R. Stalio, p. 339. Dordrecht: Reidel
253. Weigert, A. 1966. *Z. Ap.* 64:395
254. Werner, M. W., Beckwith, S., Gatley, I., Sellgren, K., Berriman, G., Whiting, D. L. 1980. *Ap. J.* 239:540
255. Westerlund, B. E. 1965. *MNRAS* 130:45
256. Westerlund, B. E. 1979. *The Messenger* 19:7
257. Westerlund, B. E., Olander, N., Richer, H. B., Crabtree, D. R. 1978. *Astron. Astrophys. Suppl.* 31:61
258. Westerlund, B. E., Olander, N., Hedin, B. 1981. *Astron. Astrophys. Suppl.* 43:267
259. Whitford, A. E., Rich, M. 1983. *Ap. J.* In press

260. Willson, L. A. 1981. In *Effects of Mass Loss on Stellar Evolution*, ed. C. Chiosi, R. Stalio, p. 353. Dordrecht: Reidel
261. Willson, L. A. 1981. In *Physical Processes in Red Giants*, ed. I. Iben Jr., A. Renzini, p. 225. Dordrecht: Reidel
262. Willson, L. A., Hill, S. J. 1979. *Ap. J.* 228:854
263. Witteborn, F. C., Strecker, D. W., Erickson, E. F., Smith, S. M., Goebel, J. H., Taylor, B. J. 1980. *Ap. J.* 238:577
264. Wood, P. R. 1974. *Ap. J.* 190:609
265. Wood, P. R. 1979. *Ap. J.* 227:220
266. Wood, P. R. 1981. In *Physical Processes in Red Giants*, ed. I. Iben Jr., A. Renzini, p. 135. Dordrecht: Reidel
267. Wood, P. R. 1981. In *Physical Processes in Red Giants*, ed. I. Iben Jr., A. Renzini, p. 205. Dordrecht: Reidel
268. Wood, P. R. 1983. *Ap. J.* Submitted for publication
269. Wood, P. R., Bessell, M. S., Fox, M. W. 1981. Preprint
270. Wood, P. R., Cahn, J. H. 1977. *Ap. J.* 211:499
271. Wood, P. R., Zarro, D. M. 1981. *Ap. J.* 247:247
272. Woodward, P. R. 1981. Preprint
273. Zinn, R., Searle, L. 1976. *Ap. J.* 209:734
274. Zuckerman, B. 1980. *Ann. Rev. Astron. Astrophys.* 18:263
275. Zuckerman, B. 1980. In *Interstellar Molecules*, ed. B. H. Andrew, p. 479. Dordrecht: Reidel